THESIS

CONTROLS ON POST-HIGH PARK FIRE CHANNEL RESPONSE,

SOUTH FORK CACHE LA POUDRE BASIN, COLORADO

Submitted by

Scott M. Shahverdian

Department of Geosciences

In partial fulfillment of the requirements

For the Degree of Master of Science

Colorado State University

Fort Collins, Colorado

Summer 2015

Master's Committee:

Advisor: Sara Rathburn

Ellen Wohl
Peter Nelson

ABSTRACT

CONTROLS ON POST-HIGH PARK FIRE CHANNEL RESPONSE,

SOUTH FORK CACHE LA POUDRE BASIN, COLORADO

Post-fire basin sediment yield is the product of multiple erosional processes operating at multiple spatial scales and in different process domains. Most post-fire erosion response studies have focused on the hillslope scale, yet land management decisions and post-fire treatments are addressed at the watershed scale. The goal of this study was to evaluate how the channel network contributes to the production, transport, and storage of sediment by monitoring post-fire channel response. A better understanding of channel production, transport, and storage of sediment post-fire is required in order to predict basin scale sediment yields and make informed management decisions. Two perennial headwater streams and two ephemeral tributaries of the South Fork Cache la Poudre River were monitored in two severely burned basins in the 2012 High Park Fire burn area of northern Colorado. The basins were either completely or partially mulched with agricultural straw and wood mulch during June 2013. Repeat cross section and longitudinal profile surveys were performed to evaluate event-driven changes. The dominant response in both basins post-fire was net degradation. Steep channel slopes promoted channel incision with no significant overbank deposition, indicating that the channel network was a substantial source of sediment and an efficient transporter of hillslope sediment. In 2013, six storms exceeded the 30 minute maximum intensity 10 mm hr^{-1} associated with hillslope sediment production while in 2014 two storms exceeded this threshold. Perennial channel response in 2014, measured by mean bed elevation change at cross sections, ranged from -20 to +17 cm, but most cross sections experienced changes between 0-3 cm. Channel response was uncorrelated with channel slope, channel slope*contributing area product, or width to depth ratio. Ephemeral channels showed an alternating cycle of aggradation and degradation on the order of 0-3 cm per event, as well as a scour and fill response during storm events. Scour and fill often resulted in minimal net changes to channel geometry, suggesting that the channel was an important temporary source and sink of sediment and that post-fire peak flow calculations must account for event-based scour. In 2013, suspended sediment concentrations in the South Fork Cache la Poudre exceeded 2500 mg L^{-1} 12 times, and exhibited a threshold response when MI_{30} exceeded 10 mm hr^{-1}. In 2014, suspended sediment concentrations exceeded 1500 mg L^{-1} once, and a MI_{30} of 40 mm hr^{-1} was insufficient to cause values to exceed 1500 mg L^{-1}. Post-fire suspended sediment concentrations from the South Fork Cache la Poudre River indicate that hillslopes were the primary source of suspended sediment. Where the straw mulch was retained on hillslopes, it was effective at limiting erosion. The channel network was largely resistant to change during the second year of post-fire monitoring due to the influence of a >200 year storm that occurred in September 2013. Following this storm, the channel network acted primarily to transport sediment rather than produce sediment. Sediment connectivity within the channel network was high in each basin due to steep channel slopes, but the development of an alluvial fan at each basin outlet as well as the morphology of the South Fork Cache la Poudre at each confluence suggest differences in the sediment delivery from each basin to downstream reaches. Sediment connectivity from the hillslopes to the channel network and along the channel network must be addressed in post-fire studies when predicting or interpreting post-fire basin sediment yields. Furthermore, assessing sediment connectivity is a useful tool for land managers making post-fire erosion mitigation decisions.

ACKNOWLEDGMENTS

There are a great many people who made this work possible without whom I would have never completed this study. This project was funded by the cities of Fort Collins and Greeley, with support from the US Forest Service Rocky Mountain Research Station and the Colorado Scientific Society. Thank you to Colorado State University Warner College of Natural Resources and the Department of Geosciences for funding, and allowing me the opportunity to pursue my love of rivers. My great thanks go to Quin Scanlon and Justin Blumenthal for tromping around through the ash and shadeless landscape for many hours, in many conditions, carrying a great assortment of equipment, and all at a moment's notice. Sandra Ryan and Mark Dixon, from the Rocky Mountain Research Station, were instrumental in providing data, guidance, and logistic support throughout the course of this study. Thank you to Dave Dust for his willingness to sit down and share his surveying experience; to Dan Brogan for teaching and trouble-shooting innumerable RTK scenarios; to US Forest service and City of Fort Collins staff for logistical support, funding, and field work. For advice, support, and therapy throughout the past few years I extend my sincere thanks to all the members of the Fluvial Family. Thank you to my committee members Dr. Ellen Wohl and Dr. Peter Nelson. My deepest appreciation and thanks go to my adviser, Dr. Sara Rathburn, for her unending patience and guidance.

TABLE OF CONTENTS

LIST OF TABLES

LIST OF FIGURES

1. INTRODUCTION

Wildfire is a natural disturbance that changes the hydrologic and geomorphic response in watersheds (Shakesby and Doerr, 2006) by lowering the intrinsic threshold for erosion (Schumm, 1973). Increased sediment yields following wildfire can degrade natural resources and aquatic habitat, promote sedimentation of reservoirs, and damage infrastructure (Benavides-Solorio and MacDonald, 2001; Goode et al., 2012; Moody and Martin, 2001a; Moody and Martin, 2001b; Wagenbrenner et al., 2006). Background erosion rates for undisturbed forests in the Colorado Front Range are low (MacDonald and Stednick, 2003; Morris and Moses, 1987). For small (< 5 km^2), forested watersheds in the interior West, erosion rates have been estimated at less than 0.2 metric tons $hectare^{-1}$ $year^{-1}$ (Patric and Evans, 1984). Long term erosion rates in arid and semi-arid regions may be heavily influenced by short duration elevated erosion rates resulting from large, infrequent disturbances (Kirchner et al., 2001; Brunsden and Thornes, 1979). Morris and Moses (1987) suggest that post-fire short term increases in sediment yield may dominate long term sediment yield in the Colorado Front Range. Infrequent, high magnitude disturbances are important drivers of physical and biological heterogeneity in riverine environments (Benda et al., 2003). In the western US, fire intensity, frequency, and extent are projected to increase due to longer fire seasons and greater temperature extremes (Westerling, 2006), causing significant increases in sediment yields (Goode et al., 2012).

Wildfire decreases ground cover and alters soil physical and chemical properties which reduce infiltration and promote runoff (Benavides-Solorio and MacDonald, 2001; DeBano, 2000; Goode et al., 2012; Larsen et al., 2009; Moody and Martin, 2001a; Shakesby and Doerr, 2006). Increased sediment yield and controls on sediment yield at the plot and hillslope scale have been well documented in the Colorado Front Range (e.g. Benavides-Solorio and MacDonald, 2001; Benavides-Solorio and MacDonald, 2005; Pietraszek, 2006; Larsen et al. 2009; Moody and Martin, 2001a; Moody and Martin, 2001b;

Schmeer, 2014). Post-fire sediment yield at the small basin (1-5 km^2) and watershed scale has received less attention (Shakesby and Doerr, 2006). Within a post-fire basin there is spatial heterogeneity in controls on runoff and sediment generation, including burn severity, ground cover, topography, and lithology (Moody and Martin, 2001a; Shakesby and Doerr, 2006). Post-fire basin sediment yield integrates hillslope and channel hydrologic and erosional processes that operate at multiple spatial scales (De Vente and Poesen, 2005) and in multiple process domains (Montgomery, 1999). Process-domains are spatially identifiable areas, such as hillslopes or channels that are characterized by specific geomorphic processes (Montgomery, 1999). Hillslope erosion processes may be dominated by sheetflow and rilling, while channel erosion processes include channel incision and widening. Both suites of processes must be addressed in post-fire basin response. Figure 1 illustrates the nested spatial scales that must be addressed in order to predict and interpret watershed sediment yield.

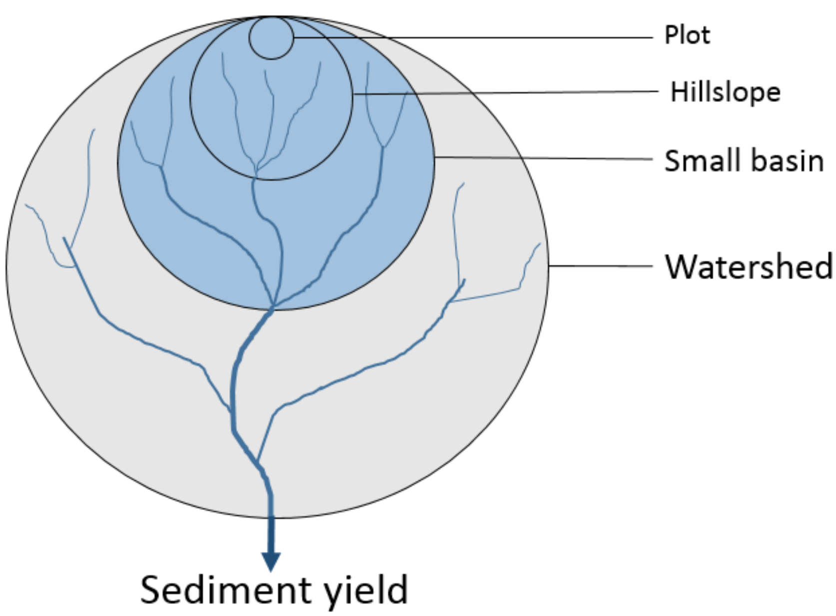

Figure 1: Schematic of the nested spatial scales within a watershed. This study focuses on the channel network at the small basin scale (highlighted in blue circles).

Interpreting and predicting watershed sediment yield and the relative importance of sediment contributions from hillslopes and channels is challenging because of increased heterogeneity and complexity at increasing spatial scales (Miller et al., 2003). Channel response and sediment dynamics in headwater streams are of critical interest because headwater streams account for the majority of total channel length in watersheds (Leopold et al., 1964; Benda et al., 2005) and are pathways that connect hillslope processes to larger order drainages.

The application of mulch to increase ground cover after wildfire has been effective at reducing erosion from hillslopes (Wagenbrenner et al., 2006; Robichaud et al., 2013a; Schmeer, 2014; Vega et al., 2015). By providing immediate ground cover, mulch reduces the impact of rainsplash, increases surface roughness, decreases flowpath length, increases soil moisture, and promotes regrowth of vegetation (Robichaud et al., 2013a). Studies on the effectiveness of mulch at reducing sediment yield have been limited to the plot and hillslope scale, but there is considerable uncertainty if unit area sediment yields can be extrapolated across spatial scales (Benavides-Solorio and MacDonald, 2001; Robichaud et al., 2013b). Post-fire treatment decisions are made at the watershed scale, therefore the efficacy of treatments at the watershed scale is most relevant to land managers (Robichaud et al., 2013b), but measuring runoff and erosion at large spatial scales is labor intensive and expensive due to extensive instrumentation requirements (Robichaud, 2005). In addition, mulch may contain seed of non-native species and thereby introduce weed seeds into remote areas. Although the seed provides quick temporary ground cover until natural regeneration stabilizes a burn area, there may be detrimental effects if non-native herbaceous species suppress native regeneration (Beyers, 2004).

The 2012 High Park Fire in northern Colorado resulted in substantial sediment delivery to the Cache la Poudre River, a vital water supply for nearly half a million users within several Front Range communities. Because of concerns about post-fire erosion degrading water quality, local municipalities conducted aerial mulching with the intent to limit sediment delivery to downstream receiving waters. This research was initiated to investigate the channel network contribution to sediment yield from two small basins in the High Park Fire burn area. A primary goal was to assess post-fire channel response in two small basins within the South Fork Cache la Poudre basin to determine controls on sediment production, transport, and storage in the channel network. A further goal was to evaluate the influence of mulch on channel response in order to determine its efficacy at mitigating sediment yield at the small basin scale. Addressing the role of the channel network as a source, transfer zone, or sink for sediment is critical to predicting sediment yields at the small basin scale and how those yields change through time.

The questions addressed by this study are, 1) At what locations within the basin does the channel network act as a source or sink for sediment?, 2) What volume of sediment is sourced from or stored in the channel network on an event basis?, 3) What rainfall, basin, and channel characteristics control the amount of sediment produced or stored within the channel network?, and 4) How does the presence of mulch influence channel response? Addressing these questions provides useful information to Front Range communities assessing post-fire sediment mitigation efforts, with broader application for land managers seeking to make informed decisions regarding the post-fire protection of natural resources.

1.1 Background

1.1.1 Post-fire sediment yield at the hillslope scale

Hillslopes exert an important control on the volume and caliber of sediment reaching the channel network, which controls channel morphodynamics and the mobility of the channel substrate (Goode et al., 2012). Table 1 provides an abbreviated list of well documented controls on post-fire sediment yield at the plot and hillslope scale in the Colorado Front Range. In the Colorado Front Range, high-intensity summer convective thunderstorms drive post-fire hillslope erosion (Morris and Moses, 1987; Pietraszek, 2006; Rough, 2007) generating more than 90% of total sediment yield (Benavides-Solorio and MacDonald, 2005). Snowmelt-driven runoff is not a significant driver of post-fire hillslope erosion in the Colorado Front Range (Benavides-Solorio and MacDonald, 2005; Pietraszek, 2006).

Table 1: Rainfall, fire-induced, and site controls on hillslope sediment yield.

Control type	Relevant Variables	Study
Rainfall	Max. 30 minute intensity	Moody and Martin, 2001a; Moody and Martin, 2009; Pietraszek, 2006; Schmeer, 2014; Spigel and Robichaud, 2007
	Erosivity	Benavides-Solorio and MacDonald, 2005; Pietraszek, 2006; Schmeer, 2014
Fire-induced	Percent ground cover	Benavides-Solorio and MacDonald, 2001; Benavides-Solorio and MacDonald, 2005; Pietraszek, 2006; Larsen et al., 2009
	Soil Water Repellency	Benavides-Solorio and MacDonald, 2001; DeBano, 1981; DeBano, 2000
	Burn Severity	Benavides-Solorio and MacDonald, 2005; Pietraszek, 2006; Schmeer, 2014
Site	Topography Soil depth	Benavides-Solorio and MacDonald, 2005; Pietraszek, 2006; Rengers et al. (in review)
	Surface roughness	Moody and Ebel, 2014

Because wildfire decreases infiltration capacity (Benavides-Solorio and MacDonald, 2001; Goode et al., 2012; Larsen et al., 2009; Moody and Martin, 2001a; Morris and Moses, 1987) and rainfall intensity determines the amount of water available for infiltration-excess overland flow (Dunne and Leopold, 1978), post-fire sediment yield increases with rainfall intensity (Moody and Martin, 2009; Pietraszek, 2006; Schmeer, 2014; Spigel and Robichaud, 2007). Infiltration rates in unburned montane forests characterized by 85% surface cover are typically greater than 100 mm hr^{-1} (Moody and Martin, 2001a). Post-fire runoff and sediment generation have been observed at rainfall intensities of 8-10 mm hr^{-1} (Moody and Martin, 2001a; Pietraszek, 2006; Schmeer, 2014). When erosion is caused by lower intensity, long duration rain events (Morris and Moses, 1987; Benavides-Solorio and MacDonald, 2005; Pietraszek, 2006) rainfall erosivity (an index of rainfall energy) may be a useful metric to explain sediment yields because high values of rainfall erosivity may be attained by brief high-intensity events and long duration low-intensity events (Schmeer, 2014). While previous studies have identified different rainfall intensity metrics (e.g. 5 minute maximum intensity, 10 minute maximum intensity, and 30 minute maximum intensity) to be correlated with different erosional processes (Moody et al., 2013), 30 minute maximum rainfall intensity (MI_{30}) has often been selected for post-fire hillslope erosion studies and has been found to correlate with peak discharge (Moody and Martin, 2001b), and is therefore the metric chosen for use in this study.

Ground cover increases infiltration and reduces erosion potential by protecting soil from rainsplash, increasing surface roughness, and limiting overland flow velocities (Larsen et al, 2009; Pietraszek, 2006). Percent ground cover is the dominant control on hillslope sediment yield (Benavides-Solorio and MacDonald, 2001; Benavides-Solorio and MacDonald, 2005; Johansen et al., 2001; Larsen et al., 2009; MacDonald and Larsen, 2009; Pietraszek, 2006; Robichaud et al., 2000; Schmeer, 2014). Previous studies have found percent bare soil explained 84% (Johansen et al., 2001), 79% (Benavides-Solorio and MacDonald, 2005), 81% (Benavides-Solorio and MacDonald, 2001) and 58% (Pietraszek, 2006) of the variability in post-fire sediment yield at the plot and hillslope scale. Benavides-Solorio and MacDonald (2005) found a nonlinear erosion response when ground cover levels reached 40%.

Burn severity reflects changes in surface cover and soil properties post-fire (Keeley, 2009). Moderate severity burns are characterized by partial consumption of the canopy, consumption of fine fuels, and loss of most soil organic matter; high severity burns are characterized by complete consumption of the canopy and all surface litter, as well as charred organic matter to several centimeters depth (Ryan and Noste, 1985). Burn severity acts as a control on erosion response through its influence on ground cover and alteration of soil properties, including the formation and/or strengthening of soil water repellency (SWR).

Fires can create or strengthen a water repellent layer at or near the soil surface by the burning and condensation of hydrophobic compounds found in ponderosa and lodgepole pine forests (Debano, 1981; DeBano, 2000; Huffman et al., 2001; MacDonald and Larsen, 2009; Rough and MacDonald, 2005). SWR decreases infiltration rates in post-fire soils and promotes runoff. Previous studies have indicated that SWR is an important control on sediment yields at the hillslope scale (Benavides-Solorio and MacDonald, 2001; DeBano, 2000; Doerr et al., 2009), but MacDonald and Huffman (2004) found that soil water repellency became statistically undetectable one year after burning and that it is therefore unlikely that SWR is the primary control on elevated hillslope sediment yields, which persist up to 5 years (MacDonald and Larsen, 2009).

Where overland flow is concentrated along the axis of a convergent hillslope (referred to as a swale in this study), sediment production is more than twice that produced on planar hillslopes (Benavides-Solorio and MacDonald, 2005; Pietraszek, 2006). Concentration of flow along the swale axis increases flow depth and shear stress leading to incision (Pietraszek, 2006). Pietraszek (2006) found that erosion of the swale axis accounted for the majority of sediment eroded from convergent hillslopes and that the channel slope*contributing area product (a proxy for stream power) explained 64% of the variability in rill incision. Because rills represent an extension of the channel network, and therefore more efficient transport of water and sediment post fire (Wester et al., 2014), understanding controls on the magnitude and direction of response has important consequences for peak discharges and channel response downstream. Eccleston (2008) attempted to predict the transition from degrading to aggrading channels using the channel slope*contributing area product but his results were inconclusive. In contrast, Rengers et al. (in review) found that the majority of sediment eroded (volumetrically) from hillslopes was the result of shallow erosion on the hillslope rather than from convergent areas.

In addition to rainfall driven production and transport, dry ravel delivers hillslope sediment to the channel network (Florsheim et al., 1991). After a 1985 wildfire in southern California, 90% of the 550 m^3 of fine gravel deposition near the tributary mouth in a 2.14 km^2 basin was derived from colluvium delivered to the channel network by dry ravel (Florsheim et al., 1991).

1.1.2 Channel response to disturbance: sediment production, transport and storage in the channel network

Post-fire channels may aggrade or degrade in response to changes in the delivery rate of water and sediment, thereby acting as a source or sink and exerting an important control on basin sediment yield. Channels are conveyors of water and sediment and can respond to changes in water and sediment inputs by multiple modes of adjustment (Phillips, 1991) that take place over different time scales (Madej and Ozaki, 1996). Post-fire studies have documented a wide range of channel responses following wildfire, including aggradation, degradation, braiding, channel narrowing, creation of alluvial fans, and extension of the channel network (Benda et al., 2003; Legleiter et al., 2003; Meyer and Wells, 1997; Moody and Martin, 2001a; Wohl, 2013). Complex response (Schumm, 1973) has been observed in post-fire channels when extensive aggradation in downstream reaches caused by degradation upstream is followed by incision as sediment delivery to the channel network decreases and elevated base flows incise into recently deposited sediments (Laird and Harvey, 1986; Moody and Martin, 2001a). The formation and headward migration of knickpoints is an indicator of a channel responding to disturbance (Schumm, 1973; Schumm and Parker, 1973). For channels at equilibrium, Lane's balance provides a conceptual framework for how channels respond to increased water or sediment (Lane, 1955). Wildfire increases the delivery of both water and sediment to the channel network, making prediction of channel response using Lane's balance challenging. A list of channel variables that may influence the direction of channel response to disturbance includes: discharge, channel slope, bed material, bank material and stability, width to depth ratio, sediment load, bedforms, and flow depth. Similarly, in order to accommodate changes in water and sediment inputs at a given location, a channel may adjust its planform, slope, bed material, width to depth ratio, and bedforms. In an ephemeral channel in an arid climate, Merrit and Wohl (2003) found flow depth to be the most important factor in predicting the direction of channel response. Legleiter et al. (2003) found that net incision was the primary response of 2^{nd}-4^{th} order streams following the 1988 Yellowstone Fires, but that site specific response was highly variable. Zelt and Wohl (2004) noted that understanding stream response post-fire is "limited by the multitude of affected processes and controls and by dependence on local site characteristics." (p. 218)

Different geomorphic processes tend to dominate at different locations within the drainage network. Schumm (1977) proposed an idealized drainage network characterized by three sediment processes; source, transfer, and deposition, which dominate at different locations within a watershed. Montgomery and Buffington (1997) expanded on work by Schumm, outlining how channel morphology, when related to characteristic relationships between sediment supply and transport capacity, can aid in predicting response to disturbance in mountain streams. Many drainage characteristics that control the dominant sediment process change in a predictable manner in the downstream direction (Figure 2).

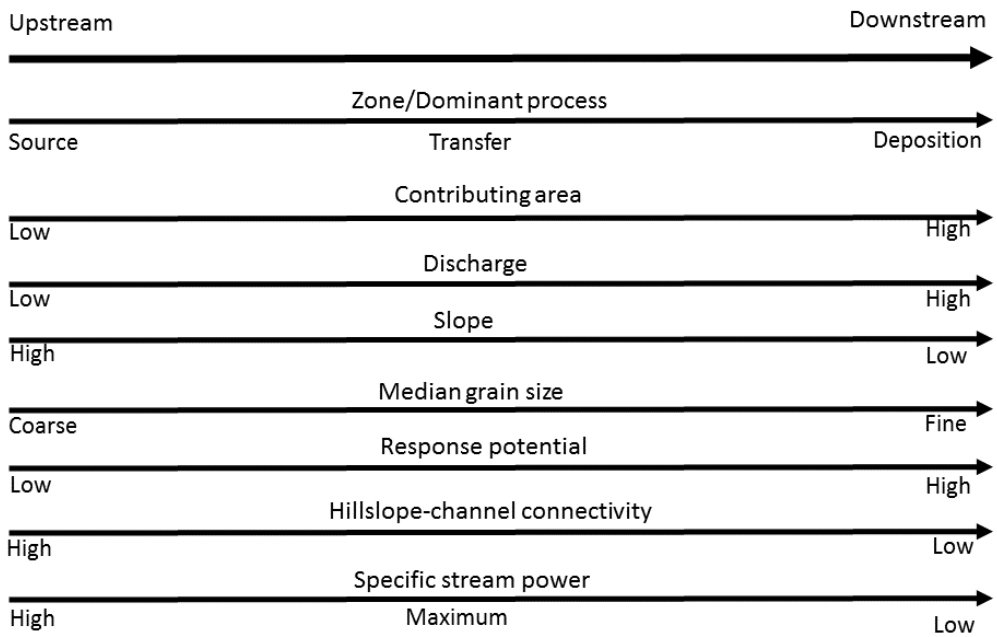

Figure 2: Downstream changes in variables controlling sediment production, transfer, and deposition in a drainage network. Modified from Schumm (1977) and Knighton (1998).

Predicting post-fire basin sediment yield requires identifying variables that control whether sediment is produced, transferred, or stored in the channel network. Despite high theoretical sediment transport capacity, mountainous headwater streams can store significant amounts of sediment (Benda, 2005). Stepped longitudinal profiles, forcing by instream wood, and high surface roughness limit bedload transport and provide significant opportunities for in-channel storage (Benda, 2005). Sediment may remain in storage for tens or hundreds of years or be quickly evacuated by debris flows or fluvial processes in high intensity episodic events (Benda, 2005).

1.1.3 Channel and hillslope contributions to post-fire basin sediment yield

Sediment delivered to the basin outlet may be derived from both hillslopes and the channel network and can be delivered as either bedload or suspended load. Bedload is of interest to geomorphologists, ecologists, and land managers because of its effects on channel morphology and stability (Leopold, 1992), the distribution of habitat patches (Benda et al., 2003), sedimentation (Moody and Martin, 2001b), and flood risk (Stover and Montgomery, 2001) while suspended load affects water quality (Wilkinson et al., 2009) and is often detrimental to fish populations (Newcombe and Macdonald, 1991). Previous studies have arrived at opposite conclusions regarding the dominance of hillslope derived and channel derived sediment. Reneau et al. (2007) found that fine sediment carried in suspension comprised 70% of the total sediment delivered to a downstream reservoir after the 2000 Cerro Grand Fire in New Mexico implying that hillslopes were the dominant source of sediment. In contrast, a study of post-fire erosion in the Colorado Front Range found 80% of basin sediment yield was eroded from the channel network whereas hillslope contributions to sediment yield were negligible following the first summer after burning (Moody and Martin, 2001a). Smith et al. (2011) found that 93% of fine sediment (< 63 μm) eroded from a 136 ha watershed originated on hillslopes, and Wilkinson et al. (2009) found that fire caused a switch in fine sediment(<10 μm) source zones from gully and bank to hillslopes. In a finding similar to Moody and Martin (2001a) and Wilkinson et al. (2009), Owens et al. (2012) concluded that fire increased the volume of sediment sourced from hillslopes, but the channel network remained the dominant source of post-fire sediment. Smith et al. (2011) caution that post-fire erosion and dominant source areas are controlled by variability in post-fire rain events which may activate differing erosion processes, therefore interpretation of results must acknowledge the importance of rainfall characteristics and timing. Consequently, the impact of fire on changes to the source area and relative contribution to sediment yield of different locations within a watershed cannot be predicted a priori (Wilkinson et al., 2009). These findings highlight the need for continued research regarding the contributions of hillslopes and the channel network to total sediment yield and with respect to grain size.

1.1.4 Post-fire recovery and return to background erosion rates

Recovery to background erosion rates post-fire depends on spatial scale. At the hillslope scale ground cover tends to reach 50% by the third or fourth year after burning (Pietraszek, 2006), resulting in erosion rates declining to pre-fire levels in roughly 5 years (Moody and Martin, 2001a; Benavides-Solorio and MacDonald, 2005; Pietraszek, 2006). Post-fire delivery of suspended sediment is immediate and fine sediment travels longer distances than coarse sediment, which may be stored in the channel as bars, overbank deposits, or alluvial fans (Hooke, 2003; Reneau et al., 2007). Suspended sediment loads decrease as hillslopes recover and return to background levels within 5 years, consistent with the time for hillslope recovery (Reneau et al., 2007), while coarse bedload sediment is transported episodically during snowmelt runoff (Reneau et al., 2007) and can persist beyond the 5 year time frame associated with hillslope recovery (Moody and Martin, 2001a; Robichaud et al., 2013b). Moody and Martin (2001a) estimated that 67% of the sediment eroded after a 1996 fire remained in the watersheds after 4 years and had an estimated residence time of greater than 300 years. The depositional features are predicted to remain as legacy sediments until the next major disturbance event (Moody and Martin, 2001a; Moody, 2001).

1.1.5 Connectivity and basin sediment yield

Not all sediment eroded within a basin is transported to the basin outlet (Walling, 1983). The ratio of total sediment eroded in a basin to sediment delivered to the basin outlet is the sediment delivery ratio (SDR), and tends to decrease with increasing area as opportunities for storage increase (Schumm, 1977; Walling, 1983). Lane et al. (1997) found a tendency for unit-area sediment yields to decrease with increasing contributing area. Sediment may be stored on hillslopes, in-channel bars, alluvial fans, and floodplains (Fryirs et al., 2007a; Meyer and Wells, 1997; May and Greswell, 2004; Walling, 1983). Understanding water and sediment flux at the watershed scale has been noted as a challenging problem in geomorphology (Baartman et al., 2013). Brierly et al. (2006) suggest that the SDR is a measure of sediment connectivity in a basin and any assessment of depositional sequences or sediment yield at the basin outlet must include an assessment of sediment connectivity. Connectivity is defined by Fryirs (2013) as the water-mediated transfer of sediment between two landscape compartments and can be assessed within hillslopes, between hillslopes and channels, and along channels (Harvey, 2002). It may also be conceptualized as the likelihood for the effects of a disturbance to be propagated through a basin (Brierly et al., 2006). Sediment connectivity may exhibit a threshold response, certain events may connect, or switch on previously unconnected parts of the basin (Fryirs et al., 2007b). The magnitude of the driving force therefore increases or decreases the effective catchment area similar to the variable source area concept (Graf, 1988). Post-fire hillslope sediment yield, or sediment eroded from the channel network, cannot be assumed to be delivered to downstream targets due to lateral (in the case of hillslopes) and longitudinal (in the case of channels) impediments to transport. Similarly, sediment measured at the basin outlet cannot be used to calculate unit area erosion rates because not all areas within a basin produce equal amounts of sediment, nor are all areas equally connected to the basin outlet. Furthermore, hillslope-channel connectivity controls channel morphology because it mediates the delivery of coarse sediment to the channel network (Harvey, 1991). Assessing connectivity is therefore critical to interpreting basin sediment yields, predicting basin sediment yields, and evaluating high risk areas for post-fire erosion mitigation treatments.

1.2 Research Objectives and Hypotheses

This study examines two small basins in the High Park Fire burn area to evaluate post-fire channel response. In addition, how rainfall, basin, and channel characteristics control the direction and magnitude of that response is assessed.

1.2.1 Objective 1: evaluate controls on channel response

Repeat cross section and longitudinal profile surveys were used to evaluate the direction and magnitude of channel response to rain events. Longitudinal profile surveys provide a contiguous record along the channel network capable of identifying reaches of aggradation and degradation not captured by cross section surveys. Identifying how rainfall, contributing area, and channel characteristics control the direction and magnitude of post-fire channel response will enable better prediction of basin scale sediment yield by providing data on sediment production and storage within the channel network. To this end, research hypotheses are as follows:

H1 – Aggradational response reaches correspond with low channel slope, whereas degradational reaches correspond to high channel slope.

H2 – Channel slope*contributing area product will predict the direction and magnitude of channel response.

H3 – MI_{30} is positively correlated with the magnitude of channel response.

1.2.2 Objective 2: evaluate the influence of mulch on channel response

Mulching immediately increases ground cover and reduces runoff and sediment generation at the hillslope scale (Wagenbrenner et al., 2006; Robichaud et al., 2013a; Robichaud et al., 2013b; Schmeer, 2014). How these reductions in runoff and sediment production affect channel response on the small basin scale have not been addressed, however. Comparing a mulched and unmulched sub-basin enables evaluation of the influence of mulch on channel response.

H4 --The magnitude of channel response in the unmulched sub-basin will be greater than the magnitude of response in the mulched basin.

1.3 Study Area

The High Park Fire burned 354 km^2 of forested land in the Arapahoe Roosevelt National Forest, west of Fort Collins, CO in June and July 2012 (BAER 2012). Burn severity within the fire perimeter was variable and included unburned (56.95 km^2), low severity (130.7 km^2), moderate severity (143.2 km^2) and high severity (23.12 km^2) areas (Figure 3).

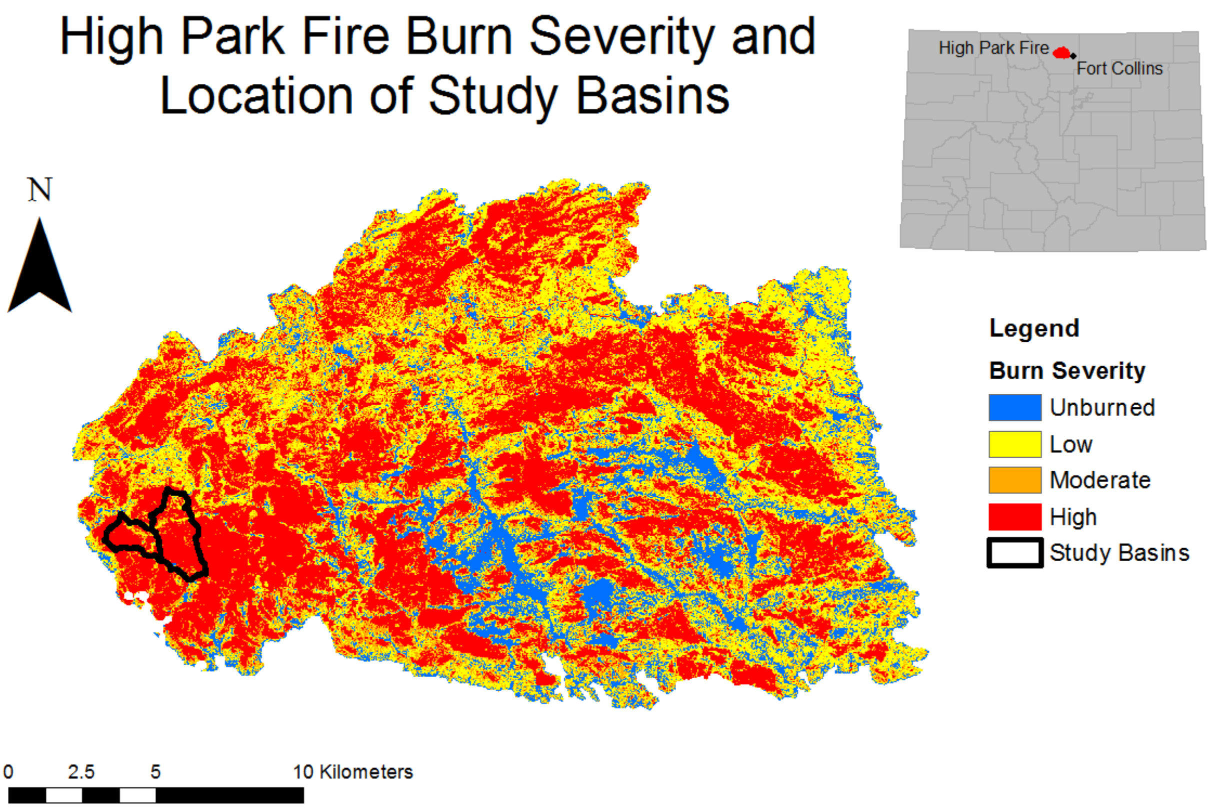

Figure 3: High Park Fire burn severity and location of study basins outlined in black (Stone, 2014, unpublished data).

The fire was located in the Cache la Poudre watershed, a vital natural and socioeconomic resource for several Front Range communities. Two small watersheds, herein referred to as Woodpecker Woods (WPW) and Rocky Top (RT), located at the western extent of the fire were selected in November 2012 for study (Figures 3 and 4). The watersheds were chosen for their accessibility (the

Old Flowers Road bisects each study basin), proximity to one another, similar burn severity and aspect, and observations that small drainages tributary to the South Fork Cache la Poudre were significant sources of sediment post-fire. Both study basins were dominated by a high burn severity (Table 2 and Appendix B).

Table 2: Burn severity area (km^2) in Woodpecker Woods and Rocky Top.

	WPW area (km^2)	WPW area (%)	RT area (km^2)	RT area (%)
Unburned	0.01	0.01	0.03	0.01
Low	0.13	0.08	0.21	0.06
Moderate	0.24	0.15	0.45	0.14
High	1.18	0.76	2.64	0.79

Both watersheds are tributary to the South Fork Cache la Poudre River approximately 20 km upstream of the confluence with the main stem Cache la Poudre River. Woodpecker Woods has an area of 1.56 km^2 and ranges from 2390 m to 2860 m in elevation. Rocky Top encompasses an area of 3.33 km^2 and ranges in elevation from 2340 m to 3030 m (Figure 4). Both watersheds are located in the upper montane zone, characterized by ponderosa pine (*Pinus ponderosa*), lodgepole pine (*Pinus contorta*), Quaking aspen (*Populus tremuloides*), and Douglas fir (*Pseudotsuga menziesii*). The fire regime in the upper montane zone is characterized by variable severity, with characteristics of the low-magnitude high-frequency fire regime of lower elevation regions and the high-magnitude low-frequency stand replacing fires of higher elevation communities, and is capable of supporting stand replacing crown fires and surface fires, creating a mosaic of tree species and cohort ages (Veblen et al., 2012). Within the montane zone elevation is the primary predictor of fire regime (Veblen et al., 2012). Charcoal samples analyzed by radiocarbon dating suggest a fire history dating back 40,000 years (S. Rathburn, unpublished data). Lithology in both study basins is characterized by Precambrian crystalline rocks

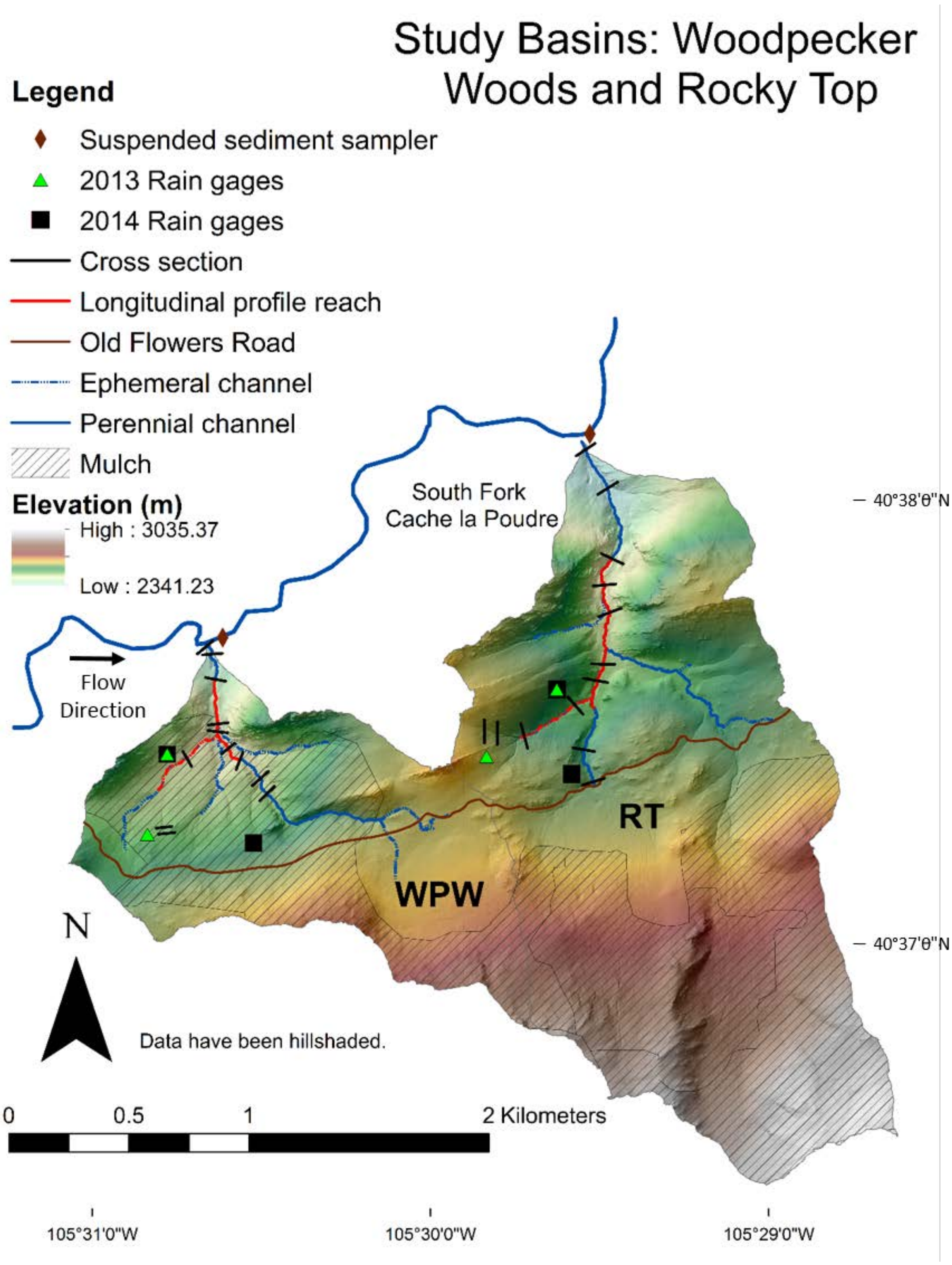

Figure 4: Study basins Woodpecker Woods (WPW) and Rocky Top (RT) and locations of mulching, cross sections, rain gages, and longitudinal profile surveys.

including schist, quartz monzonite, and gneiss (Abbot, 1976; Braddock and LaFountain, 1988; Nesse and Braddock, 1989; Shaver et al., 1988). Mulch was applied in both study basins, but a sub-basin in RT was left unmulched as a control basin in order to test the influence of mulch on channel response. Precipitation across the Cache la Poudre watershed varies with elevation. Values for annual precipitation range from 330 mm at lower elevations to 1350 mm at the highest elevations. The mean precipitation for the basin is 540 mm (Richer, 2009). Average annual precipitation in the study basins ranges from 450 mm at lower elevations to 625 mm at higher elevations (Richer, 2009). Precipitation falls as snow during the winter months and is characterized by brief-duration high-intensity convective thunderstorms in the summer months (Benavides-Solorio and MacDonald, 2005; Veblen and Donnegan, 2005). Table 3 shows the recurrence interval for the average maximum 30 minute intensity (MI_{30}) and depth for a 60 minute storm for the two study basins.

Table 3: Recurrence interval for MI_{30} and 60 minute storm depth for study basins (NOAA Atlas 14).

Recurrence interval	MI_{30} (mm hr^{-1})	Depth for 60 minute storm (mm)
1 yr	25.20	15.67
2 yr	30.48	18.67
5 yr	40.89	24.66
10 yr	50.55	30.73

1.3.1 Cross section locations

Cross sections along the main stem perennial channel and one ephemeral tributary were selected for survey within each study basin (Figure 4). Along the perennial channel in each basin, cross sections were selected in order to maximize variability of potential controls on channel response. In order to test the influence of mulch on channel response, three cross sections were selected in a mulched and unmulched sub-basin within WPW (unmulched) and RT (mulched) based on similarity of geomorphic processes. Two of the three cross sections were established in swales and one in an ephemeral channel. Cross sections were named by basin location (i.e. WPW or RT), followed by XS (cross section), a number, and finally *p* or *e* or *s*, in order to differentiate between cross sections along the perennial reach, ephemeral reach or swale (e.g. WPW XS 4p, Woodpecker Woods, cross section 4, perennial reach). Figure 5 shows the location of cross sections along the longitudinal profile of each perennial reach.

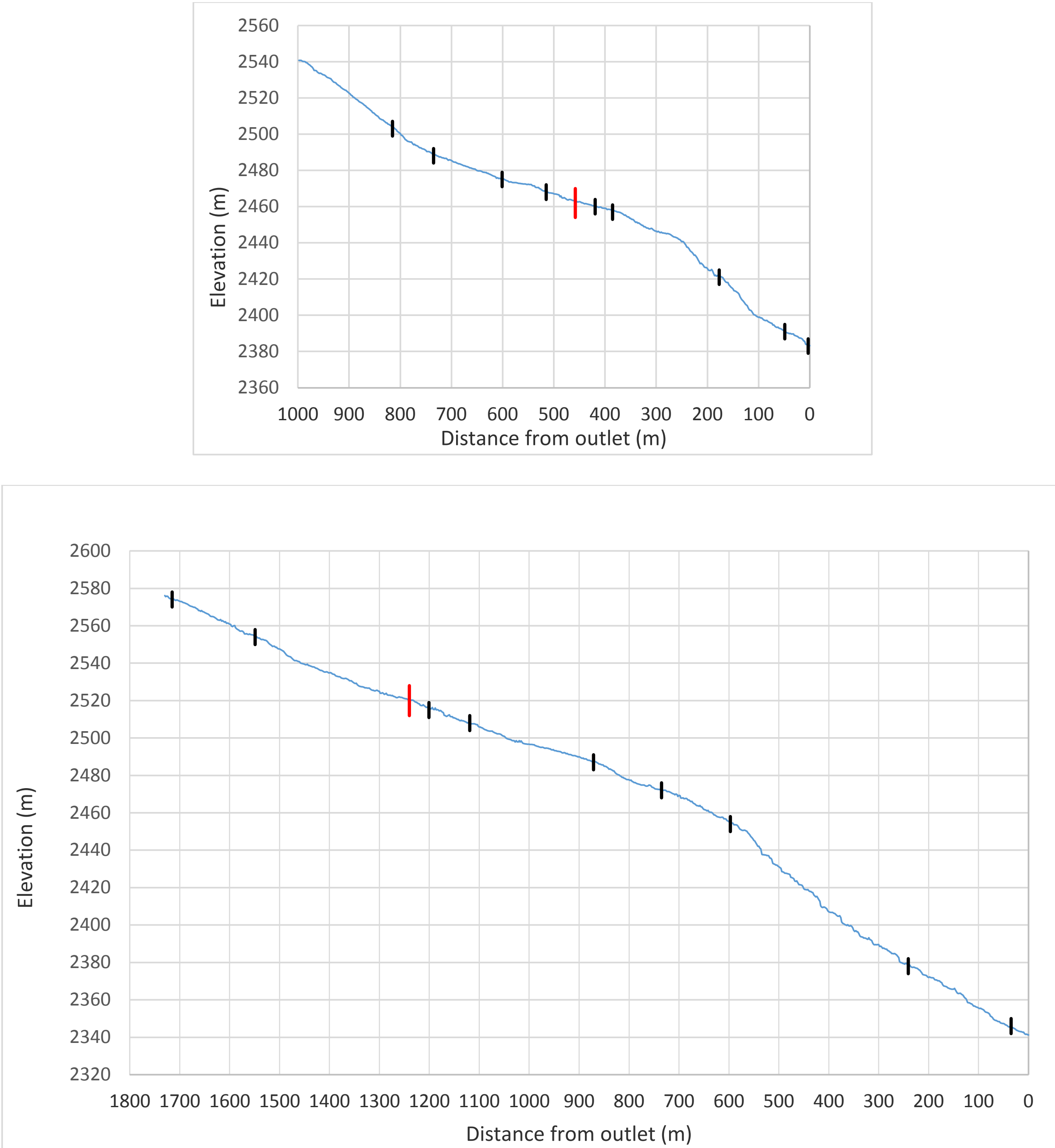

Figure 5: Longitudinal profiles in WPW (top) and RT (bottom). Locations of cross section are marked in black, confluence with the ephemeral reach in red. Figures differ in size in order to maintain consistency in scale.

Table 4: Cross section contributing area, slope, width: depth ratio and initial survey date. An * indicates presence of a scour chain.

Cross Section	Contributing Area (km^2)	Channel Slope	Width to Depth ratio	Initial Survey date
WPW XS 1s	0.005	0.25	18.4	July 2013
WPW XS 2s	0.010	0.22	11.6	July 2013
WPW XS 3e*	0.264	0.06	11.3	July 2013
WPW XS 4p	0.678	0.20	11.0	June 2014
WPW XS 5p	0.709	0.14	24.3	June 2014
WPW XS 6p	0.775	0.07	12.4	June 2014
WPW XS 7p	0.783	0.13	4.8	June 2014
WPW XS 8p	1.291	0.08	4.5	June 2014
WPW XS 9p*	1.482	0.08	22.1	June 2014
WPW XS 10p	1.507	0.11	5.9	June 2014
WPW XS 11p*	1.551	0.16	5.6	June 2014
WPW 12p	1.554	0.09	2.8	June 2014
RT XS 1s	0.002	0.32	15.9	July 2013
RT XS 2s	0.023	0.28	9.2	July 2013
RT XS 3e	0.078	0.14	12.2	June 2014
RT XS 4e*	0.166	0.13	36.6	July 2013
RT XS 5p	0.350	0.09	12.6	June 2014
RT XS 6p	0.847	0.12	4.0	June 2014
RT XS 7p	1.109	0.09	7.3	June 2014
RT XS 8p*	1.115	0.07	15.3	June 2014
RT XS 9p	2.795	0.09	6.6	June 2014
RT XS 10p	2.944	0.05	7.4	June 2014
RT XS 11p	2.976	0.15	10.7	June 2014
RT XS 12p	3.131	0.10	9.6	June 2014
RT XS 13p	3.339	0.11	7.3	June 2014

Figure 6: Photographs of cross section variability.
A: Cross section WPW XS 6p (6/25/2014). Approximate slope is 0.07, contributing area is 0.78 km^2.
B: Cross section RT XS 13p (6/24/2014). Approximate slope is 0.11, contributing area is 3.40 km^2.
C: Cross Section WPW XS 8p (7/15/2014). Approximate slope is 0.08, contributing area is 1.29 km^2.
D: Cross Section RT XS 10p (7/15/2014). Approximate slope is 0.05, contributing area is 2.9 km^2.

2. METHODS

The majority of data collected and analyzed for this study was based on traditional field survey methods. However, certain elements such as the sediment connectivity analysis and calculation of many basin metrics relied on a 1 m LiDAR-derived digital elevation model (DEM). The first field surveys were performed in summer 2013, one year after the fire, therefore any changes that occurred during 2012 are undocumented by this study. The study evolved between summer 2013 and summer 2014 based on collected data and field observations. Changes that took place between the 2013 field season and the 2014 field season are described in this section.

A total of six cross sections (3 per basin) were identified for repeat cross section surveys in November 2012 based on similar geomorphic processes, and initial surveys took place in July 2013 (Table 4). In each basin, two of the three cross sections were located in swales, and one in an ephemeral channel. One scour chain per basin, located at the cross section in the ephemeral reach, was installed in July 2013. Field work in summer 2013 could not begin until 7/1/2013 after aerial mulching in the two study basins had been completed. On 7/1/2013, a storm producing 16 mm of precipitation (E. Berryman, pers. communication, 2013) affected the study area. Photographs document significant transport of mulch during the storm as well as the highest discharge in swale and ephemeral channels as evidenced by preserved stage indicators. The initial study design paired one mulched basin (WPW) and one control basin (RT), but field observations in summer 2013 indicated mulch was also applied to the control basin (Figure 4; RT south of Old Flowers Road) and therefore the effects of mulch on channel response can only be assessed within one ephemeral sub-basin.

Data and field observations collected during summer 2013 suggested that changes in geometry in the swales were below the resolution of our survey and thus not included in this analysis. Evidence of significant degradation was observed in the perennial reaches downstream of cross sections surveyed in

2013. Consequently, 18 additional cross sections were surveyed along the perennial channel in June 2014 and monitored on an event basis (Table 4). Initial longitudinal profile surveys were performed in June 2014 and re-surveyed on an event basis. Additional scour chains were installed in June 2014 in both the ephemeral and perennial channels.

2.1 Rainfall

Rainfall was measured using Rainwise tipping bucket rain gages with a resolution of 0.254 mm with data recorded on Campbell CR 10x data loggers. Two rain gages were installed in each basin (Figure 4). Additional cross sections in 2014 required relocating rain gages in order to better characterize rainfall contributing to the newly surveyed cross sections (Figure 4). In 2014 HOBO Pendant Event loggers replaced Campbell CR 10x data loggers for their advantages in installation, maintenance, data collection, and processing.

Rainfall analysis was performed using the Rainfall Intensity Summarization Tool (RIST) developed by the USDA Agricultural Research Service (ARS 2013, http://www.ars.usda.gov/Research/docs.htm?docid=3251). A rainfall event was defined as any event with greater than 2 mm total depth and separated by 1 hour without rainfall (Eccleston, 2008; Pietraszek, 2006). A depth of 2 mm was selected in order to create a data set capable of highlighting storm variability, rather than an assumption that a 2 mm storm was sufficient to generate runoff and sediment. RIST was used to calculate the total depth, duration, maximum 30 minute rainfall intensity (MI_{30}), and rainfall erosivity index (EI_{30}) per storm event. EI_{30} is a measure of the total erosive power of an event and is the product of the MI_{30} and the total energy of the storm where total energy, *E*, is calculated:

$$E = 0.29\,[1 - 0.72^{(-0.05*MI_{30})}] \quad (2.1)$$

Where MI_{30} is in mm hr^{-1}, E, is in MJ ha^{-1} mm^{-1}, and EI_{30} is in MJ mm ha^{-1} hr^{-1}.

In order to perform statistical analyses basin rainfall metrics were averaged for each basin on an event basis.

2.2 At-A-Station: Cross Section Surveys and Scour Chains

Repeat cross section surveys were performed using a hand level and monopod. This methodology was chosen over other traditional survey methods (e.g. Leica Total Station, auto-level, etc.) due to the logistical challenges of carrying such equipment to field sites. It was decided that the precision, accuracy, and repeatability of hand level monopod measurements were adequate for the surveys in question. Repeat cross section surveys indicate that the uncertainty associated with cross sections surveys was < 2 cm. Cross sections were monumented with rebar and extended past all high water indicators to ensure channel change would be captured and were surveyed after each storm event greater than 5 mm. Because of the inability to obtain accurate rainfall data remotely, and the close spacing of some storms, some surveys reflect changes caused by two events.

Cross section area was calculated after every storm event. Net change in cross section area at time *n* was computed as:

$$\Delta A_n = A_{n-1} - A_n \tag{2.2}$$

Net change in area was converted to mean bed elevation change (ΔMBE) after Madej and Ozaki (1996) defined as:

$$\Delta MBE = \Delta A/W \tag{2.3}$$

where ΔA is the difference in cross section area computed between two surveys, and W is bankfull width. Bankfull width was determined in the field based on geomorphic characteristics. Positive values of ΔMBE indicate aggradation and negative values of ΔMBE indicate degradation. Degradation can take place as either channel incision or channel widening. ΔMBE was calculated between all surveys. Change in maximum depth (ΔD) was also calculated between all surveys.

All subsets multiple linear regression model selection was performed in R to determine whether a combination of contributing area, channel slope, channel slope*contributing area, or width to depth ratio (w:d) could predict ΔMBE or ΔD on an event basis. Univariate analysis was performed in R to test the importance of each predictor variable in determining channel response. Data were analyzed on an event basis. Data were analyzed both per basin and in a combined data set. Due to a limited sample size of runoff generating storms, rainfall metrics could not be statistically assessed as predictors of channel response in 2014.

Contributing area, channel slope, and width to depth ratio were assessed by a combination of field surveys and analysis using ArcGIS. Basin delineation, contributing area, and average basin slope were computed using the hydrological toolbox available in ArcGIS. (Basin slopes were not included in the analysis because they were similar for all cross sections, range 15-17 %.) Channel slopes were calculated in ArcGIS based on slope breaks at the reach scale of 10-12 channel widths. Width to depth ratio was based on field surveys.

Scour chains are used to measure maximum scour depth and subsequent deposition resulting from elevated discharges during storm events providing data on channel response not evident in cross section surveys (Laronne et al., 1994; Lisle and Eads, 1991; Nawa and Frissel, 1993). Observations following the 7/1/2013 storm suggested that despite elevated discharge channel geometry remained stable, and that cross section surveys would reveal only minor changes, leading to low estimates of channel sediment production and storage. Scour chains 1 m in length were installed approximately 1 m downstream of the ephemeral cross sections in 2013. In 2014 an additional seven scour chains were installed, two were installed upstream of pre-existing scour chains in the ephemeral channel, four in perennial reaches (two per basin) and one in an alluvial fan in WPW. Scour chains were installed in channel segments with sand and gravel beds due to the challenges associated with installation in bed material dominated by pebbles and cobbles. A storm on 7/12/2014 removed three of the five scour chains in WPW, and two of the four scour chains in RT, which were immediately replaced. One scour chain in WPW was relocated due to a significant deposition of coarse material on the previous site.

2.3 Bed Material

Bed material samples were collected from the ephemeral cross sections in both basins at the beginning and end of the 2013 and 2014 field seasons in order to assess changes in bed material post-fire. Pebble counts were performed at the beginning and end of the 2014 field season at three cross sections along the perennial reach in both basins.

2.4 Suspended Sediment

Automated suspended sediment samplers were installed below the outlet of each study basin (Figure 4) in order to assess the relative fine sediment contribution of each basin, to evaluate the relationship between rainfall and suspended sediment, and to evaluate how rainfall thresholds for fine sediment generation compare to thresholds for coarse sediment generation. Data were processed by Sandra Ryan (US Forest Service Rocky Mountain Research Station) and shared for this analysis. The values used in this analysis were those produced by the general model, rather than the model calibrated to individual storm events, in order to more easily compare values between 2013 and 2014, as well as small storm events for which an individual model calibration was not performed. Because suspended sediment concentration (SSC) was measured below the outlets of both basins it reflects the contribution of both a given study basin and all upstream areas, therefore analysis is limited to demonstrating large scale patterns and relationships rather than establishing a quantitative relationship between rainfall and SSC. All analyses performed in this study refer to the maximum SSC for a given event, referred to hereafter as SSC.

2.5 Ground Cover

Ground cover surveys were performed in mid-July during 2013 and 2014 to assess differences in ground cover between WPW and RT as well as monitor changes between 2013 and 2014. Transects 50 m in length were established every 50 m along the ephemeral channel, and ground cover was surveyed at 1 m intervals along each transect. This resulted in 50 points per transect, for a total of 450 points in WPW and 500 points in RT. Ground cover was classified as rock, bare soil, ash, live vegetation, organics, mulch, charcoal, or wood. Because ground cover was surveyed in the ephemeral sub-basin, which experienced the greatest differences in burn severity (Figure 29, Appendix B), results from the survey should not be used to infer differences between the two study basins. The results of the ground cover survey are reported in Appendix B.

2.6 Longitudinal Profile Surveys

Longitudinal profile surveys were performed using a Topcon GR-5 Real Time Kinematic Global Positioning System (RTK-GPS). Reaches were selected for repeat longitudinal profile survey based on field observations that indicated a responsive channel segment. Bedrock and steep cascade reaches were assumed to be resistant to change and avoided. This resulted in a longitudinal profile of approximately 400 m in WPW, and approximately 800 m in RT. Static data collected by the base station were processed using the free online software OPUS (Online Positioning User Service) provided by National Geodetic Survey (http://www.ngs.noaa.gov/OPUS/) and used to correct daily survey data in order to align repeat longitudinal profiles. The average root mean square error (RMS) associated with the base station was 1.5 cm for summer 2014. Data on survey specific RMS were not obtained during this study, but previous studies using an RTK-GPS have found maximum horizontal root mean square error of 0.05 m and vertical root mean square of 0.08 m (Brogan, 2014).

Longitudinal profiles were aligned by converting Cartesian coordinates to a channel fitted coordinate system (Smith and McLean, 1984) using a procedure developed by Legleieter and Kyriakidis (2007). Reaches were defined by slope breaks in order to test the hypothesis that low slope areas correspond with areas of aggradation and high slope areas with degradation, and labeled according to basin location, location within the drainage network, and flow regime. Reach lengths varied between the two basins. In general, reach lengths were longer in RT due to a longer available channel profile. Reach characteristics are described in Appendix F. Longitudinal profiles were assessed visually in order to determine slope breaks, identify erosional and depositional areas, and mechanisms of degradation (e.g. headward migration of knickpoints). Quantitative analysis was performed by calculating the difference in area between consecutive profiles and dividing by reach length in order to calculate mean thalweg elevation change (ΔMTE) between surveys. All reaches were characterized by bedforms including plane-bed, step-pool, and cascade, and all three bedforms were often found within a single study reach. Post-fire channel adjustments in 2012 and 2013 also formed numerous knickpoints throughout each study reach.

2.7 Sediment Connectivity Analysis

A sediment connectivity analysis was performed in ArcGIS using the method proposed by Borselli et al. (2008) and modified by Cavalli et al. (2013). The connectivity model developed by Borselli et al. (2008) integrates characteristics of the upslope contributing area with downslope flowpath characteristics in order to calculate an index of connectivity (IC) which describes the likelihood of sediment from a given location being delivered to a pre-defined target. In this study, the target chosen was the basin outlet. Cavalli et al. (2013) modified the original model by making topographic roughness, rather than vegetation, the dominant control on sediment connectivity. The analysis was performed as a first order approximation of basin scale sediment connectivity, to compare sediment connectivity between the two basins, and to evaluate if field data and observations could corroborate the results of the ArcGIS model. This analysis was undertaken following the 2014 field season to provide additional information useful to interpreting the results of cross section and longitudinal profile surveys which revealed a channel largely resistant to changes in morphology. Quantitative model results are reported as qualitative high-low values.

2.8 Flow Depth

Sonic and radar depth sensors were installed in order to monitor stage response to rain events of different depths and intensities. Sensors were mounted on a 0.5” stainless steel pipe mounted between two t-posts that spanned the width of the channel. Due to data loss resulting from storage capacity limitations of the Campbell CR 10x data loggers, battery failures that went unnoticed, unexplained errors in the observed data, and limited runoff-generating events in 2014, the data set provided by the depth sensors is limited. Despite these limitations, results from the depth sensor mounted at WPW XS 3e provide valuable insight into runoff generating precipitation thresholds that may have important consequences for channel response and are therefore included in Appendix A of this report.

2.9 September 2013 event

In September 2013, a 200-500 year rain storm took place over the Colorado Front Range (NOAA-NWS, 2013), herein referred to as the September 2013 event. Seven days of rain occurred from September 9-15, 2003 in an area of approximately 3400 km^2. Record-breaking cumulative rainfall, especially in Boulder County (429 mm over the 7 day period) (Lukas et al., 2013), caused extensive flooding and debris flows. Despite cumulative rainfall between 169 -180 mm, minimal changes were observed in the 2013 study area. Extensive channel degradation was observed downstream of the ephemeral reaches established in summer 2013, however. The influence of the September 2013 event is discussed in Chapter 4.

3. RESULTS

3.1 Rainfall

In summer 2013, six storms exceeded the MI_{30} and depth thresholds associated with hillslope sediment production in WPW and RT. Figure 7 shows the basin-averaged depth and MI_{30} in both study basins for all storms. A total depth threshold of 8 mm hr^{-1} was observed in summer 2013 by Schmeer (2014) as required in order to generate hillslope sediments following the High Park fire.

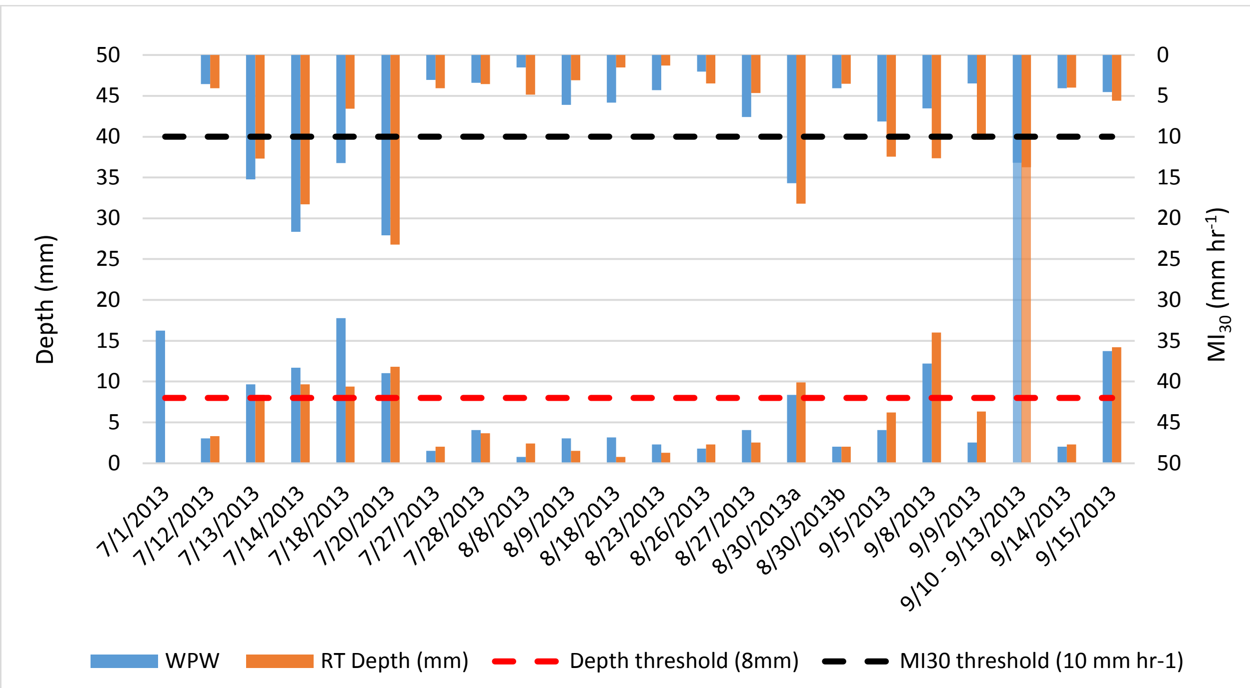

Figure 7: 2013 basin-averaged rain depth and MI_{30} for all storms in WPW and RT. Six storms exceeded threshold values of MI_{30} and total depth associated with hillslope sediment production in each basin. Values reported for the 7/1/2013 storm are courtesy of E. Berryman, pers. communication (2013). MI_{30} values were not available for the 7/1/2013 storm. The depth totals for the period of 9/10 – 9/13/2013 cannot be displayed on this graph, and were 166.1mm and 152.7mm in WPW and RT, respectively.

During summer 2014 two storms exceeded the MI_{30} of 10 mm hr^{-1} threshold for hillslope sediment production (Figure 8). Channel response results are therefore limited to changes that took place following the 7/12/2014 and 7/29/2014 storms. Surveys were performed after other storms, but photographic evidence indicates that no change took place and calculated differences from surveying were minimal. A complete record of rainfall metrics for 2013 and 2014 are reported in Appendix C.

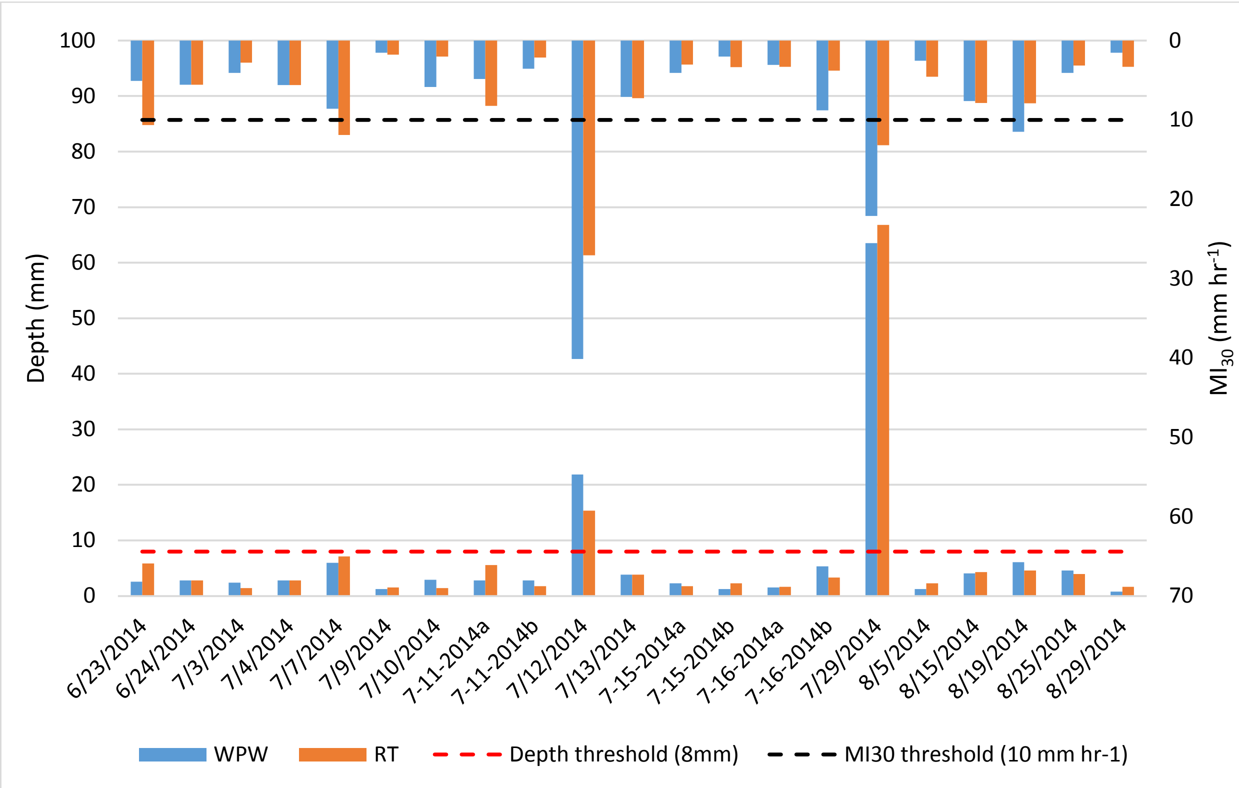

Figure 8: 2014 basin-averaged rain depth and MI_{30} per storm for WPW and RT. Two storms exceeded threshold MI_{30} values in each basin during summer 2014. Note: scales of Figure 7 and Figure 8 are not equal, however threshold values are the same. Threshold values increase as hillslopes recover after fire, so this is a conservative approach.

3.2 At-A-Station: Cross Section Change, Scour Chains, and Bed Material

At-a-station results for 2013 include repeat surveys from one ephemeral cross section and one scour chain in each basin. Results from 2014 include data from the 2013 cross sections as well 18 additional cross sections in the perennial reach.

3.2.1 Ephemeral cross section, scour chain, and bed material

Channel response in 2013, measured by ΔMBE and ΔD, was variable in both basins, alternating between net aggradation and net degradation, and < |3| cm for all events. In WPW, ΔD > ΔMBE for three of the five events and ΔMBE < ΔD for two of the five storms. Scour or fill quantities exceeded values for ΔMBE in three of the five events, and ΔD in one storm (Table 5). In RT, ΔMBE < |2| cm for all storms. ΔD exceeded ΔMBE for three of the five events. Scour or fill values exceeded ΔMBE for four of the five events. There is no significant relationship between rainfall depth, MI_{30}, or EI_{30} and ΔMBE, ΔD, or scour and fill at either location in 2013 or 2014. However, the data suggest that higher values of MI_{30} may promote aggradation and the lack of statistical significance may be the result of a small sample size.

The two rain events in 2014 caused opposite responses in both cross sections. As in 2013, the higher MI_{30} caused net aggradation while the lower MI_{30} resulted in net degradation. Comparing results from the two summers indicates that a much higher MI_{30} was required in 2014 to cause the same response measured in 2013. Despite low absolute values of channel response, repeat photographs clearly demonstrate the channel is a source and sink for sediment on an event basis (Figure 9).

Table 5: 2013 and 2014 ΔMBE, ΔD, scour and fill at WPW XS 3e and WPW SC 2e. A range of values indicates that the burial depth of the scour tapered from 0 at the end to the maximum value at the elbow.

Storm Date	MI_{30} (mm hr^{-1})	ΔMBE (cm)	ΔD (cm)	Scour (cm)	Fill (cm)
7/13/2013	15.2	-1.5	-2	0	0.5
7/14/2013	21.7	2.8	7	2.5	3.5
7/18/2013	13.2	-1.5	-1	NA	NA
7/20/2013	22.1	1.2	0	4.5	5
9/10/2013	13.2	-1.7	-7	6	3
7/12/2014	40.1	2.6	4	2	4.5
7/29/2014	22.1	-0.55	-7	6	0-2

Table 6: 2013 and 2014 ΔMBE, ΔD, scour and fill at RT XS 4e and RT SC 2e. An * indicates presence of running water in the channel during the time of measurement.

Storm Date	MI_{30} (mm hr^{-1})	ΔMBE (cm)	ΔD (cm)	Scour (cm)	Fill (cm)
7/13/2013	12.7	0.5	0	3	2
7/14/2013	18.3	-1.0	-2	9	6
7/18/2013	6.6	-0.1	0	NA	NA
7/20/2013	23.2	1.7	3	0	2
9/10/2013	13.7	1.7	-6	8.5	0*
7/12/2014	27.1	1.3	1.5	0	3-6.5
7/29/2014	13.2	-0.8	-1	0	0

Bed material coarsened at WPW XS 3e during 2013 and 2014, while at RT XS 4e coarsening occurred during 2013 but bed material remained similar over the 2014 field season (Table 7). Figure 9 highlights the importance of the timing of bed material sampling in interpreting post-fire bed material and grain size trends through time.

Table 7: Changes in bed material at WPW XS 3e and RT XS 4e illustrated by contrasting the fraction of each grain size class per sample during 2 sampling dates in 2013 and 2014.

WPW	7/12/2013	10/13/2013	7/2/2014	10/16/2014
Grain size (mm)				
<2	0.87	0.55	0.58	0.46
2-4	0.10	0.14	0.08	0.10
>4	0.04	0.32	0.33	0.44
RT				
<2	0.84	0.40	0.55	0.53
2-4	0.11	0.12	0.10	0.07
>4	0.05	0.48	0.35	0.40

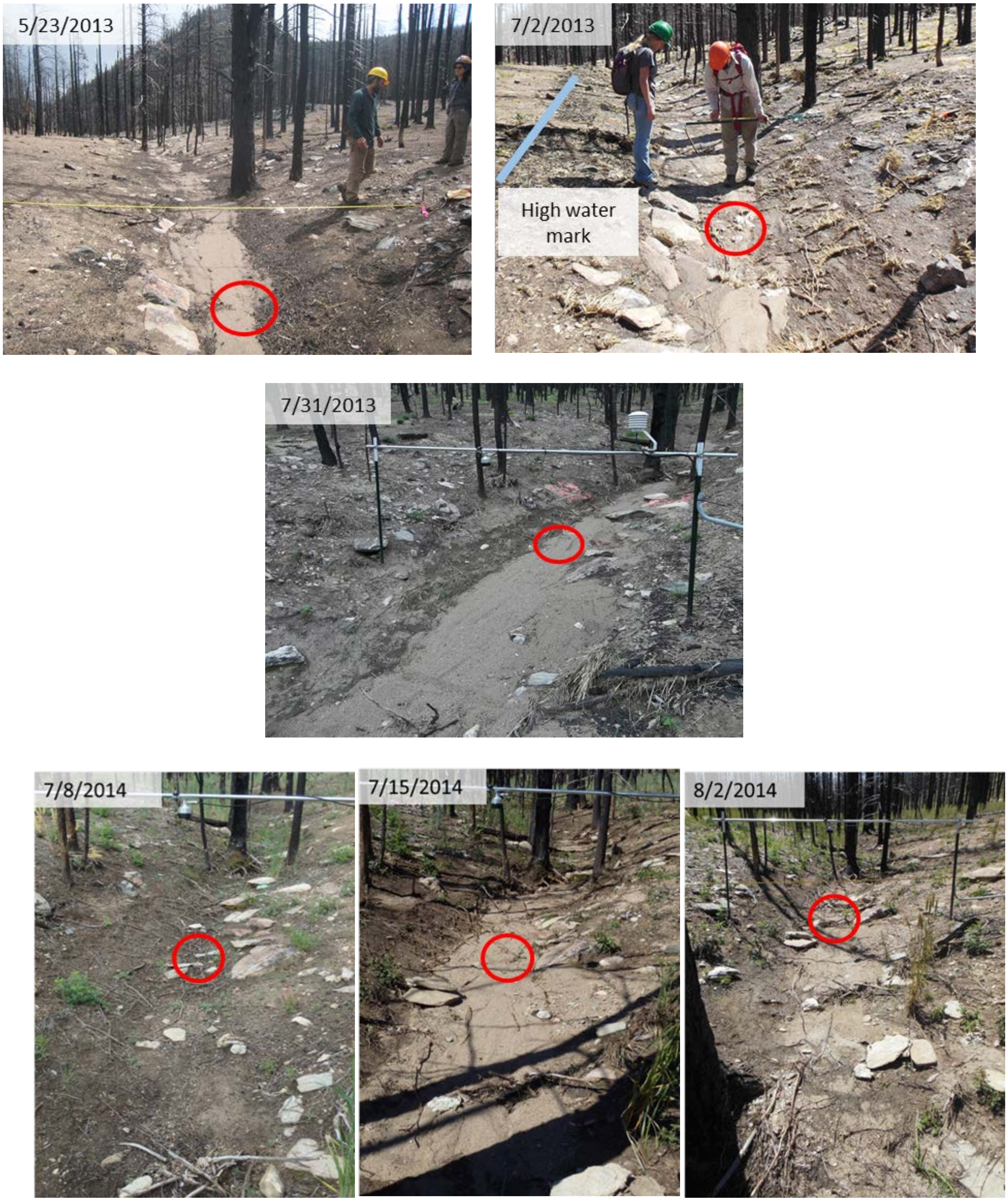

Figure 9: Repeat photographs of WPW XS 3e that illustrate the ephemeral channel is a temporary source and sink for sediment by alternating response between degradation and aggradation. Despite statistical insignificance, the direction of response appears to correspond to MI_{30}. The red circle in the photographs indicates a common bed location.

3.2.2 2014 perennial cross sections

Despite clear signs of significant previous degradation in perennial channels in both basins, ΔMBE and ΔD were limited in 2014. The range of ΔMBE values from both storms was -20 to +17 cm, but the majority of cross sections experienced absolute ΔMBE on the order of 0-3 cm per event (Table 7). Multiple linear regression analysis as well as univariate analysis revealed no significant relationships between the predictor variables channel slope, channel slope*contributing area, contributing area, and w:d to ΔMBE or ΔD. P-values for all tests are reported in Appendix D.

Table 8: ΔMBE and ΔD in perennial cross sections for 7/12/2014 and 7/29/2014 storms. Multiple linear regression and univariate analysis revealed no significant relationships between predictor and response variables.

Cross Section	Area (km^2)	Channel Slope	Ch. slope* cont. area	ΔMBE (cm) 7/12/2014	ΔMBE (cm) 7/29/2014	ΔD (cm) 7/12/2014	ΔD (cm) 7/29/2014
WPW XS 4p	0.678	0.20	0.13	0.90	0.53	2	1
WPW XS 5p	0.709	0.14	0.10	1.73	-0.02	2	1.5
WPW XS 6p	0.775	0.07	0.06	0.54	0.24	-2	1
WPW XS 7p	0.783	0.13	0.10	0.15	-0.69	7.5	-1
WPW XS 8p	1.291	0.08	0.10	-20.20	-13.59	-24.5	-22.5
WPW XS 9p	1.482	0.08	0.12	-9.30	-0.66	-14	-1.5
WPW XS 10p	1.507	0.11	0.17	1.03	-1.40	4	0
WPW XS 11p	1.551	0.16	0.25	2.69	-5.24	-6	2.5
WPW 12p	1.554	0.09	0.13	-12.30	2.43	-36	8
RT XS 5p	0.350	0.09	0.03	2.21	-0.92	5	-2.5
RT XS 6p	0.847	0.12	0.10	1.26	-1.07	0	-1
RT XS 7p	1.109	0.09	0.10	-3.32	-4.61	7.5	-0.5
RT XS 8p	1.115	0.07	0.07	3.87	0.01	3.5	-0.5
RT XS 9p	2.795	0.09	0.24	-6.90	-1.39	-11	1.5
RT XS 10p	2.944	0.05	0.13	12.65	0.03	28	3
RT XS 11p	2.976	0.15	0.45	-0.63	2.02	-19	2.5
RT XS 12p	3.131	0.10	0.31	-2.93	-0.13	-23.5	1.5
RT XS 13p	3.339	0.11	0.38	16.90	-2.60	31	-6

3.2.3 2014 Scour chains

Scour chain response showed high variability between storms, basins, and flow regime. Five of nine scour chains were lost during the 7/12/2014 storm, including all scour chains installed in the perennial channel. Estimates of scour were based on the known depth of the scour chain and the assumption that the chain was capable of being removed when only 10 cm remained buried. The estimates are likely conservative because scour beyond that required to remove the scour chains could have occurred and is not reflected in the estimate. Because the scour chain measurements were not linked to a permanent datum, deposition could not be calculated for the 7/12/2014 event. Responses included (1) scour > deposition (2) scour = deposition (3) scour < deposition. There is no significant relationship between the depth of scour and fill and channel slope or rainfall characteristics. The greatest scour was observed at WPW SC 3e located in a small alluvial fan at the confluence between the ephemeral reach and the perennial reach.

Table 9: Scour chain results after 7/12/2014 and 7/29/2014. An* indicates scour chain was lost during event. At WPW SC 5p deposition of coarse material at the scour chain site prevented an estimate of scour.

Scour Chain	Contributing Area (km^2)	Channel Slope	Ch.slope* cont. area	7/12/2014 Scour (cm)	Fill (cm)	7/29/2014 Scour (cm)	Fill (cm)
WPW SC 1e	0.23	0.03	0.008	11	0-1.5	2.5	0
WPW SC 2e	0.26	0.06	0.016	2	4.5	6	0-2
WPW SC 3e	0.30	0.12	0.036	35*	NA*	0.5	0
WPW SC 4p	1.48	0.08	0.124	13*	NA*	9	7-10
WPW SC 5p	1.55	0.16	0.249	NA*	NA*	12	0
RT SC 1e	0.12	0.08	0.010	0	3-8.5	0	0
RT SC 2e	0.17	0.13	0.022	0	3-6.5	0	0
RT SC 3p	1.11	0.07	0.075	15*	NA*	0.05	0.02
RT SC 4p	2.73	0.08	0.205	24*	NA*	0.21	0.11

3.2.4 Perennial channel bed material

Pebble counts at three perennial cross sections in each basin at the beginning and end of the 2014 field season show that bed material 1) coarsened, 2) fined, and 3) remained the same at different cross sections in summer 2014 (Table 10).

Table 10: Changes in D_{50} and D_{84} at 6 cross sections in WPW and RT.

WPW Cross Section		Date 7/7/2014	10/16/2014	RT Cross Section		Date 7/7/2014	10/16/2014
XS 9p	D_{50}	2	7.7	XS 8p	D_{50}	5.1	5.3
	D_{84}	6.6	32		D_{84}	18.2	22.5
XS 10p	D_{50}	10.7	12.5	XS 10p	D_{50}	2	10.4
	D_{84}	128	45		D_{84}	3.9	104.3
XS 11p	D_{50}	15.5	6.7	XS 12p	D_{50}	14.9	33.6
	D_{84}	57.7	41.8		D_{84}	45	138.4

3.3 Suspended Sediment

3.3.1 2013 results

Suspended sediment concentrations (SSC) in 2013 were generally correlated with MI_{30} (Figure 10, Appendix E). All storms with MI_{30} >10 mm hr^{-1} resulted in SSC values > 2500 mg L^{-1}. Storms where MI_{30} ranged between 5-10 mm hr^{-1} were capable of producing SSC levels between 500-1500 mg L^{-1}. It is important to note that the SSC levels recorded near the RT outlet are a function of both rainfall characteristics in the RT basin as well as delivery from upstream, including the delivery from WPW, and therefore it should not be implied that a MI_{30} of 3.1 mm hr^{-1} generated a SSC level of 419 mg L^{-1} (Appendix E). Dam releases from small irrigation reservoirs upstream from the study sites that caused significant increases in stage do not correspond to increases in SSC, suggesting that hillslopes are the dominant source of fine sediment (Appendix E). In three events, SSC decreased downstream, suggesting that the rain event caused hillslope sediment production in WPW but not RT. Other storms are indicated by a sharp spike below RT and little increase below WPW suggesting the rain event generated sediment production in RT but little in WPW. The variable direction of SSC in the downstream direction highlights the importance of high spatial variability in rainfall.

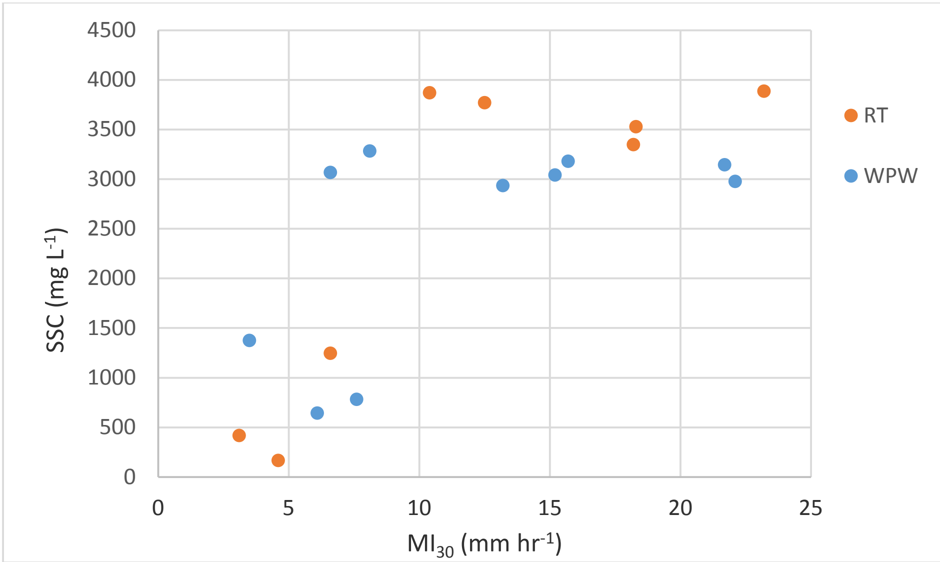

Figure 10: 2013 SSC as a function of MI_{30} in WPW and RT. All storms greater with MI_{30} > 10 mm hr^{-1} generated SSC values greater than 2500 mg L^{-1}. Increases in SSC due to upstream dam releases are not included in this figure.

3.3.2 2014 results

In 2014 higher MI_{30} values were required to produce SSC comparable to values observed in 2013 (Figure 11, Figure 12, Appendix E). SSC exceeded 1500 mg L^{-1} only once, when MI_{30} = 27.1 mm hr^{-1}. An event where MI_{30} reached 40.1 mm hr^{-1} was not enough to cause SSC to exceed 1500 mg L^{-1} at the outlet of WPW (Figure 11 and Appendix E). Decreases in SSC between WPW and RT correspond with MI_{30} values in each basin. When MI_{30} was 5-10 mm hr^{-1}, SSC did not exceed 500 mg L^{-1}. Dam releases during 2014 provide additional data demonstrating that increases in stage height are not the cause of increased SSC as the two greatest increases in stage were not correlated with a correspondingly large increase in SSC (Figure 13, Appendix E).

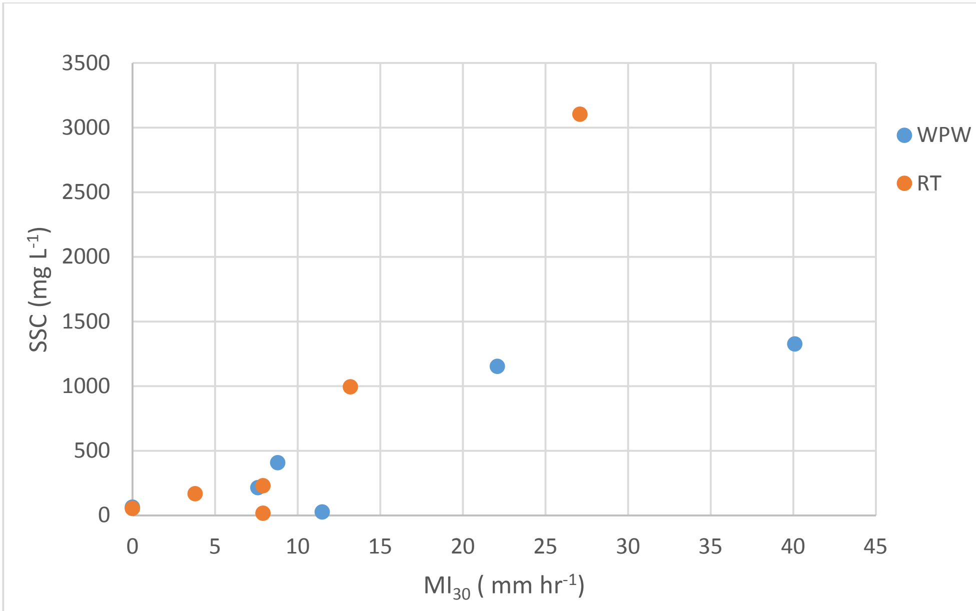

Figure 11: 2014 SSC as a function of MI$_{30}$ in WPW and RT. Fewer runoff generating events, as well as lower SSC values illustrate the difference in rain event frequency and intensities between 2013 and 2014, as well as indicating hillslope recovery. SSC values recorded at near both basin outlets exceeded 1500 mg L^{-1} only once in 2014, compared to 12 times in 2013.

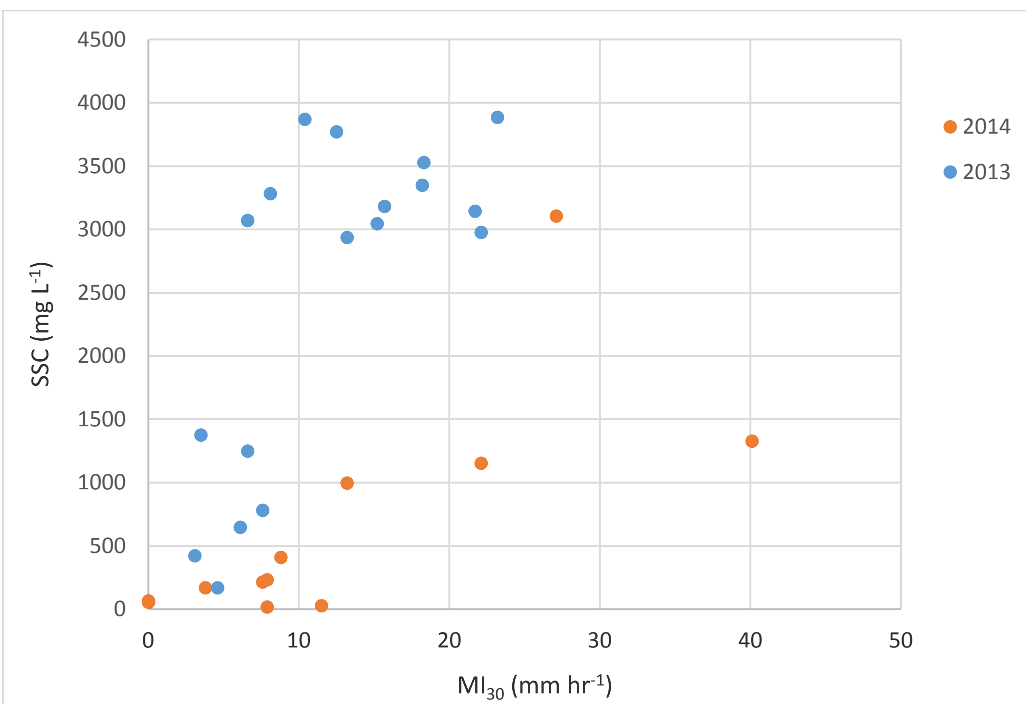

Figure 12: Comparison of MI$_{30}$ and SSC in 2013 and 2014 based on data collected at the outlet of both study basins. The results suggest that as hillslopes recovered greater MI$_{30}$ was required in 2014 to cause SSC levels observed in 2013.

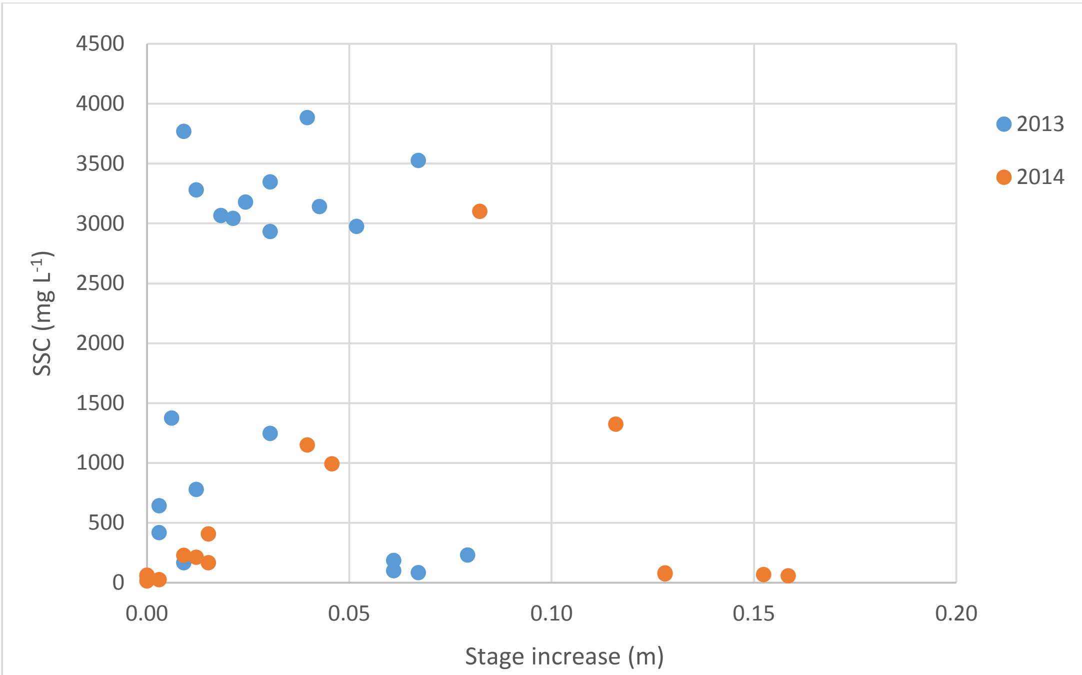

Figure 13: SSC as a function of stage in 2013 and 2014 for the South Fork Cache la Poudre River. Maximum rises in stage due to upstream dam releases caused very low increases in SSC. All stage increases greater than 0.06 m and with SSC less than 500 mg L^{-1} are the result of upstream dam releases.

3.4 2014 Longitudinal Profile Surveys

Longitudinal profiles indicate a largely stable channel in summer 2014. Mean thalweg elevation change (ΔMTE) for both storms and all reaches ranged from -9 cm to +5 cm (Figure 14). Among the perennial reaches five of the eight experienced the same direction of response for both storms (Table 11). Logistical problems prevented surveying of the ephemeral channels after the 7/12/2014 storm, therefore the survey on 8/5/2014 represents the cumulative effect of the 7/12/2014 and 7/29/2014 storms. A univariate analysis showed slope could not be used to predict ΔMTE in the perennial reaches when data were analyzed per storm (p-value = 0.74) or when data from both storms were combined (p-value = 0.49). Statistical analysis was not performed for the ephemeral channels due to the inability to distinguish between the effects of two storms. Figure 15 shows a scatterplot of slope vs ΔMTE for both storms.

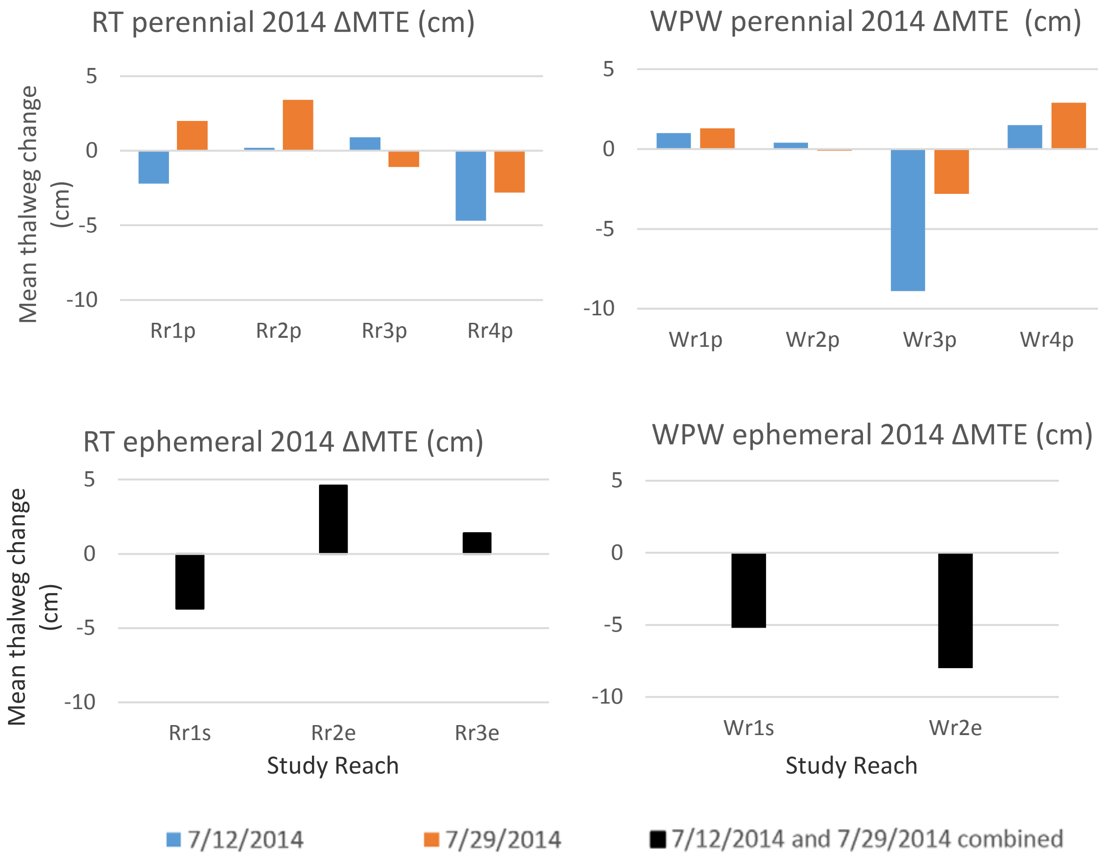

Figure 14: Mean thalweg elevation change (cm) for WPW and RT study reaches.

Table 11: Differences in response by study reach to the two 2014 rain events. *High MI_{30}* refers to the 7/12/2014 rain event, *Low MI_{30}* refers to the 7/29/2014 rain event. *A* signifies aggradation, *D* signifies degradation, *NR* signifies no response. A "+" or "-" in the second column indicates how the magnitude of response differs between storms when the direction is the same.

	High MI_{30}	Low MI_{30}
Wr1p	A	A+
Wr2p	A	NR
Wr3p	D	D-
Wr4p	A	A+
Rr1p	D	A
Rr2p	A	A+
Rr3p	A	D
Rr4p	D	D-

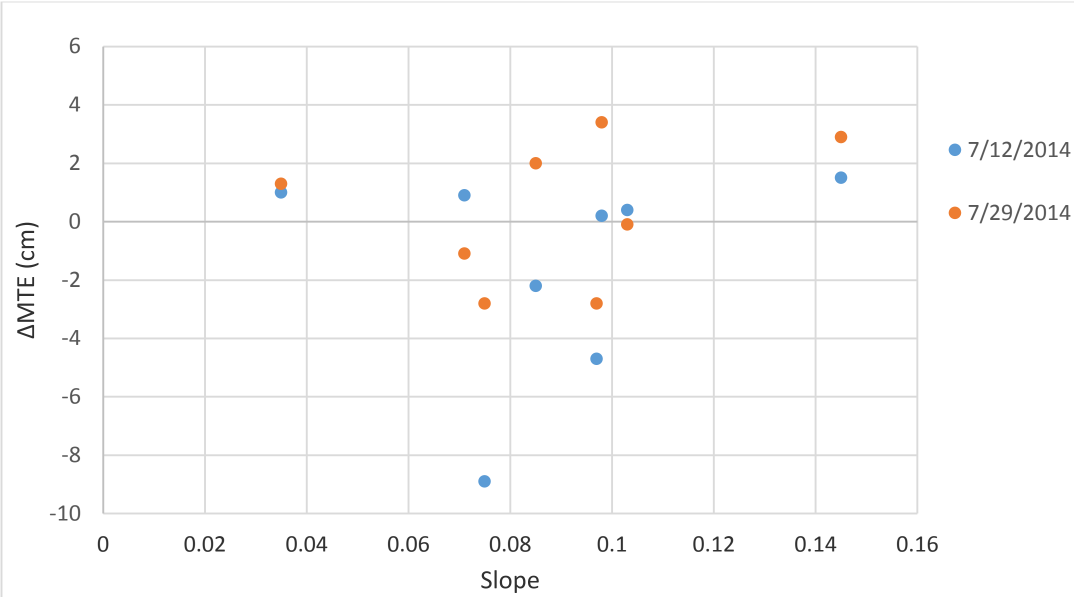

Figure 15: ΔMTE as a function of slope in the perennial study reaches in response to the 7/12/2014 and 7/29/2014 rain events.

Longitudinal profiles in both basins revealed numerous knickpoints, often an indicator of channel adjustment to changes in energy and sediment inputs (Schumm, 1973; Schumm and Parker, 1973). However, in summer 2014, visual assessment of the longitudinal profile suggests that knickpoints were stable. One exception was a knickpoint found in Wr3p that experienced significant degradation during the 7/12/2014 storm and is responsible for the high value of ΔMTE experienced by that study reach (Appendix E). Both swales experienced net degradation over the two storms surveyed. The ephemeral channel reaches experienced different directions of response in each basin. Net degradation occurred in WPW (slope 0.06) and net aggradation took place along both reaches in RT (slopes 0.15 and 0.11). Figure 16 shows channel gradients throughout both study basins. Longitudinal profiles for perennial and ephemeral reaches are located in Appendix E.

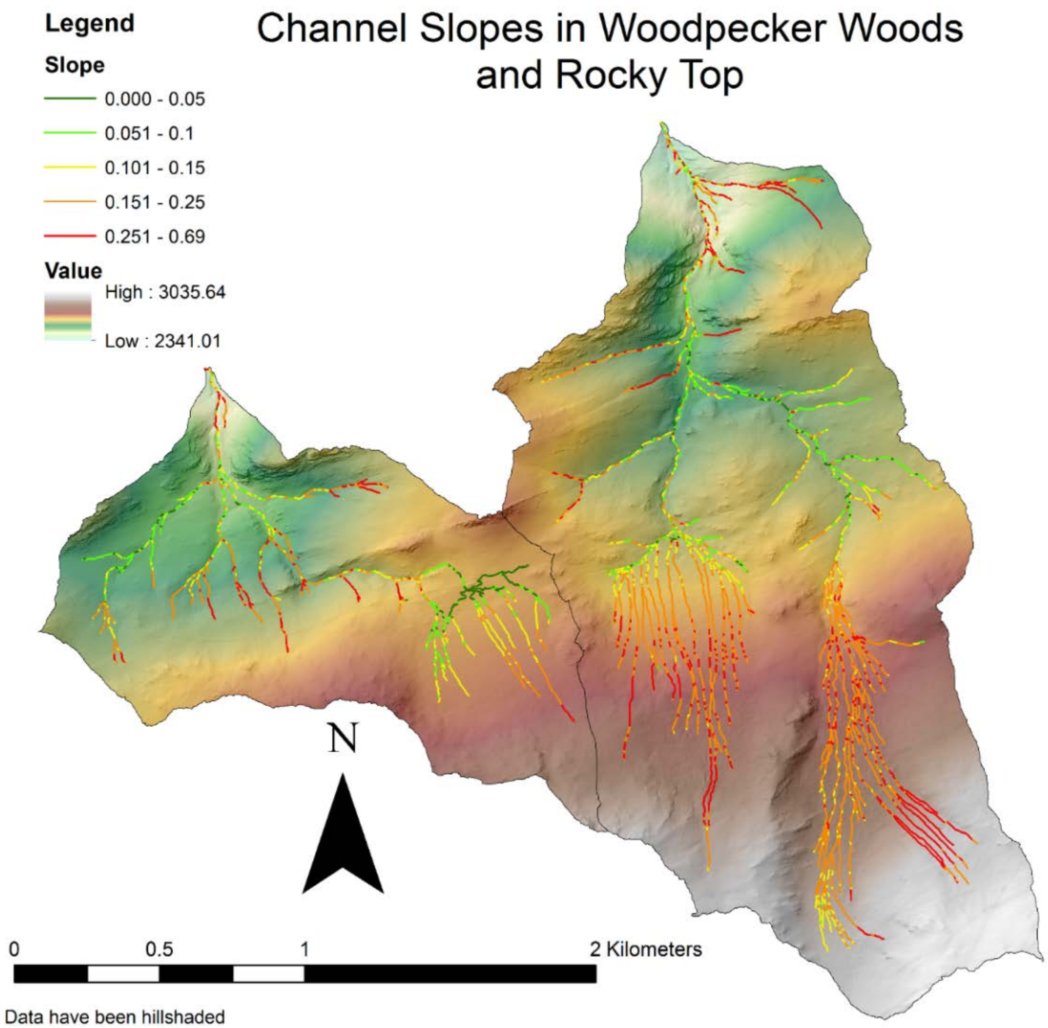

Figure 16: Channel gradients in WPW and RT. Very few channel segments have slopes less than 0.05.

3.5 September 2013

Rainfall depths in the study basins over the seven day September 2013 event totaled 169-180 mm and MI_{30} values ranged from 13.2-13.7 mm hr^{-1}. The effects of the September storms on the ephemeral cross sections were comparable to those caused by events throughout the 2013 summer, but field observations indicated that the perennial channel in each basin experienced extreme degradation. Surveys were not performed along the perennial reach in summer 2013 but field observations, corroborated by repeat photos, show extreme channel degradation. A knickpoint approximately 1 m tall and 1.5 m wide migrated roughly 50 m due to the September 2013 event (Figure 17). The immobility of the knickpoint shown in Figure 17 during summer 2013, despite six runoff-generating storms, suggests that it is unlikely that it would have experienced headward migration during the following summer as hillslopes continued to recover.

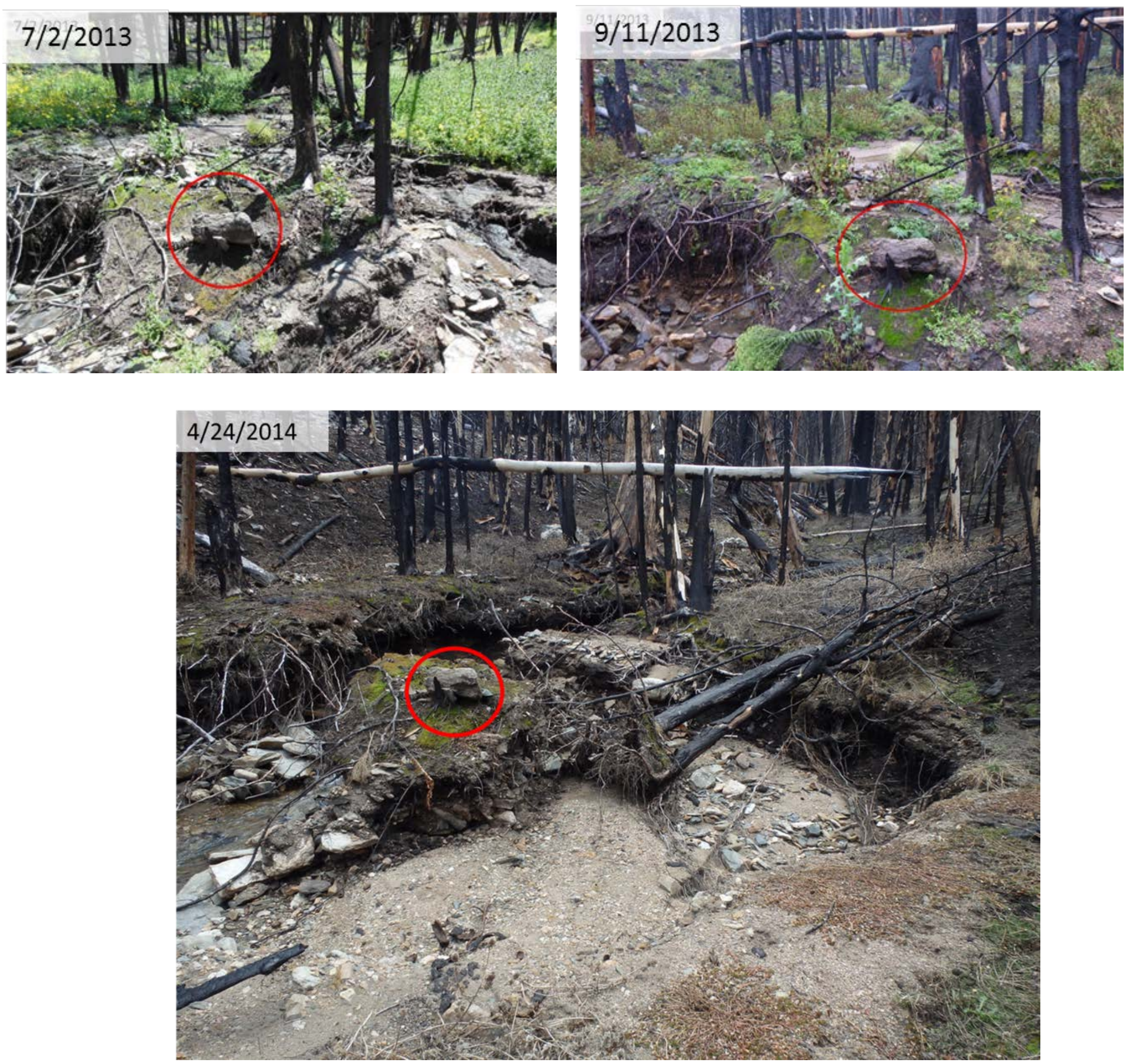

Figure 17: Repeat photographs of a knickpoint located in Rocky Top that migrated approximately 50m during the September 2013 rain event. Storms throughout summer 2014 were did not generate enough discharge to cause headward migration.

3.6 Connectivity Analysis

The connectivity analysis performed in ArcGIS (Cavalli et al.,2013) suggests that at the basin scale both basins exhibit low intra-basin sediment connectivity (Figure 17). However, results from repeat cross section survey, longitudinal profiles, and field observations suggest minimal sediment storage and hence high connectivity of sediment transport within the basin. Values calculated for the two basins range between -5.9 – 0, which are reported in qualitative low-high values. While basin-specific interpretation of model results should be based on qualitative field observations (Cavalli et al., 2013; Cavalli, pers. communication, 2015), other researchers have found values less than -3.5 to correspond to low sediment connectivity, and values of 1-2 to be found in close proximity to the channel network (Cavalli, pers. communication, 2015.) Challenges to interpreting the model output as well as the importance of assessing sediment connectivity in a post-fire setting are addressed in Chapter 4.

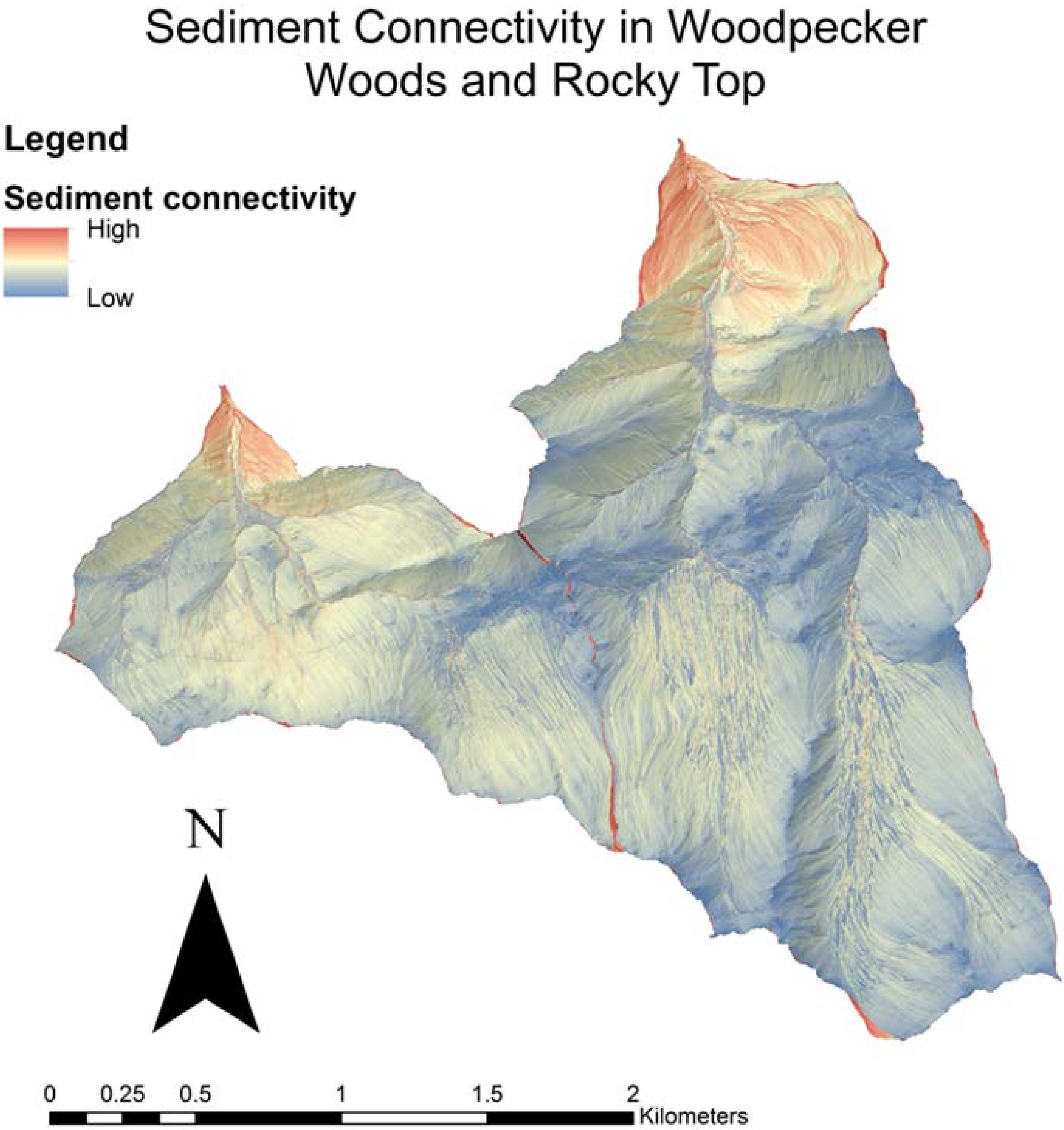

Figure 18: Connectivity analysis after Cavalli et al. (2013). Both study basins show low intra-basin sediment connectivity, with increased connectivity near the basin outlets. Areas of high connectivity at the basin perimeter are assumed to be inaccurate.

4. DISCUSSION

4.1 Rainfall

In 2013, with the exception of the September 2013 event, most summer storms were short duration events. The maximum MI_{30} reached in both basins was 23.2 mm hr^{-1}, which is approximately the 1 year recurrence interval for MI_{30} in the study area (Table 3, Chapter 1). The maximum depth (not including the September event) was 16.3 mm, approximately equal to the 1 year recurrence interval for a 60 minute storm (Table 3, Chapter 1). The total depth from the September 2013 event ranged from 169-182 mm (Appendix B) in WPW and RT, which is approximately 64% of the total depth received at other heavily monitored High Park Fire study areas at lower elevations (Schmeer, 2014). While the September 2013 event was not a brief duration, high intensity event, it highlights potential rainfall-elevation patterns. At higher elevations the likelihood of intense convective summer thunderstorms is lower than at lower elevations (MacDonald and Stednick, 2003). Above 2300 m (approximately the lowest elevation of the study area), peak discharge is driven by snowmelt, below 2300 m peak flows are caused primarily by rainfall (Jarrett, 1990).

In comparison to 2013, two storms exceeded the MI_{30} threshold and depth for hillslope sediment production in summer 2014. The maximum MI_{30} experienced in either study basin was 40.1 mm hr^{-1}, which is approximately the 5 year recurrence interval (Chapter 1, Table 3). The two significant storms show the potential for dramatic differences in storm characteristics at the small basin scale. MI_{30} was 48% larger in WPW for the 7/12/2014 storm, and erosivity was 112% greater. A similar pattern was observed for the 7/29/2014 storm. MI_{30} was 67% greater in WPW and erosivity was 63% greater. These findings corroborate previous studies that demonstrate the high spatial variability of convective storms in semi-arid regions (Faures et al., 1995; Goodrich et al., 1997). The implications for predicting and interpreting basin sediment response are addressed in Chapter 5.

4.2 At-A-Station: Cross Section Change, Scour Chains, and Bed Material

4.2.1 Ephemeral cross sections, scour chain, and bed material

Results from ephemeral cross section surveys in both years and basins suggest that MI_{30} may determine the direction of response in ephemeral channels. Higher intensity events resulted in net aggradation in the ephemeral channel, as measured by ΔMBE and ΔD, while lower intensity events produced net degradation. This suggests that high intensity storms generate hillslope runoff and sediment in proportions such that at small spatial scales ephemeral channels may become transport limited, while at lower intensities sediment production decreases both absolutely and relative to runoff generation, and the system is sediment limited. Based on data collected in summer 2014, this relationship appears to be limited to the ephemeral channel environment. The lack of a statistically significant relationship may be attributable to a small sample size. Given a limited sample size of ephemeral channel cross sections, it is unclear how slope and contributing area determine the direction of response.

The alternating nature of channel response through time suggests that an alternative explanation of channel response depends on the direction of the previous response. Degradation is more likely to follow deposition during a previous event (complex response). Rengers et al. (in review) found that hilllslope erosion response was heavily influenced by the preceding event. Unfortunately for this study, channel response alternates in concert with storm intensities, making it difficult to separate these competing hypotheses. Repeat photographs clearly demonstrate that rain events were acting on very different channel environments (Figure 9), varying between a channel with a significant amount of available sediment and one with limited sediment availability.

Scour chain results suggest that ephemeral channels act as a source and sink for sediment on an event basis whereby scour occurs on the rising limb of the hydrograph and deposition occurs on the receding limb. Maximum scour or deposition revealed by the scour chains generally exceeded the values for ΔMBE for a given event. The absence of a significant relationship between scour or fill and channel slope or MI_{30} is likely attributable to the dependence on previous response, complex response, and a limited data set. Scour chains installed upstream of the 2013 scour chains in the ephemeral channel were characterized by a single response direction in 2014. In WPW the response to both storms was net degradation (scour > fill) while in RT the response to the 7/12/2014 storms was net aggradation (scour < fill), and there was no observed response to the 7/12/2014 storm. The observed responses highlight the importance of site-specific interactions among factors such as channel slope, w:d, lateral connectivity to sediment sources, and location within the channel network that result in differences in transport capacity. The scour chains also provide evidence for potential complex response. The 7/12/2014 rain event produced the greatest amount of scour (and limited deposition) at WPW SC 1e, while the downstream scour chain and cross section (WPW SC 2e and WPW XS 3e) experienced fill > scour and net aggradation. During the 7/29/2014 rain event, scour at the upstream scour chain produced less sediment i.e. lower magnitude of scour, and the downstream scour chain and cross section experienced net degradation that may have been caused by a lack of sediment delivery from upstream.

These results highlight an important dynamic in post-fire channels that may be unaccounted for in repeat cross section and longitudinal profile surveys, which may result in underestimating channel sediment production. Furthermore, it illustrates a response that needs to be accounted for when calculating peak flows even when reliable stage data are present. Peak flow calculations that rely on stage data, whether recorded by depth sensors or geomorphic indicators, must assume a bed elevation in order to accurately assess stage, and therefore discharge. These results demonstrate that the post-event bed elevation is likely higher than the elevation during the event due to a scour and fill sequence, and therefore will tend to underestimate peak flow calculations.

Changes in bed material during the 2013 and 2014 storm season varied between the two ephemeral cross sections. Coarsening of bed material took place at WPW XS 3e during both summers, while at RT XS 4e coarsening occurred over summer 2013 but remained constant over 2014. Because the ephemeral channels in both basins were characterized by a sequence of storage and evacuation of sediment, results from the bed material survey likely reflect the influence of the preceding storm event, rather than a trend through time. Figure 9 illustrates how the timing of sampling would lead to very different conclusions regarding trends in bed material. Furthermore, bed material samples at the end of each field season were taken after events that were dominated by channel degradation, which would promote a coarsening of the bed material.

4.2.2 At-a-station perennial channel cross sections, scour chains, and bed material

The direction and magnitude of channel response at perennial cross sections in 2014 was not correlated with the predictor variables slope, channel slope*contributing area, or w:d. A multiple linear regression model failed to identify significant relationships between the predictor and response variables when the data were analyzed using individual basin response as well as when data sets were combined. Previous studies have noted the difficulty of predicting at a station channel responses post-fire based on the myriad variables impacted as well the capacity for rivers to respond to disturbance through multiple modes of adjustment (Eccleston, 2008; Hooke, 2003; Legleiter et al., 2003; Lane et al., 2008; Phillips, 1991). Lane et al. (2008) further suggest that predicting channel response remains a challenge even when rates of sediment delivery are known due to variability in the timing and magnitude of discharge and sediment delivery, and considerations of reach morphology and valley slope (Hooke, 2003). Rice (1999) and Harvey (1991; 1997; 2002) highlight the importance of lateral sediment inputs in disturbing downstream finding trends and as an important control on channel morphology and response to disturbance. Consequently, a better understanding of the influence of lateral sediment sources and their influence on downstream bed material characteristics as well as channel morphology and response to disturbance would aid in interpreting at-a-station results. Harvey (1991; 1997) found that channel morphology immediately downstream of lateral sediment supply areas was characterized by channel instability and braiding, while other reaches were stable and characterized by single thread morphology. Determining significant relationships between predictor variables and response variables is further complicated by complex response and the episodic movement of sediment slugs which have been observed by other researchers (Moody, 2001). As a sediment slug travels through the channel network, cross sections may experience both aggradation and degradation, confounding the ability to determine statistically significant relationships.

The obvious signs of net degradation post-fire, the absence of significant deposition, and the relative resistance to channel change in 2014 can be explained by (1) channel slope and (2) events that occurred prior to summer 2014. In the idealized basin proposed by Schumm (1977), depositional zones are characterized by increased contributing area and decreased channel gradient, which results in decreased sediment transport capacity. Both study basins demonstrate a significant departure from this idealized basin (Figure 5). Rather than a decreasing channel gradient to the basin outlet, there is an inflection point below which channel gradient increases dramatically. The average slope below the inflection point is 0.23 in WPW and 0.19 in RT. High slope values, which are directly related to stream power and shear stress, explain the lack of depositional features found lower in the basin. The dramatic increase in slope is controlled by basin lithology. Highly incised reaches, large knickpoints, and a poorly-sorted coarse alluvial fan in RT suggest that debris flows may have taken place prior to this study. Gabet and Bookter (2008) found that progressively bulked debris flows were a significant source of sediment post-fire, whereby increased runoff from hillslopes caused rilling that initiated a debris flows at a channel slope*contributing area threshold.

The relative stability of the channel in 2014 can be explained by the timing of the surveys, which did not begin until summer 2014. (Relative stability is used here to refer to ΔMBE values in the range observed during summer 2014 in channels that had experienced net degradation up to an order of magnitude larger than observed changes, i.e. ΔMBE of 5 cm in a channel that had previously incised 50 cm.) Because cross section surveys in the perennial channel were not initiated until two years post-fire, these results should only be used to evaluate response in the 3rd storm season post fire. In a post-fire study of channel head locations in WPW, Wohl (2013) found that the drainage area required to initiate channel heads was more than two orders of magnitude lower than in unburned catchments. However, by the summer 2013 channel head were migrating downslope (E. Wohl, pers. communication, 2014), indicating hillslope recovery, and decreased sediment delivery from both hillslopes and the upstream-most portions of the channel network. A more detailed description of the importance of the timing of cross section surveys and the influence of the September 2013 rain events is undertaken later in this chapter.

Bed material changes illustrated by pebble count data highlight the difficulty of evaluating long term trends in highly dynamic systems. Changes in grain size distribution at a given location may change based on 1) deposition of sediment, 2) removal of fine sediment, 3) channel degradation that exposes new sediment or 4) a combination of 1-3. Results from RT XS 11p highlight scenario 1, whereby aggradation was accompanied by dramatic increase in D_{50} and D_{84}. Changes at RT XS 8p likely demonstrate scenario 2, where minor changes in channel geometry and coarsening indicate the selective transport of fine sediment. Changes demonstrated by WPW XS 8p illustrate scenarios 2 and 3, whereby incision exposes larger clasts and removes fines, resulting in a general coarsening. Changes that result in fining of the bed material may take place by the same mechanisms. The importance of the timing of surveying is further evidenced in Figure 18. A sample taken on 7/28/2014 (pre-event) would lead to different conclusions than a sample taken on 8/2/2014 (post-event). Bed material in steep headwater streams post-fire therefore likely reflects the effects of the previous event, rather than long-term geomorphic trends.

Figure 19: WPW XS 11p illustrating that bed material surveys reflect changes caused by the most recent event rather than trends through time.

4.3 Suspended Sediment

Suspended sediment concentrations monitored in the South Fork Cache la Poudre highlight and provide evidence of three important findings: (1) hillslopes are the dominant source of suspended sediment, (2) rain events with MI_{30} <10 mm hr^{-1} can produce and transport suspended sediment at the small basin scale, and (3) convective storms exhibit high spatial variability such that adjacent basins may not experience equal rainfall, runoff, and erosion response.

Dam releases upstream from the study basins caused the largest increases in stage throughout the study period, but resulted in some of the lowest increases in SSC, suggesting that fine sediments are not stored or produced from the South Fork Cache la Poudre in the reaches immediately above the study basins. Channel complexity and beaver activity may promote the storage of fine sediment in headwater reaches, resulting in minimal SSC increases observed at our basin outlets. However, these results suggesting that the channel is not the source of fine sediment may reasonably be extrapolated to the channel network within each study basin (high slopes discourage the deposition of fine sediment in the channel network), suggesting that hillslopes are the source of fine sediment.

Increases in SSC at MI_{30} values below the often cited threshold of 10 mm hr^{-1} suggest that low intensity storms are capable of generating runoff and fine sediment. Rainfall events that caused elevated suspended sediment concentrations but no changes in channel geometry illustrate a threshold response and differences in connectivity between fine and coarse sediment. Because persistent inputs of fine sediment can have detrimental ecological impacts (Goode et al., 2012), low intensity rainfall events that occur more frequently than high intensity events can have important ecological consequences. Post-fire sediment yield studies therefore need to address both fine and coarse sediment delivery, which may require different study methodologies and present different logistical challenges at different spatial scales. Changes in cross section geometry or longitudinal profiles, which focus on coarse sediment, may not account for the transport of fine sediment, which in some post-fire basins may comprise the majority of basin sediment yield (Reneau et al., 2007). The results also provide evidence for a threshold erosion response in the first year post-fire when MI_{30} is approximately 10 mm hr^{-1}. SSC during events when MI_{30} exceeded 10 mm hr^{-1} were in general twice as high as SSC when MI_{30} was less than 10 mm hr^{-1}. This finding would support previous work that identifies 10 mm hr^{-1} as a threshold intensity for hillslope generation of sediments.

Downstream observations of SSC highlight the localized nature of convective storms. Uniform storm coverage would likely produce increasing SSC as downstream tributaries deliver sediment to the mainstem, but SSC both increased and decreased in the downstream direction, indicating that both study basins did not experience equal erosion response on an event basis. Decreasing downstream SSC corresponded to decreased MI_{30} values in RT (the downstream basin), and increasing values corresponded with higher MI_{30} values. In one storm, a dramatic increase in SSC below RT appears to be directly related to MI_{30} values that were approximately twice that of WPW (12.6 mm hr^{-1} vs 6.6 mm hr^{-1}). These findings illustrate the challenges in interpreting watershed suspended sediment yields and the relative contribution of specific sub-basins.

Comparing 2013 and 2014 SSC suggests significant hillslope recovery between summer 2013 and summer 2014. In 2013 storms where MI_{30} exceeded 10 mm hr^{-1} produced SSC greater than 2500 mg L^{-1}, while in 2014 SSC exceeded 1500 mg L^{-1} only once. A storm with MI_{30} of 40.1 mm hr^{-1} was not sufficient to generate SSC above 1500 mg L^{-1}. This suggests that hillslopes in both study basins experienced significant recovery between 2013 and 2014 and peak levels of SSC are most likely to occur immediately post-fire.

4.4 Longitudinal Profile Surveys

Repeat longitudinal profiles in both study basins reveal channel networks largely resistant to change, in both perennial and ephemeral channels. Visual and quantitative evaluation of the repeat longitudinal profile surveys in 2014 indicate that channels in both basins experienced neither significant aggradation nor degradation. Numerous knickpoints identified in 2013 suggest that channels in both basins were in the process of adjusting to post-fire increases in water and sediment inputs, but the stability of those knickpoints during summer 2014 indicate that they are unlikely to continue moving in the future without large scale disturbance. Longitudinal profiles covered a range of channel characteristics (i.e. w:d, slope, and D_{50}) which were expected to exhibit varying degrees of sensitivity to change. The resistance to change across all channel segments, however, suggests channel stability cannot be attributed to a single variable. The stability of the channel network as well as cross sections is addressed in the September 2013 part of this chapter.

Swale longitudinal profiles in each basin showed net degradation between 4-6 cm. Previous researchers have suggested that swale incision is responsible for the majority of post-fire hillslope sediment yield (Pietraszek, 2006). Swales, which represent the upstream-most extension of the drainage network, are characterized by steep slopes that promote sediment production and transport. Sediment may be stored in clast-controlled steps and local areas of low slope such as plunge pools, but the volume is generally limited. Field observations of unsurveyed swales in both study basins suggest swale incision was a significant source of sediment post-fire.

The response of the ephemeral reaches differed between study basins, with the steeper ephemeral reach in RT experiencing aggradation and the more gentle ephemeral reach in WPW experiencing degradation. This finding may be explained by the differences in upstream contributing areas and the position along the longitudinal profile. In WPW the ephemeral reach is disconnected from the upstream swale by an alluvial fan that prevents sediment produced in the swale from reaching the channel. Furthermore, directly above the study reach in WPW there is a large clast-controlled step that limits channel incision and promotes upstream deposition. By contrast, the ephemeral study reach in RT begins at the confluence of three steep swales. The abrupt transition from a steep swale to a lower slope channel results in a transport limited system that promotes aggradation within the study reach. The reach is then characterized by high roughness due to instream wood and vegetation, both of which are absent in the WPW ephemeral channel.

Differences in the direction and magnitude of change in the perennial study reaches caused by the two storms in 2014 are challenging to interpret. Response to the lower intensity storm (ΔMTE), compared to the higher intensity storm in the study reaches included: (1) increased aggradation, (2) decreased aggradation, (3) decreased degradation, (4) a switch from aggradation to degradation, and; (5) a switch from degradation to aggradation. Five of the eight reaches experienced the same direction of response to both storms. There does not appear to be evidence to suggest that degradation of upstream reaches resulted in aggradation in downstream reaches. It is worth noting that with the exception of Wr3p, all values of ΔMTE were < 4 cm during summer 2014, which is less than the value of uncertainty associated with RTK-GPS surveys (Brogan, 2014; Mekik and Arslanoglu, 2009).

Changes in mean thalweg elevation cannot account for channel degradation that occurs by channel widening. It is possible to produce sediment from the channel network that is not captured by repeat longitudinal profile surveys. However, when combined with data from cross section surveys that suggest a stable channel, the limited changes experienced by the channel as shown by the longitudinal profile surveys indicate that in 2014 the channel was not producing or storing large amounts of sediment.

4.5 Revisiting Hypotheses

4.5.1 Hypothesis 1

Hypothesis 1 predicted that aggradational response reaches corresponded with low channel slope, whereas degradational reaches correspond to high channel slope. H1 is not supported by the results. Slope did not correspond to channel response measured at cross sections or along the longitudinal profile. The greatest degradation took place at channel cross sections with low (relative to other cross sections) slopes, suggesting that site specific factors and their interaction with slope may be more important than channel slope alone. Channel slopes throughout the basin were generally in excess of 0.05 (Figure 16). Montgomery and Buffington (1997) found that channels with slopes 0.03-0.065 were characterized by a step-pool morphology, those with slopes greater than 0.06 were characterized by cascade morphology, both of which are characterized as transport, rather than response reaches. The lack of channel slopes less than 0.06 means it is difficult to fully evaluate Hypothesis 1.

4.5.2 Hypothesis 2

Hypothesis 2 tested whether the channel slope*contributing area product could predict the direction and magnitude of channel response. H2 is not supported by the results. The channel slope*contributing area product does not correlate with the direction and magnitude of response measured at cross sections. The lack of correlation between channel slope*contributing area product and the direction and magnitude of channel response is likely due to a number of factors, including; (1) the importance of site-specific variable interactions such as w:d, bank stability, grain size distribution, bedforms, and spatial location along the longitudinal profile and with respect to upstream and downstream controls, (2) field surveys of perennial channels that were not initiated until after two storm seasons, (3) the lack of low-slope reaches, and (4) inherited channel geometry after the September 2013 event.

4.5.3 Hypothesis 3

Hypothesis 3 predicted that the magnitude of channel change was controlled by MI_{30}. Due to the need for multiple events that caused changes in channel geometry, H3 can only be tested using the data set from 2013, which is limited to the ephemeral channel cross sections. An implicit assumption of H3 was that the direction of channel response is consistent. Results from cross section surveys of the ephemeral channel in 2013 demonstrate that the direction of channel response varies between net aggradation and net degradation, therefore H3 is not supported. There is evidence to suggest, however, that the direction of channel change is controlled by the MI_{30} at the ephemeral cross sections. Because there were only two storms that caused changes in channel geometry in the study basins in 2014, H3 cannot be statistically tested. Results from the two storms support the hypothesis that higher rainfall intensities produce a greater magnitude of channel change, but variability in the direction of channel change and a limited sample size make determination of the role of rainfall intensity difficult.

4.5.4 Hypothesis 4

Hypothesis 4 predicted that the magnitude of channel response in the unmulched sub-basin will be greater than the magnitude of response in the mulched basin. The variable response of the ephemeral channel to storm events, the importance of site specific factors in determining channel response, a limited data set and the mobilization of mulch before the initial surveys makes a quantitative assessment challenging. A further complication is that ground cover was greater in the unmulched basin than the mulched basin due to differences in burn severity. Because mulch reduces erosion response by increasing ground cover, the disparity between the mulched and control basins makes evaluating the effects of mulch unrealistic. Photographic documentation provides the best evidence of the role mulch played in stabilizing hillslopes and promoting infiltration. Aerial mulching was completed at the end of June 2013, with field access allowed only after mulching was complete. Field observations and photographic evidence show a variable distribution of mulch, ranging from uniform to clumped, and concentrated in swale axes and channels (Figure 18). The rain event on 7/1/2013 transported much of the mulch that was located in swales and channels (Figure 18), which suggests that mulch may be ineffective at reducing sediment yields during large storm events (Wagenbrenner et al., 2006) especially from channel areas. Where mulch remained in place, it was effective at stabilizing the hillslope (Figure 19), promoted infiltration, and reduced runoff and sediment production.

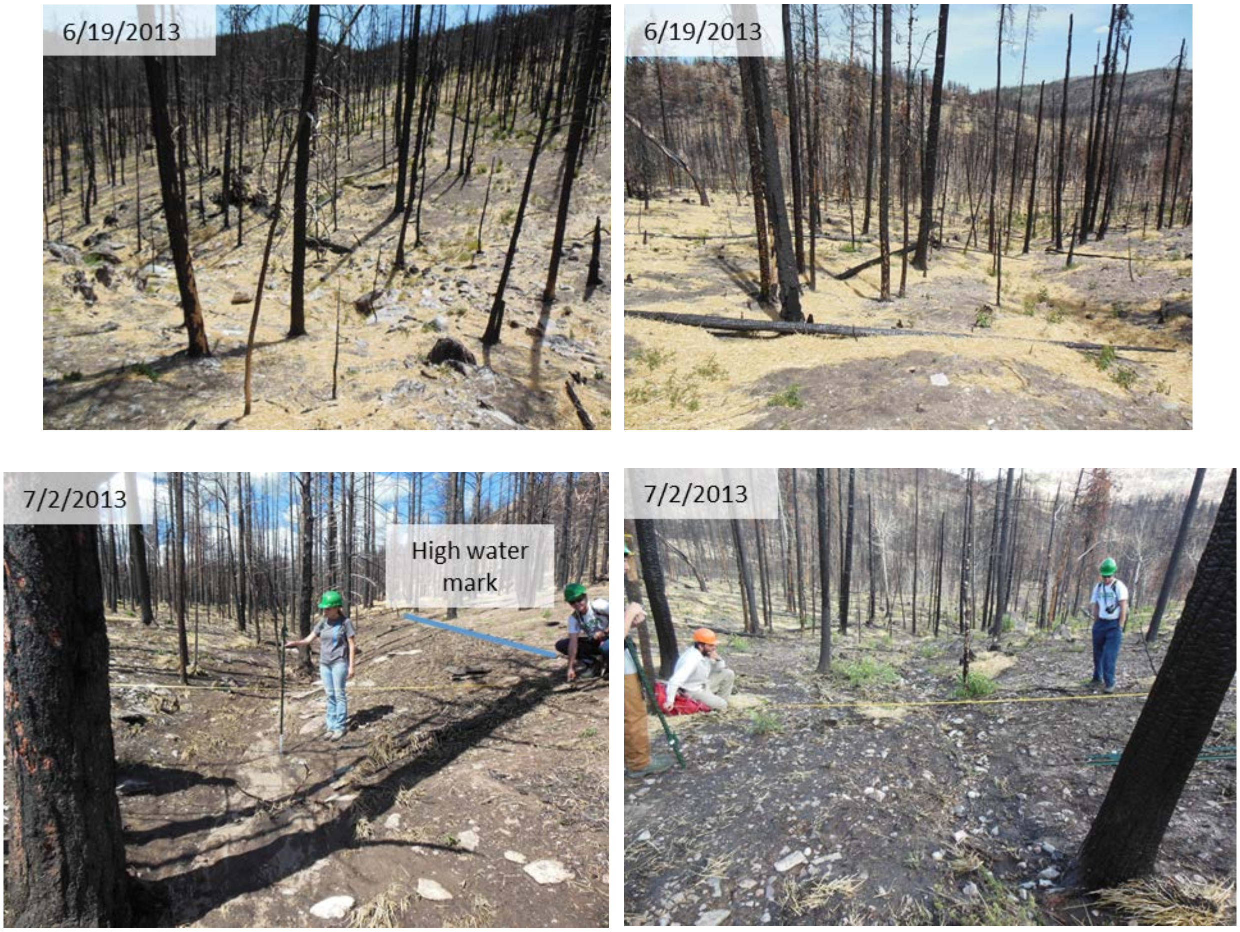

Figure 20: Examples of the mulch distribution and transport in WPW. Mulch distribution was variable and concentrated in topographic depressions such as swales and channels making it vulnerable to transport during the 7/1/2013 rain event.

Figure 21: Mulch stabilization of hillslopes. High water marks along the swale due to the 7/1/2013 storm show where mulch was transported.

4.7 September 2013

The September 2013 rain event presents significant challenges when interpreting results from this study and also illustrates important long term geomorphic patterns. The minimal changes observed along the ephemeral channel supports previous research that MI_{30} is a better predictor of runoff and sediment yield than total depth, and that infiltration excess overland flow generates more runoff and sediment than saturation excess overland flow at the hillslope scale. However, based on changes that took place at locations with larger contributing areas, an alternative explanation suggests that the ephemeral channel, due to a combination of moderate slope and limited contributing area, acted as a transport reach rather than a source or storage reach and that response was controlled by site characteristics rather than rainfall characteristics.

The immobility of the knickpoint shown in Figure 17 suggests that significant amounts of sediment produced by the degradation of the perennial reach would likely have remained in storage during summer 2014 and until the next large disturbance event. This highlights the importance of high magnitude, low frequency events in controlling long term sediment yields. The significant degradation and relatively low MI_{30} of the September 2013 event also illustrates the challenges associated with linking rainfall characteristics with runoff response and discharge. The long duration of the September 2013 event may have generated runoff by both infiltration excess overland flow as well as saturation overland flow. Temporal variability and the timing of the MI_{30} may also have been an important factor in determining peak discharges. The large spatial extent of the September 2013 event suggests that all portions of the basin experienced rainfall capable of generating runoff, unlike convective storms that cover only isolated portions of a basin.

The September 2013 event exerted an important control on channel response in 2014 by creating the template upon which the storms of summer 2014 acted. The relative stability of the channel in summer 2014, despite evidence of previous degradation, suggests that the discharges resulting from the September 2013 event increased the threshold for discharges capable of causing channel degradation in summer 2014 by transporting much of the available sediment in the channel network. This new threshold combined with continued recovery of hillslopes explains the relative stability of the channel during summer 2014. Most sediment produced in the channel network during summer 2014 occurred during the 7/12/2014 storm, which had a MI_{30} of 40 mm hr^{-1} and 27 mm hr^{-1} in WPW and RT respectively, which is the highest MI_{30} recorded during this study. Despite a total depth more than twice that of the 7/12/2014 storm (Figure 8), the storm on 7/29/2014 caused less change, as calculated by ΔMBE, ΔD, and ΔMTC, due to lower rainfall intensities. Based on changes observed in 2014 and given continued hillslope recovery, the threshold for rainfall intensities required to cause changes in channel geometry will likely be in excess of 20 mm hr^{-1}.

4.8 Sediment Connectivity Analysis

The sediment connectivity analysis performed in this study indicates low intra-basin connectivity in both study basins. The connectivity model developed by Cavalli et al. (2013) integrates characteristics of the upslope contributing area with downslope flowpath characteristics in order to calculate an index of connectivity (IC). The model was developed for alpine catchments where topographic roughness rather than vegetation is the dominant control on sediment connectivity. Because vegetation was largely absent due to high burn severity in the study basins, the model was run as a first order approximation of sediment connectivity. The absence of significant deposition within the channel network suggests that the channel network is a very efficient transporter of both hillslope derived and channel derived sediments. Extensive rilling on hillslopes and observations of swale incision throughout the basin further indicate that hillslopes are delivering sediments to the channel network. The importance of hillslope-channel connectivity on determining channel morphology and downstream geomorphic trends has been highlighted by previous studies (Harvey, 1991; Rice, 1999). Rice (1999) defined sediment links as channel segments that experience downstream trends that result from fluvial processes, and showed that these trends may be disrupted by discrete sediment supply zones. Such zones were not explicitly identified in this study, but field observations indicating high hillslope-channel connectivity confirm the importance of assessing hillslope-channel connectivity when interpreting channel response. Generally, field observations support high sediment connectivity in both basins, which is not suggested by the model.

A limitation of the model is the inability to account for the presence of vegetation in the study basins. While some studies have suggested that percent ground cover is an important control on sediment yields (Benavides-Solorio and MacDonald, 2005), others have highlighted the importance of the spatial distribution of ground cover such that even low total percent of vegetation may act as a significant barrier to sediment connectivity (Cawson et al., 2013), as in the presence of riparian vegetation. The influence of vegetation therefore needs to be integrated into post-fire sediment connectivity models. Ultimately, the connectivity model results must be confirmed by qualitative field observations (Cavalli et al., 2013; Cavalli, pers. communication, 2015). The lack of observed sediment storage on hilllopes, or in the channel and near-channel environment, suggests high sediment connectivity within the study basins which were not captured by the model. It is also important to address differences in sediment availability and sediment connectivity. The areas with high connectivity in the study basins were bedrock outcrops that, despite a high capacity to transport sediment, are unlikely to produce sediment. It is essential therefore to assess not only sediment connectivity but also sediment availability in post-fire basins. A further challenge to post-fire sediment connectivity analysis is that changes to connectivity change through time as vegetation recovers as well as by the creation of depositional features that may act as barriers to sediment transport, as in formation of alluvial fans, or as inputs of wood to the channel increase as dead trees fall and promote deposition. In such a highly dynamic setting, a static assessment of connectivity may only be useful immediately post-fire.

4.9 Integrating Spatial Scales: From Hillslopes to Watersheds Post-Fire Erosion Response

The specific goal of this study was to evaluate sediment production, transfer and storage within the channel network by monitoring channel response. The broader aim was to apply results from this study to improve understanding of basin-scale sediment yields. Numerous variables contribute to sediment yield at different spatial scales and sediment may exhibit different degrees of connectivity with and between those spatial scales, influencing basin sediment yield (Figure 22).

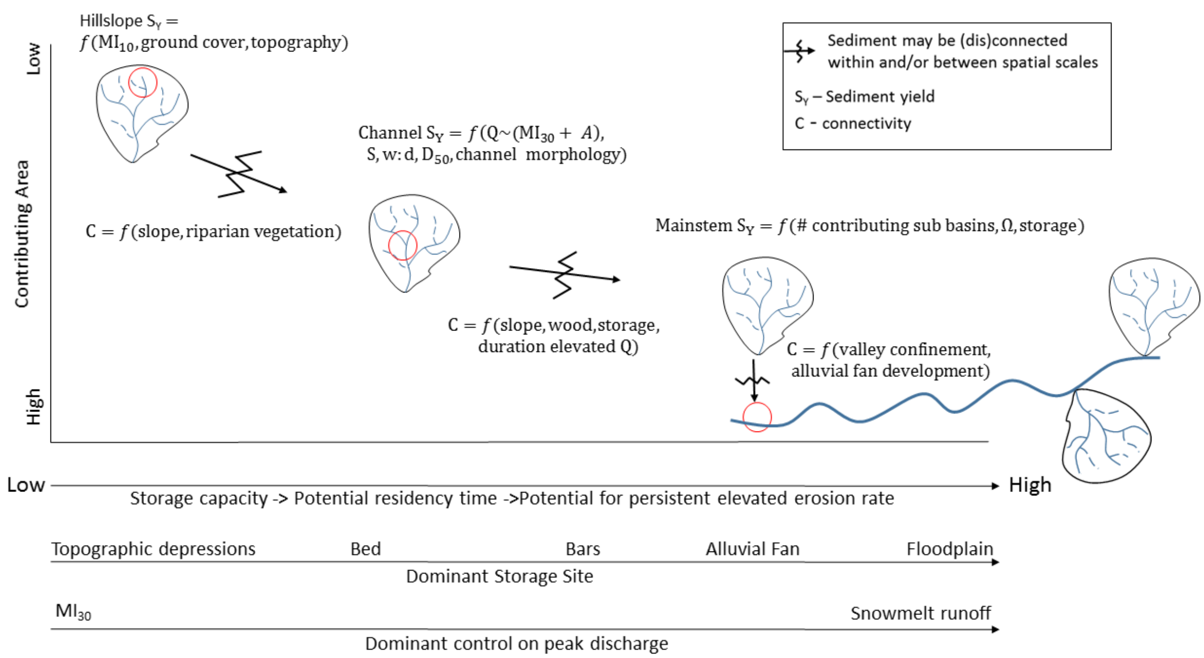

Figure 22: Conceptual illustration of variables contributing to sediment yield and connectivity from the hillslope to watershed scale post-fire.

Hillslope sediment production is a function of ground cover, topography and rainfall intensity. Previous researchers have identified both the MI_{30} and MI_{10} as correlated with hillslope sediment yield. MI_{10} is used in Figure 22 to illustrate that different metrics may be necessary when analyzing different spatial scales. Sediment produced by hillslopes may be disconnected from the channel network by areas of low slope or riparian vegetation. Channel response is influenced by water and sediment inputs (from hillslopes and upstream reaches), slope, discharge, w:d, D_{50}, and channel morphology. Sediment connectivity within the channel network may be disrupted by instream wood, low slope, the duration of elevated discharge, and in-channel or overbank storage. Furthermore sediment that reaches the basin outlet may be disconnected from the receiving channel by the presence of depositional features such as alluvial fans and floodplains. Figure 22 illustrates the complexity that must be addressed in order to predict and interpret post-fire basin sediment yields. It demonstrates the need to address not only sediment dynamics within a given spatial scale, when outputs from one scale become the inputs for another, but also the linkages between them. Post-fire basin-scale sediment yield studies therefore require extensive cooperation between researchers operating at different spatial scales in order to address scale dependent processes and connectivity between those scales.

Figure 23 provides a conceptual illustration of the results and observations from WPW and RT. Field observations of extensive rilling and rock pedestals indicated that planar hillslopes produced moderate amounts of sediment post-fire. The lack of deposition in these areas suggests that planar

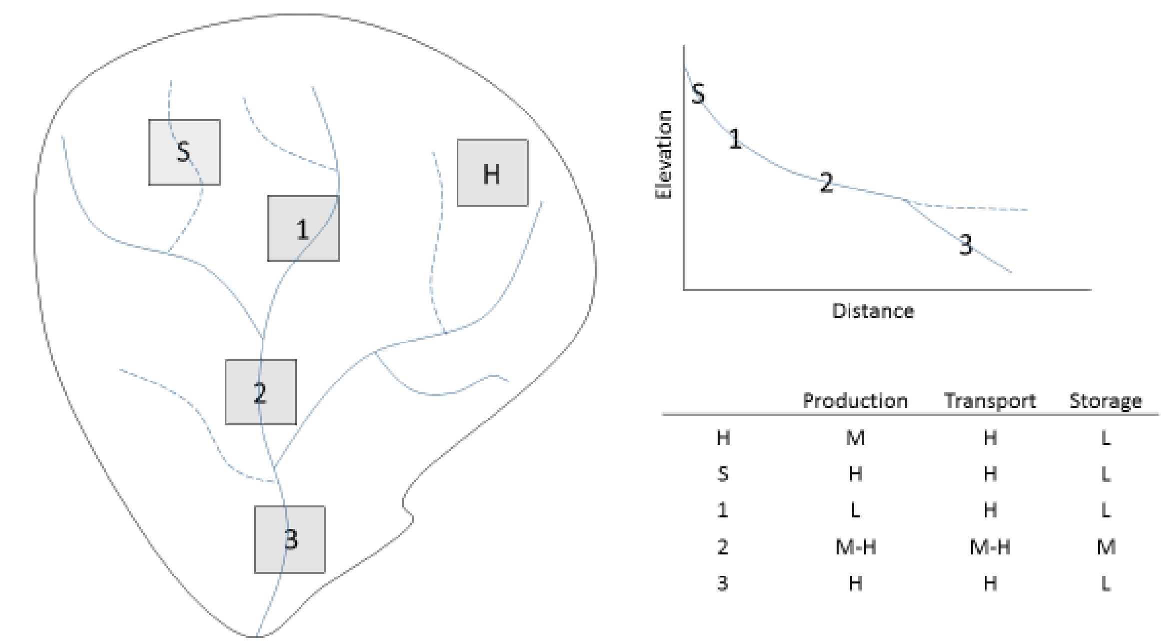

	Production	Transport	Storage
H	M	H	L
S	H	H	L
1	L	H	L
2	M-H	M-H	M
3	H	H	L

H=hillslope, S=swale, 1=1st order stream, 2=2nd order stream, 3=3rd order stream H=high M=medium L=low

Figure 23: Illustration of how sediment dynamics vary at different locations within a basin. The dotted line in the longitudinal profile represents an idealized basin, the solid line represents the profile within each study basin.

hillslopes were effective at delivering sediment to the channel network. Significant swale incision indicated that swales produced large amounts of sediment post-fire. The resistance to change shown during the course of this study is the result of a limited sample size of survey swales and surveys that were not initiated until after a significant storm on 7/1/2013, sediment yields can decline substantially within a few months to years post-fire (Wohl, 2013). Significant net incision and limited deposition indicate that swales produced and transported significant sediment post-fire. The uppermost reaches of the perennial channels in both basins showed little evidence of post-fire channel changes (Figure 23). Despite high slopes, limited contributing areas may have resulted in discharges incapable of degrading the channel. A lack of depositional features suggests that these areas were capable of transporting sediment delivered from hillslopes.

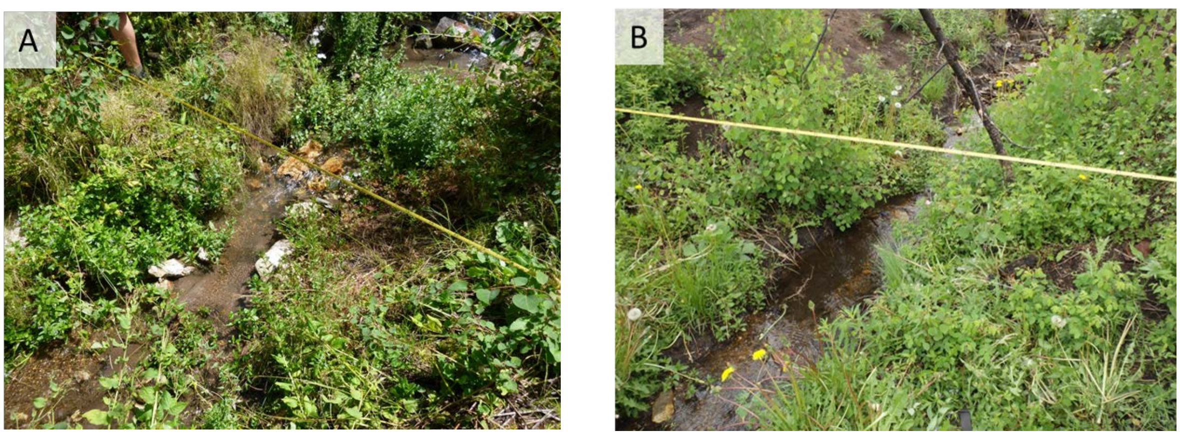

Figure 24: A: RT XS Rp, B: WPW XS Sp. Both cross sections showed little evidence of post-fire change, indicating that they acted predominately to transport hillslope sediments to downstream reaches.

Mid-basin channel segments were characterized by net degradation post-fire (changes that happened before summer 2014), and similarly to upstream channel segments showed few signs of providing significant sediment storage, suggesting they produced sediment as well as transported sediment from upstream reaches. Channel segments lower in the basin were characterized by high slopes, net degradation, and minimal storage areas in both basins. High slopes promote a positive feedback loop whereby initial incision decreases the probability of overbank flows that would lead to deposition by an increase in roughness, and instead promote higher shear stress leading to further incision (Figure 24).

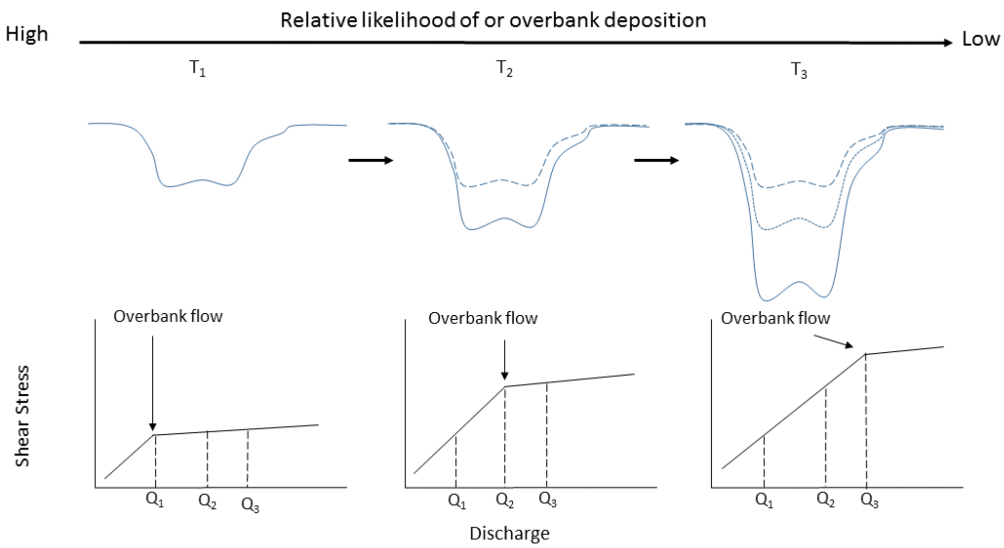

Figure 25: Conceptual illustration of how high channel slopes promote initial incision which reduces the likelihood of overbank deposition during subsequent events.

Once incision has taken place (T_2 and T_3), shear stress for a given discharge will be greater than at the previous time step such that for Q_3 shear stresses increase ($\tau_1 < \tau_2 < \tau_3$) (Figure 25). Overbank deposition becomes increasingly less likely as the channel continues to incise. Any deposition therefore will occur in the channel rather than overbank, with a correspondingly lower residence time and higher probability of transport during subsequent events.

As vegetative regrowth takes place, landscape sensitivity and the potential for erosion decrease (Figure 25). Erosion mitigation measures as well as significant storm events also affect erosion potential. The potential for erosion is highest immediately post-fire when ground cover is at its minimum and sediment availability at its maximum. As sediment is removed, which may cause armoring of the surface, and vegetation recovers, the potential for erosion declines. Treatments such as mulching immediately provide increased ground cover, thereby further lowering the erosion potential. Large storm events further decrease the erosion potential by removing available sediment. This suggests that the time to recovery may be a function of both hillslope recovery as well as the number and characteristics of erosive events, such that basins that experience significant erosion immediately post-fire will be more likely to experience less erosion during subsequent events, and therefore return to background rates of sediment yield more quickly.

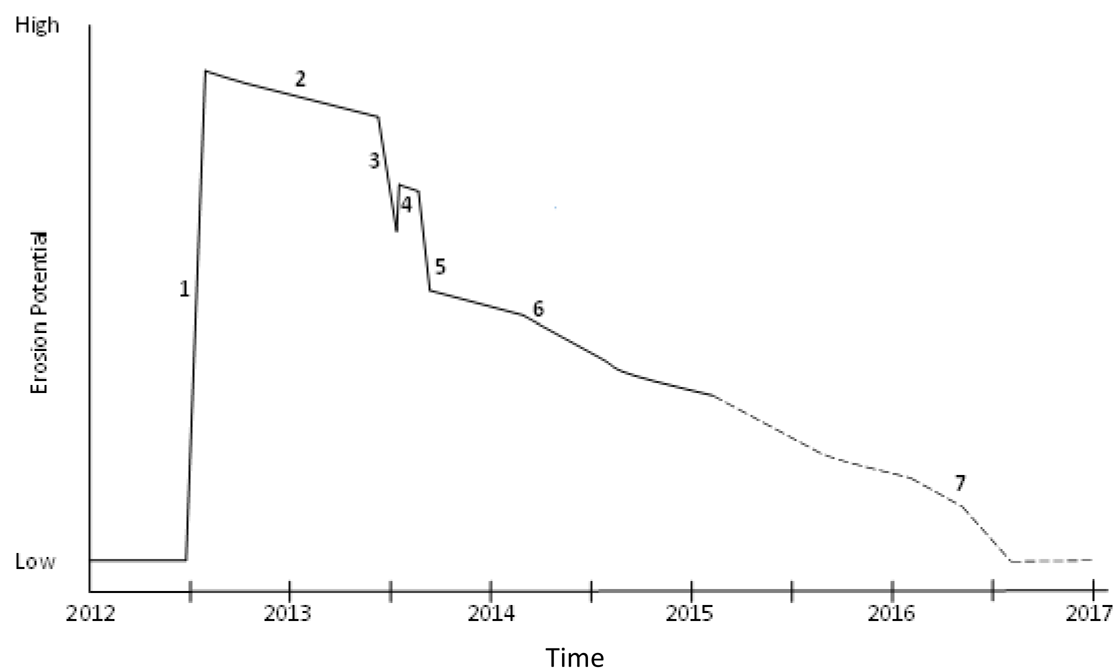

Figure 26: Schematic of erosion potential through time post-fire in our study basins. 1) High Park Fire dramatically increases erosion potential, 2) Erosion potential declines immediately post-fire as easily erodible sediment is transported, 3) Mulching provides immediate ground cover, reducing erosion potential, 4) 7/1/2013 storm removes significant quantities of mulch, 5) September 2013 event causes significant erosion, reducing sediment availability for future storms, 6) Basins continue to recover as vegetation regrowth occurs, 7) Vegetation cover reaches threshold values and erosion potential returns to background levels.

5. FUTURE RESEARCH AND MANAGEMENT RECOMMENDATIONS

5.1 Future research

5.1.1 Spatial and temporal variability in rainfall and sequence of rainfall events

High spatial and temporal variability rainfall events are the driving force in post-fire erosion in the Colorado Front Range (Chapter 1). Moody et al. (2013) identify meso-scale precipitation patterns as an important area of future post-fire research. Spatial variability exhibited by convective storms in semi-arid regions has been observed at spatial scales as low as 5 ha (Faures et al., 1995; Goodrich et al., 1995), suggesting that the assumption of uniform rainfall is invalid at such low spatial scales (Goodrich et al., 1995). Spatial and temporal variability have a significant effect on hillslope runoff and discharge (Goodrich et al., 1995). Unlike hillslope studies where rainfall is uniform across the study area, rainfall may vary significantly at the small basin scale, therefore linking rainfall characteristics to discharge and geomorphic response requires high resolution spatial rainfall data. In addition to high spatial variability, model simulations indicate that temporal variability exerts a strong control on runoff generation, discharge and consequent geomorphic effects (Reaney et al., 2007). Partial storm coverage of a watershed can result in highly localized geomorphic changes. A dense network of rain gages may permit statistical interpolation to calculate a more appropriate average rainfall, but such an approach may still obscure the importance of individual sub-basins and/or maximum rainfall intensities in controlling response at the watershed scale. In a storm immediately after containment of the High Park Fire on 7/6/2012, significant changes in channel geometry were observed within a lower elevation basin, while no changes were observed in an adjacent sub-basin (Brogan, pers. communication, 2015).

Watershed sediment yield integrates responses from multiple sub-basins experiencing different rainfall intensities and depths. The selection and calculation of a single rainfall metric is therefore challenging. Previous studies have used a number of rainfall metrics in order to predict erosion response, including total depth, 10, 15, and 30 minute maximum intensities, and erosivity (Moody et al., 2013). Soil erosion rate has been found to correlate best with MI_{10} (Spigel and Robichaud, 2007), debris flow timing with MI_{15} (Kean et al., 2011), and peak discharge with MI_{30} (Moody and Martin, 2001b). Cammeraat (2002) found that rainfall events that generate runoff at the plot scale may not necessarily generate runoff at the hillslope scale, and Lane et al. (2008) demonstrated that the thresholds for hillslope sediment production differed from the rainfall thresholds required to mobilize sediment in the channel network. Photographs from the ephemeral channel illustrate differences between hillslope and channels in the rainfall intensity thresholds required to produce and transport sediment (Figure 26). The

Figure 27: In-channel deposition of hillslope sediments during a storm event < 3mm depth illustrating hillslope sediment production and an absence of in-channel discharge. Measurement of sediment transport during the following event incorporates the erosion response of the preceding event.

storm that produced the deposition shown in Figure 26 had a total depth of 2.8 mm and MI_{30} of 5.6 mm hr^{-1}, well below the commonly cited threshold of 10 mm hr^{-1}. However, the MI_{15} was 10.6 mm hr^{-1} (the MI_5 was 26 mm hr^{-1}). This evidence illustrates two points that must be addressed in post-fire studies: (1)

rainfall thresholds that activate erosional processes on hillslopes may differ from those that activate erosional processes within the channel network, requiring the use of different rainfall threshold metrics, and (2) event-based, basin-scale sediment yield must account for the sequence of storms because short duration storms with high MI_{10} and low MI_{30} may be capable of transporting hillslope sediments to the channel network but be incapable of transporting sediment downstream to the basin outlet. Rengers et al. (in review) suggest that hillslope erosion response is heavily influenced by previous events. Sediment yield for a given storm therefore reflects the storm history in the basin rather than the effect of a single storm.

5.1.2 Evaluating sediment connectivity: interpreting and predicting post-fire sediment yields

Assessment of connectivity within a post-fire basin is critical to assessing the effective source area of sediment and informing post-fire erosion mitigation measures (Bracken and Croke, 2007; Brierly et al., 2006). Reneau et al. (2007) implicitly adopted such an approach when calculating unit area sediment yield after the Cerro Grande fire by assuming all sediment was produced from areas of high and moderate burn severity. Understanding sediment flux at a basin outlet requires an understanding of (1) sediment delivery from source areas, (2) entrainment thresholds, (3) transport (as suspended load or bedload,) and; (4) deposition in temporary or long term storage sites (Fryirs, 2013). Connectivity in a post-fire basin must take into account site topographic characteristics that control sediment dynamics such as channel slope, channel confinement, and presence/absence of floodplain, as well as post-fire vegetation patterns. Geomorphic characteristics can be assessed independent of fire, while vegetation coverage can only be evaluated post-fire.

Assessing lateral connectivity between hillslopes and channels is essential because hillslopes control the amount of water and volume and caliber of sediment reaching the channel network, which controls channel response (Harvey, 1991; Harvey, 1997). Previous studies have suggested that the spatial arrangement of areas of high and low infiltration capacity may be more important than the total area covered by each (Bracken and Croke, 2007). Ambroise (2004) cites ‘tiger-bush’ banding patterns as an example of the importance of the spatial variability of ground cover wherein more than 50% of a hillslope may produce runoff but no runoff reaches the outlet (contributing area 0% and disconnected). Cawson et al. (2013) found that the hillslope position and width of vegetation buffer strips significantly affected post-fire hillslope sediment yields. However, not all sediment that is delivered to the channel network can be assumed to be delivered to the basin outlet (Cavalli et al., 2013). River systems have been described as “jerky conveyor belts” (Ferguson, 1981) that transport sediment episodically in response to external disturbances. Longitudinal connectivity (connectivity within the channel network) is controlled by slope, which may be controlled by basin lithology and geologic history, as well as fluvial processes. Lateral sediment inputs also exert a strong control on bed material and channel morphology and may disrupt downstream trends (Harvey, 1991; Rice, 1999). Bed material, for example, may fine within a sediment link (Rice, 1999) but experience coarsening when influenced by inputs from hillslopes. Assessing hillslope-channel connectivity is important to interpreting channel morphology and response to disturbance.

Alluvial fan development and valley characteristics of the receiving river valley are important controls on the amount of sediment delivered from small basins to larger order channels. In a survey of 63 debris flows in the Oregon Coast Range, May and Gresswell (2004) found that 52% of debris flows delivered sediment directly to the main channel, 18% were deposited within the tributary valley, and 30% were deposited on an existing alluvial fan before reaching the mainstem channel.

Total basin sediment yield includes both fine and coarse material, but sediment connectivity differs greatly with respect to grain size (Hooke, 2003; Lane et al., 1997), and events that transport fine sediment may differ from those that transport coarse sediment. Fine sediment exhibits a greater degree of connectivity than coarse sediment (Hooke, 2003). Because coarse and fine sediment have different geomorphological, ecological, and water quality implications (See Chapter 1), differentiating fine sediment connectivity and coarse sediment is important to addressing specific questions about channel form and response and water quality.

Connectivity can be assessed on hillslopes where it may be controlled by topography and vegetation; within the channel network where it may be controlled by discharge, slope, and channel geometry; and at the basin scale where it may be controlled by morphologic complexity. Basin sediment yield requires an understanding of all scales and how sediment connectivity is affected post-fire. For land managers faced with post-fire management decisions, assessing basin scale connectivity may be more important, and more easily addressed as a “black box” rather than the product of nested spatial scales and processes. Basin morphological complexity was found to be inversely related to sediment connectivity in a study by Baartman et al. (2013), who suggest that information regarding sediment connectivity at the watershed scale is most relevant for soil and water conservation measures. While their approach does not address the role of different processes operating at different locations within a basin, it may provide a useful approach for land managers when identifying basins capable of delivering the greatest amount of sediment.

An alternative approach would be to analyze sediment connectivity by process domains. On hillslopes where sheetflow and rilling are the dominant erosion processes, ground cover, roughness, and flow length (Mayor et al., 2008) may provide a useful index by which to assess sediment connectivity. However, in the channel network, such characteristics may no longer be the dominant controls on connectivity and connectivity could be assessed using the channel slope*contributing area product as a surrogate for stream power. It may be useful, therefore, to assess hillslope-channel lateral connectivity and longitudinal connectivity within the channel network separately.

5.1.3 Evaluating the effectiveness of mulch on small watershed scale

Evaluating the effectiveness of mulch on the small watershed scale presents researchers with a complex problem. Not only must researchers address precipitation concerns and connectivity (as outlined in the previous two sections), they must address how mulch influences erosion response and sediment yield, which themselves are the product of multiple processes acting at multiple spatial scales. In order to compare sediment yields between basins, sediment connectivity and rainfall inputs need to be comparable, a factor that cannot be controlled. Also, because channels may respond to disturbance through multiple modes of adjustment, assessing channel response does not necessarily provide information regarding the role of mulch in altering that response.

Evaluating the effectiveness of mulch at the basin scale, therefore, should focus on changes in response that are most easily attributable to mulch. Because mulch is applied in order to promote infiltration and reduce runoff, and therefore suspended sediment, monitoring discharge and suspended sediment at multiple locations within a post-fire basin may be the best way to evaluate the effectiveness of mulch. Fine sediment that causes elevated SSC exhibits a higher degree of connectivity than coarse sediment, therefore measurements at the basin outlet more directly reflect hillslope processes than measurements of bedload would. Decreased levels of SSC, therefore, would indicate a reduction in hillslope runoff, and effectiveness of mulch at mitigating sediment yields. Such a finding may then assume reduced runoff from hillslopes, decreased discharge in channels, and a muted magnitude of channel response. Monitoring discharge at multiple points within the basin may also provide insight into the effectiveness of mulch at mitigating erosion, under the assumption that lower discharges will produce a decreased erosion response. Both of these methods are ways to indirectly assess the effectiveness of mulch at the basin scale.

5.2 Management Recommendations

5.2.1 Evaluate risk based on precipitation patterns and sediment connectivity

In order to maximize the benefits of erosion mitigation measures, land managers should evaluate the precipitation regime in the affected area. Additional research into the relationship between precipitation frequency-intensity and elevation would provide land managers with valuable information to guide effective application of erosion mitigation treatments and target areas more likely to experience erosion causing events. The lack of high intensity rain events in the second year of this study suggests that the 2300 m threshold suggested by Jarrett (1990) may provide guidance to land managers when evaluating risk in post-fire areas due to differences in the precipitation regime. This is not to suggest that areas above 2300 m are incapable of producing significant amount of sediment, but rather to suggest that lower elevation areas should be prioritized based on the increased likelihood of sediment producing events.

Identification of impediments to sediment yield at the appropriate spatial scale is critical in evaluating basin sediment connectivity when prioritizing erosion mitigation measures. Furthermore, assessing basin scale sediment connectivity can be quickly and inexpensively performed post-fire using data acquired through remote sensing. Sediment (dis)connectivity can occur at multiple locations within a basin. Because land managers need to make decisions at the basin scale, this is the scale at which analysis should be undertaken. Alluvial fans and the confinement of the receiving river valley both exert a strong control on sediment connectivity between small basins and the main channel (Figure 27).

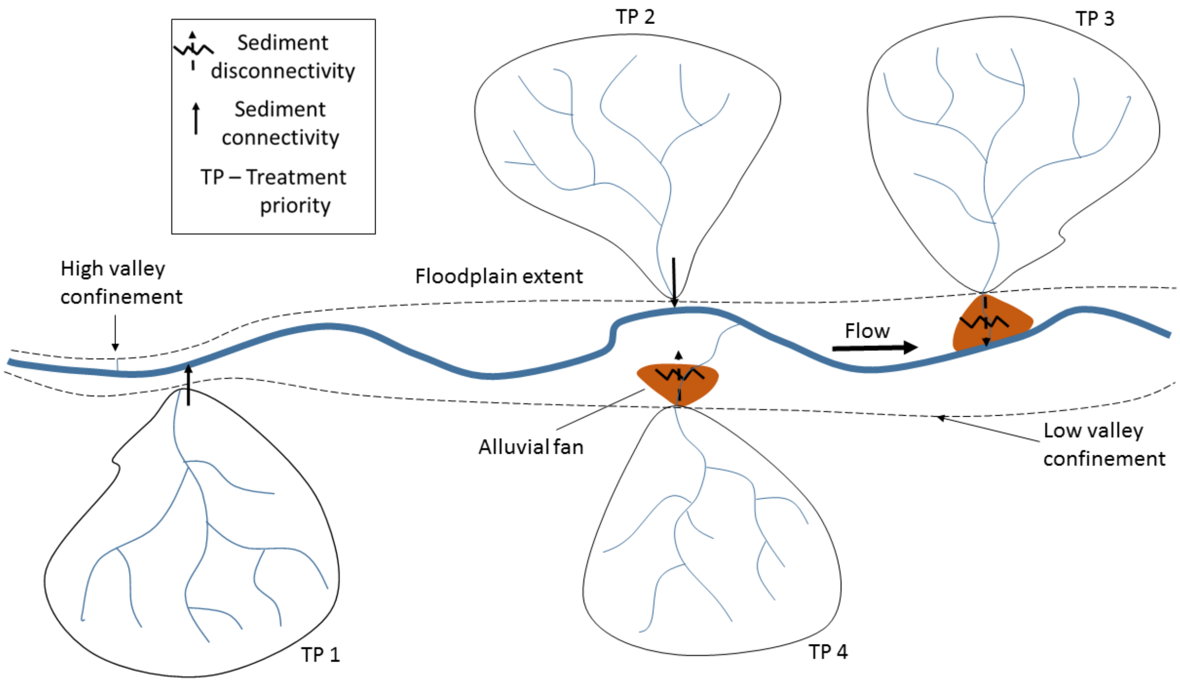

Figure 28: Conceptual model illustrating how identification of sediment connectivity at the basin scale based on the development of alluvial fans, valley confinement, and floodplain-sub-basin, receiving channel spatial arrangement can be assessed to prioritize erosion mitigation measures at the basin scale.

The spatial arrangement of the sub-basin outlet-floodplain and receiving channel, presence of alluvial fans, and valley confinement of the receiving channel all influence whether sediment eroded from a sub-basin will be delivered to the main channel (Figure 27). Sub-basin TP 1 (Figure 27) exhibits high connectivity to the main channel due to high valley confinement of the receiving channel and the lack of an alluvial fan that could act as a barrier to sediment connectivity. By contrast, sub-basin TP 4 is disconnected from the main channel by the development of an alluvial fan at the basin outlet as well as a floodplain that has developed as the result of lower valley confinement.

Assessing small basin connectivity to the main channel provides land managers a valuable tool when designing erosion mitigation measures by acknowledging that basins that may be characterized as high risk based on slope, burn severity and high intra-basin connectivity may not require erosion mitigation due to disconnectivity at larger spatial scales (Table 11).

Table 12: Erosion mitigation treatment prioritization based on analysis of sub-basin connectivity (Figure 27) to the receiving channel based on valley confinement, alluvial fan development, and basin outlet-floodplain-main channel spatial arrangement.

Sub-basin TP	Connectivity	Justification
1	High	high valley confinement of receiving channel, lack of floodplain, no alluvial fan development
2	High	despite low valley confinement, main channel is located in close proximity to basin outlet and not buffered by the floodplain
3	Moderate	low valley confinement, and alluvial fan development act to disrupt connectivity but alluvial fan extents to main channel suggesting moderate connectivity
4	Low	low valley confinement, extensive floodplain separates basin outlet from main channel, alluvial fan acts as barrier

6. CONCLUSIONS

Two small basins were selected in order to study post-fire channel sediment production, transport, and storage. During the study period, the channel network was characterized by resistance to change despite evidence of significant post-fire degradation. The direction and magnitude of channel response could not be predicted by channel slope, channel slope*contributing area, or width to depth ratio due to site specific variables, unique channel history, the ability of channels to respond to disturbance through multiple modes of adjustment and the changing rates of inputs of water and sediment post-fire. Both basins lacked significant depositional zones due to a steepening of channel gradient close to the basin outlet, indicating that sediment eroded in both basins was delivered to the basin outlet. Observations of significant post-fire net degradation suggest that channel sediment production peaked during the first two storm seasons and September 2013 event. Aerial mulching occurred in both basins. Where the mulch was retained on hillslopes, it was effective at limiting erosion.

Evidence for different rainfall thresholds for hillslope and channel sediment erosion response was observed during this study, supporting previous studies that have recognized that post-fire sediment yield at the basin scale requires integrating multiple spatial scales and geomorphic processes that may be governed by rainfall thresholds. Ephemeral channels exhibited a scour and fill response while maintaining consistent channel geometry, indicating that they were acting as a temporary source and storage site for sediments that may not be recognized by cross section or longitudinal profile surveys.

Assessing sediment connectivity is of critical interest to both researchers and land managers attempting to interpret or predict basin sediment yields. In a post-fire context, topography and vegetation patterns exert strong controls on sediment delivery which must be accounted for when interpreting or predicting sediment yields. While most previous research on sediment connectivity has focused on a qualitative analysis, there has been a recent increase in quantitative sediment connectivity analyses. Post-fire researchers should recognize connectivity analyses as essential to studying post-fire sediment dynamics. Land managers can also use connectivity analyses to prioritize erosion mitigation treatments. By identifying areas, from hillslopes to basins, that are disconnected from the potentially impacted target, land managers can focus mitigation on relevant areas for the most cost-effective treatment.

In addition to creating conditions of channel resistance to change that characterized channel response during this study, the September 2013 event caused dramatic channel degradation, transporting sediment that would likely have remained in storage until the next disturbance. The degradation that occurred as a result of the combination of high post-fire erosion potential and a 200-500 year rain event provide evidence for the importance of short duration increases in sediment yield on long term erosion rates.

7. WORKS CITED

Abbott, J.T., 1976. Geologic map of the Big Narrows quadrangle, Larimer County, Colorado: U.S. Geological Survey, Geologic Quadrangle Map GQ-1323, scale 1:24,000.

Ambroise, B., 2004. Variable 'active' versus 'contributing' areas or periods: a necessary distinction. Hydrological Processes 18, 1149-1155.

Burned Area Emergency Response, 2012. High Park Fire Burned Area Emergency Response (BAER) Report. High Park Fire Emergency Stabilization Plan, 12, July 2012.

Baartman, J.E.M., Masselink, R., Keesstra, S.D., Temme, A.J.A.M., 2013. Linking landscape morphological complexity and sediment connectivity. Earth Surface Processes Landforms 38, 1457-1471.

Benavides-Solorio, J. and MacDonald, L.H., 2001. Post-fire runoff and erosion from simulated rainfall on small plots, Colorado Front Range. Hydrological Processes 15, 2931–2952.

Benavides-Solorio, J. and MacDonald, L.H., 2005. Measurement and prediction of post-fire erosion at the hillslope scale, Colorado Front Range. International Journal of Wildland Fire 14, 1-18.

Benda, L., Miller, D., Bigelow, P., Andras, K., 2003. Effects of post-wildfire erosion on channel environments, Boise River, Idaho. Forest Ecology and Management, 178, 105-119.

Benda, L., Hassan, M.A., Church, M., May, C.L., 2005. Geomorphology of steepland headwaters: the transition from hillslopes to channels. Journal of the American Water Resources Association 41, 835-851.

Beyers, J., 2004. Postfire seeding for erosion control: effectiveness and impacts of native plant communities, Conservation Biology 18, 947-956.

Borselli, L., Cassi, P., Torri, D., 2008. Prolegomena to sediment and flow connectivity in the landscape: A GIS and field numerical assessment. Cantena, 75, 268–277.

Bracken, L.J. and Croke, J., 2007. The concept of hydrological connectivity and its contribution to understanding runoff-dominated geomorphic systems. Hydrological Processes 21, 1749-1763.

Braddock, W.A. and LaFountain, L.J., 1988. Geologic map of the Crystal Mountain quadrangle, Larimer County, Colorado: U.S. Geological Survey, Geologic Quadrangle Map GQ-1623, scale 1:24,000

Brierley, G., Fryirs, K., Jain, V., 2006. Landscape connectivity: the geographic basis of geomorphic applications. Area 38, 165–174.

Brogan, D, 2014. Extreme post-wildfire flooding in the Colorado Front Range. Master's thesis, Department of Civil and Environmental Engineering, Colorado State University, Fort Collins, Colorado. 57 pp.

Brunsden, D. and Thornes, J.B., 1979. Landscape sensitivity and change. Transactions of the Institute of British Geographers NS4, 463-484.

Cammeraat, L.H., 2002. A review of two strongly contrasting geomorphological systems within the context of scale. Earth Surface Processes and Landforms 27, 1201-1222.

Cavalli, M., Trevisani, S., Comiti, F., Marchi, L., 2013. Geomorphometric assessment of spatial sediment connectivity in small Alpine catchments. Geomorphology 188, 31–41.

Cawson, J.G., Sheridan, G.J., Smith, H.G., Lane, P.N.J., 2013. Effects of fire severity and burn patchiness on hillslope-scale surface runoff, erosion and hydrologic connectivity in a prescribed burn. Forest Ecology and Management 310, 219-233.

De Vente, J. and Poesen, J., 2005. Predicting soil erosion and sediment yield at the basin scale: Scale issues and semi-quantitative models. Earth-Science Reviews 71, 95-125.

DeBano, L.F., 1981. Water repellent soils: a state-of-the-art. US Department of Agriculture, Forest Service, Pacific Southwest Forest and Range Experiment Station.

DeBano, L.F., 2000. The role of fire and soil heating on water repellency in wildland environments: a review. Journal of Hydrology 231, 195–206.

Doerr, S.H., Shakesy, R.A., McDonald, L.H., 2009. Fire Effects on Soils and Restoration Strategies. Volume Ed. Cerda, A., Robichaud, P.R.—Land Reconstruction and Management Series. Vol.5

Dunne, T. and Leopold, L.P., 1978. *Water in Environmental Planning*. W.H. Freeman and Company. New York, NY. 818 pp.

Eccleston, D.T., 2008. Post-fire Channel Change in Two Small Watersheds in the Colorado Front Range. Master's Thesis, Department of Forest, Rangeland and Watershed Stewardship, Colorado State University, Fort Collins, Colorado. 151 pp.

Faures, J., Goodrich, D.C., Woolhiser, D.A., Sorooshian, S., 1995. Impact of small-scale spatial rainfall variability on runoff modeling. Journal of Hydrology 173, 309-326.

Ferguson, R.I., 1981. Channel forms and channel changes in *British Rivers*, Ed. Lewin J., Allen and Unwin, London; 90-125.

Florsheim, J.L., Keller, E.A., Best, D.W., 1991. Fluvial sediment transport in response to moderate storm flows following chaparral wildfire, Ventura County, southern California. Geol. Soc. Am. Bull. 103, 504–511.

Fryirs, K., 2013. (Dis)Connectivity in catchment sediment cascades: a fresh look at the sediment delivery problem. Earth Surface Processes and Landforms 38, 30–46.

Fryirs, K.A., Brierley, G.J., Preston, N.J., Kasai, M., 2007a. Buffers, barriers and blankets: The (dis)connectivity of catchment-scale sediment cascades. Catena 70, 49–67.

Fryirs, K.A., Brierley, G.J., Preston, N.J., Spencer, J., 2007b. Catchment-scale (dis)connectivity in sediment flux in the upper Hunter catchment, New South Wales, Australia. Geomorphology 84, 297–316.

Gabet, E.J. and Bookter, A., 2008. A morphometric analysis of gullies scoured by post-fire progressively bulked debris flows in southwest Montana, USA. Geomorphology 96, 298-309.

Goode, J.R., Luce, C.H., Buffington, J.M., 2012. Enhanced sediment delivery in a changing climate in semi-arid mountain basins: Implications for water resource management and aquatic habitat in the northern Rocky Mountains. Geomorphology 139-140, 1–15.

Goodrich, D.C., Faures, J., Woolhiser, D.A., Lane, L.J., Sorooshian, S., 1995. Measurment and analysis of small-scale convective storm rainfall variability. Journal of Hydrology 173, 283-308.

Graf, W.L., 1988. *Fluvial Processes in Dryland Rivers*. Blackburn Press, New Jersey, USA. 346 pp.

Harvey, A.M., 1991. The influence of sediment supply on the channel morphology of upland streams: Howgill Fells, Northwest England.

Harvey, A.M., 1997. Coupling between hillslope gully systems and stream channels in the Howgill Fells, northwest England: temporal implications. Geomorphologie: Relief, Processus, Environnement 1, 3-20.

Harvey, A.M., 2002. Effective timescales of coupling within fluvial systems. Geomorphology 44, 175-201.

Hooke, J., 2003. Coarse sediment connectivity in river channel systems: a conceptual framework and methodology. Geomorphology 56, 79–94.

Huffman, E.L., MacDonald, L.H., Stednick, J.D., 2001. Strength and persistence of fire-induced soil hydrophobicity under ponderosa and lodgepole pine, Colorado Front Range. Hydrological Process 15, 2877–2892.

Jarrett, R.D., 1990. Paleohydrologic techniques used to define the spatial occurrence of floods. Geomorphology 3, 181-195.

Johansen, M.P., Hakonson, T.E., Breshears, D.D., 2001. Post-fire runoff and erosion from rainfall simulation: contrasting forests with shrublands and grasslands. Hydrological Process 15, 2953–2965.

Kean, J.W., Staley, D.M., Cannon, S.H., 2011. In situ measurements of post-fire debris flows in southern California: Comparisons of the timing and magnitude of 24 debris-flow events with rainfall and soil moisture conditions. Journal of Geophysical Research 116, 1-21.

Keeley, J.E., 2009. Fire intensity, fire severity and burn severity: a brief review and suggested usage. International Journal of Wildland Fire 18, 116-126.

Kirchner, J.W., Finkel, R.C., Riebe, C.S., Granger, D.E., Clayton, J.L., King, J.G., Megahan, W.F., 2001. Mountain erosion over 10 yr, 10 ky, and 10 my time scales. Geology 29, 591–594.

Knighton, D., 1998. *Fluvial Forms and Processes: A New Perspective*. Arnold, London, 383 pp.

Laird, J.R. and Harvey, M.D., 1986. Complex-response of a chaparral drainage basin to fire. In *Drainage Basin Sediment Delivery Symposium*, Albuquerque, New Mexico. IAHS Publication No. 159, 165-183.

Lane, E.W., 1955. The importance of fluvial geomorphology in hydraulic engineering. American Society of Civil Engineers Proceedings 81, 1-17.

Lane, L.J., Hernandez, M., Nichols, M., 1997. Processes controlling sediment yield from watersheds as functions of spatial scale. Environmental Modelling and Software 12, 355–369.

Lane, S.N. and Thorne, C.R., 2007. River Processes in *Future Flooding and Coastal Erosion Risks*, Ed. Thorne, C.R, Evans, E.P., Penning-Roswell, E. Thomas Telford Publishing, London.

Lane, S.N., Reid, S.C., Tayefi, V., Yu, D., Hardy, R.J., 2008. Reconceptualising coarse sediment delivery problems in rivers as catchment-scale and diffuse. Geomorphology 98, 227–249.

Laronne, J.B., Outhet, D.N., Carling, P.A., McCabe, T.J., 1994. Scour chain employment in gravel bed rivers. Catena 22, 299–306.

Larsen, I.J., MacDonald, L.H., Brown, E., Rough, D., Welsh, M.J., Pietraszek, J.H., Libohova, Z., de Dios Benavides-Solorio, J., Schaffrath, K., 2009. Causes of post-fire runoff and erosion: water repellency, cover, or soil sealing? Soil Science Society of America Journal 73, 1393-1407.

Legleiter, C.J. and Kyriakidis, P.C., 2007. Forward and Inverse Transformations between Cartesian and Channel-fitted Coordinate Systems for Meandering Rivers. Mathematical Geology 38, 927–958.

Legleiter, C.J., Lawrence, R.L., Fonstad, M.A., Andrew Marcus, W., Aspinall, R., 2003. Fluvial response a decade after wildfire in the northern Yellowstone ecosystem: a spatially explicit analysis. Geomorphology 54, 119–136.

Leopold, L.B., 1992. Sediment size that determines channel morphology. In *Dynamics of Gravel-Bed Rivers*. Ed. Billi, P., Hey, R.D., Thorne, C.R., Tacconi, T. John Wiley and Sons Ltd. 297–311.

Leopold, L.B., Wolman, M.G., and Miller, P., 1964. *Fluvial Processes in Geomorphology*. W.H. Freeman and Company. 522 pp.

Lisle, T.E. and Eads, R.E., 1991. Method to measure sedimentation of spawning gravels. Research, PWS-411. Berkeley, CA: Pacific Southwest Research Station, Forest Service, p 1-7.

Lukas, J., Wolter, K., Mahoney, K., Barsugli, J., Doesken, N., Ryan, W., Rangwala, I., Livneh, B., Gordon, E., Hoerling, M., Kiladis, G., and Nacu-Schmidt, A., 2013, Severe flooding on the Colorado Front Range, September 2013: A preliminary assessment from the CIRES Western Water Assessment at the University of Colorado, NOAA ESRL Physical Science Division, and the CSU Colorado Climate Center, 4 pp.

MacDonald, L.H. and Stednick, J.D., 2003. Forests and water; a state-of-the-art review for Colorado. Colorado Water Resources Research Institute, Completion Report No. 196: Fort Collins, CO 65 pp.

MacDonald, L.H. and Huffman, E.L., 2004. Post-fire soil water repellency. Soil Science Society of America 68, 1729–1734.

MacDonald, L.H. and Larsen, 2009. Effects of Forest Fires and Post-Fire Rehabilitation: A Colorado, USA Case Study. In *Fire Effects on Soils and Restoration Strategies*. Ed. Cerda, A., and Robichaud, P.R. Science Publishers, Enfield, NH, 423-452.

Madej, M.A. and Ozaki, V., 1996. Channel response to sediment wave propagation and movement, Redwood Creek, California, USA. Earth Surface Processes and Landforms 21, 911–927.

May, C.L. and Gresswell, R.E., 2004. Spatial and temporal patterns of debris-flow deposition in the Oregon Coast Range, USA. Geomorphology 57, 135–149.

Mayor, Á.G., Bautista, S., Small, E.E., Dixon, M., Bellot, J., 2008. Measurement of the connectivity of runoff source areas as determined by vegetation pattern and topography: A tool for assessing potential water and soil losses in drylands. Water Resources Research 44, 1-13.

Mekik, C. and Arslangolu, M., 2009. Investigation on Accuracies of Real Time Kinematic GPS for GIS Applications. Remote Sensing 1, 22-35.

Merritt, D.M. and Wohl, E.E., 2003. Downstream hydraulic geometry and channel adjustment during a flood along an ephemeral, arid-region drainage. Geomorphology 52, 165–180.

Meyer, G.A. and Wells, S.G., 1997. Fire-related sedimentation events on alluvial fans, Yellowstone National Park, USA. Journal of Sedimentary Research 67, 776-791.

Miller, J.D., Nyhan, J.W., Yool, S.R., 2003. Modeling potential erosion due to the Cerro Grand Fire with a GIS-based implementation of the Revised Universal Soil Loss Equation. International Journal of Wildland Fire 12, 85-100.

Montgomery, D.R., 1999. Process domains and the river continuum. Journal of the American Water Resources Association 35, 397-410.

Montgomery, D.R. and Buffington, J.M., 1997. Channel-reach morphology in mountain drainage basins. Geological Society of America Bulletin 109, 596-611.

Moody, J.A., 2001. Sediment transport regimes after a wildfire in steep mountainous terrain, in: Proceedings of the Seventh Federal Interagency Sedimentation Conference, Reno, 41–48.

Moody, J.A. and Martin, D.A., 2001a. Initial hydrologic and geomorphic response following a wildfire in the Colorado Front Range. Earth Surface Processes and Landforms 26, 1049–1070.

Moody, J.A. and Martin, D.A., 2001b. Post-fire, rainfall intensity–peak discharge relations for three mountainous watersheds in the western USA. Hydrological Process.es 15, 2981–2993.

Moody, J.A. and Martin, D.A., 2009. Synthesis of sediment yields after wildland fire in different rainfall regimes in the western United States. International Journal of Wildland Fire 18, 96-115.
Moody, J.A. and Ebel, B.A., 2014. Infiltration and runoff generation processes in fire-affected soils. Hydrological Process 28, 3432–3453.

Moody, J.A., Shakesby, R.A., Robichaud, P.R., Cannon, S.H., Martin, D.A., 2013. Current research issues related to post-wildfire runoff and erosion processes. Earth-Science Reviews 122, 10–37.

Morris, S.E. and Moses, T.A., 1987. Forest fire and the natural soil erosion regime in the Colorado Front Range. Annals of the Association of American Geographers 77, 255-264.

Nawa, R.K. and Frissell, C.A., 1993. Measuring scour and fill of gravel streambeds with scour chains and sliding-bead monitors. North American Journal of Fisheries Management 13, 634–639.

Nesse, W.D. and Braddock, W.A., 1989, Geologic map of the Pingree Park quadrangle, Larimer County, Colorado: U.S. Geological Survey, Geologic Quadrangle Map GQ-1622, scale 1:24,000.

Newcombe, C.P. and Macdonald, D.D., 1991. North American Journal of Fisheries Management 11, 72-82.

NOAA Atlas 14 Point Precipitation Frequency Estimates: CO. http://hdsc.nws.noaa.gov/hdsc/pfds/pfds_map_cont.html?bkmrk=co. Accessed March, 2015.

NOAA-NWS, 2013. Exceedance Probability analysis for the Colorado flood event 9-16 September 2013. Hydrometerological Design Studies Center, Silver Springs, MD.

Owens, P.N., Blake, W.H., Giles, T.R., Williams, N.D., 2012. Determining the effects of wildfire on sediment sources using 137Cs and unsupported 210Pb: the role of landscape disturbances and driving forces. Journal of Soils Sediments 12, 982–994.

Patric, J.H. and Evans, J., 1984. Summary of sediment yield data from forested lands in the United States. Journal of Forestry 82, 101-104.

Phillips, J.D., 1991. Multiple modes of adjustment in unstable river channel cross-sections. Journal of Hydrology 123, 39-49.

Pietraszek, J.H., 2006. Controls on post-fire erosion at the hillslope scale, Colorado Front Range. Master's Thesis, Department of Forest, Rangeland, and Watershed Stewardship, Colorado State University, Fort Collins, Colorado, 124 pp.

Reaney, S.M., Bracken, L.J., Kirkby, M.J., 2007. Use of the Connectivity of Runoff Model (CRUM) to investigate the influence of storm characteristics on runoff generation and connectivity in semi-arid areas. Hydrological Processes 21, 894-906.

Reneau, S.L., Katzman, D., Kuyumjian, G.A., Lavine, A., Malmon, D.V., 2007. Sediment delivery after a wildfire. Geology 35, 151–154.

Rengers, F.K., Tucker, G.E., Moody, J.A. Illuminating Wildfire Erosion and Deposition Patterns with Repeat Terrestrial LiDAR (in review).

Rice, S., 1999. The Nature and Controls on Downstream Fining within Sedimentary Links. Journal of Sedimentary Research 69, 32-39.

Richer, E.E., 2009. Snowmelt runoff analysis and modeling for the Upper Cache la Poudre Basin, Colorado. M.S. Thesis, Department of Forest, Rangeland and Watershed Stewardship, Colorado State University, Fort Collins, Colorado, 117 pp.

Robichaud, P., 2005. Measurement of post-fire hillslope erosion to evaluate and model rehabilitation treatment effectiveness and recovery. International Journal of Wildland Fire 14, 475-485.

Robichaud, P.R., Beyers, J.L., Neary, D.G., 2000. Evaluating the effectiveness of postfire rehabilitation treatments. US Department of Agriculture, Forest Service, Rocky Mountain Research Station Fort Collins, CO, USA.

Robichaud, P.R., Lewis, S.A., Wagenbrenner, J.W., Ashmun, L.E., Brown, R.E., 2013a. Post-fire mulching for runoff and erosion mitigation. Catena 105, 75–92.

Robichaud, P.R., Wagenbrenner, J.W., Lewis, S.A., Ashmun, L.E., Brown, R.E., Wohlgemuth, P.M., 2013b. Post-fire mulching for runoff and erosion mitigation Part II: Effectiveness in reducing runoff and sediment yields from small catchments. Catena 105, 93–111.

Rough, D., 2007. Effectiveness of rehabilitation treatments in reducing post-fire erosion after the Hayman and Schoonover fires, Colorado Front Range. M.S. Thesis, Department of Forest, Rangeland and Watershed Stewardship, Colorado State University, Fort Collins, CO, 177 pp.

Rough, D. and MacDonald, L.H., 2005. Effectiveness of BAER treatments in reducing post-fire erosion after the Hayman Fire, Colorado Front Range. Proceedings, AGU Hydrology Days, Colorado State University, Fort Collins, Colorado.

Ryan, K. and Noste, N., 1985. Evaluating prescribed fires, pp. 230-238 in: JE Lotan et al.(tech. coor) Proceedings - Symposium and Workshop on Wilderness Fire. USDA Forest Service Intermountain Forest and Range Experiement Station, General Technical Report INT-182.

Schmeer, S., 2014. Post-fire erosion response and recovery, High Park Fire, Colorado. M.S. Thesis, Department of Environmental Science and Stewardship, Colorado State University, Fort Collins, CO, 159 pp.

Schumm, S.A., 1973. Geomorphic thresholds and complex response in drainage systems. In *Fluvial geomorphology*. Ed. M.Morisawa, SUNY Binghamton Publications in Geomorphology, 299-310.

Schumm, S.A., 1977. *The fluvial system*. John Wiley & Sons, New York, 338 pp.

Schumm, S.A. and Parker, R.S., 1973. Implications of complex response of drainage systems for Quaternary alluvial stratigraphy. Science 243, 99-100.

Shakesby, R. and Doerr, S., 2006. Wildfire as a hydrological and geomorphological agent. Earth-Science Reviews 74, 269–307.

Shaver, K.C., Nesse, W.D., and Braddock, W.A., 1988, Geologic map of the Rustic quadrangle, Larimer County, Colorado: U.S. Geological Survey, Geologic Quadrangle Map GQ-1619, scale 1:24,000.

Smith, J.D. and McLean, S.R., 1984. A model for flow in meandering streams. Water Resources Research 20, 1301-1315.

Smith, H.G., Sheridan, G.J., Lane, P.N.J., Noske, P.J., Heijnis, H., 2011. Changes to sediment sources following wildfire in a forested upland catchment, southeastern Australia. Hydrological Processes 25, 2878–2889.

Spigel, K.M. and Robichaud, P.R., 2007. First-year post-fire erosion rates in Bitterroot National Forest, Montana. Hydrological Processes 21, 998–1005.

Stover, S.C. and Montgomery, D.R., 2001. Channel change and flooding, Skokomish River, Washington. Journal of Hydrology 243, 272–286.

Veblen, T.T. and Donnegan, J.A., 2005. Historical Range of Variability for Forest Vegetation of the national Forests of the Colorado Front Range. USDA Forest Service Rocky Mountain Region, Golden, CO.

Veblen, T.T., Romme, W.H., Regan, C., 2012. Regional Application of Historical Ecology at Ecologically Defined Scales: Forest Ecosystems in the Colorado Front Range. In Historical Environmental Variation in Conservation and Natural Resource Management, 149–165.

Vega, J.A., Fernández, C., Fonturbel, T., 2015. Comparing the effectiveness of seeding and mulching+seeding in reducing soil erosion after a high severity fire in Galicia (NW Spain). Ecological Engineering 74, 206–212.

Walling, D.E., 1983. The Sediment Delivery Problem. Journal of Hydrology 65, 209-237.

Wagenbrenner, J.W., MacDonald, L.H., Rough, D., 2006. Effectiveness of three post-fire rehabilitation treatments in the Colorado Front Range. Hydrological Processes 20, 2989–3006.

Wester, T., Wasklewicz, T., Staley, D., 2014. Functional and structural connectivity within a recently burned drainage basin. Geomorphology 206, 362–373.

Westerling, A.L., 2006. Warming and Earlier Spring Increase Western U.S. Forest Wildfire Activity. Science 313, 940–943.

Wilkinson, S.N., Wallbrink, P.J., Hancock, G.J., Blake, W.H., Shakesby, R.A., Doerr, S.H., 2009. Fallout radionuclide tracers identify a switch in sediment sources and transport-limited sediment yield following wildfire in a eucalypt forest. Geomorphology 110, 140–151.

Wohl, E., 2013. Migration of channel heads following wildfire in the Colorado Front Range, USA: Channel heads following wildfire. Earth Surface Processes and Landforms 38, 1049–1053.

Zelt, R.B. and Wohl, E.E., 2004. Channel and woody debris characteristics in adjacent burned and unburned watersheds a decade after wildfire, Park County, Wyoming. Geomorphology 57, 217–233.

APPENDIX A: RAINFALL-PEAK STAGE RELATIONSHIP

Peak stage-rainfall relationships are drawn from data collected at WPW XS 3e during 2013. A variety of logistics problems, including battery failures, storage capacity limitations, and unexplained errors render data collected at other depth sensors unsuitable for analysis.

Peak stage-rainfall relationships observed at WPW XS 3e illustrate the importance of selecting rainfall metrics when evaluating runoff and erosion response at the hillslope and small basin scale. Storms with MI_{30} and MI_{15} < 10 mm hr^{-1} were capable of generating runoff in the ephemeral channel. This result, combined with data collected by automated suspended sediment samplers suggests that low intensity storms can produce increases in discharge that are capable of delivering suspended sediment. It also supports the hypothesis that low intensity events may deliver sediments to the channel network and perhaps transport sediments within the channel network, but perhaps not to the basin outlet due to the short duration of increased discharge. Interpretation of the subsequent events must then take into account previous storm history.

There is a strong positive correlation between both MI_{15} and MI_{30} and maximum flow depth (Figure 28). Two rainfall events highlight the importance of selecting an appropriate rainfall metric when evaluating runoff and erosion response, 1) a minor increase in MI_{30} results in a dramatic increase in stage and 2) A significant increase in MI_{30} results in a minimal increase in stage. As discussed previously, the temporal variability of a given rainfall event may exert a significant influence on runoff response. An alternative explanation suggests that at small spatial scales runoff response, and therefore stream discharge may be better predicted by MI_{15}. Examining the same two events reveals that in scenario (1) there was a significant increase in the MI_{15} (27.1 to 34.6 mm hr^{-1}) despite a minimal increase in MI_{30} (21.7 to 22.1 mm hr^{-1}) and (2) There was little increase in MI_{15} (26.4 to 27.1 mm hr^{-1}) despite a significant increase in MI_{30} (15.2 to 21.7 mm hr^{-1}). These results provide a limited data set that suggests that MI_{15}

may be a better predictor of peak discharge than MI_{30} at small spatial scales. The coefficients of each regression (MI_{30}, 1.21 and MI_{15}, 0.84) indicate that a unit increase in MI_{30} will have a greater increase in stage than an equal unit increase in MI_{15}. This difference results because an increase in MI_{30} requires a longer period of more intense rainfall, and therefore a greater total depth, increasing the amount of rainfall capable of being converted to discharge, while increases in MI_{15} are more sensitive to very short bursts of intense rainfall but may not produce enough total depth to cause as large an increase in stage. Both MI_{15} and MI_{30} are strong predictors of stage depth, r-squared 0.87 and 0.85, respectively. Using erosivity as a predictor of maximum flow depth produced a lower r squared value (0.82) and exhibited the same trend as using MI_{30} where, 1) an increase in erosivity corresponded to a decrease in peak stage 2) an equal increase in erosivity corresponded to both small and large increases in peak stage. Interpretation of these results is also made more difficult by the potential for different threshold responses.

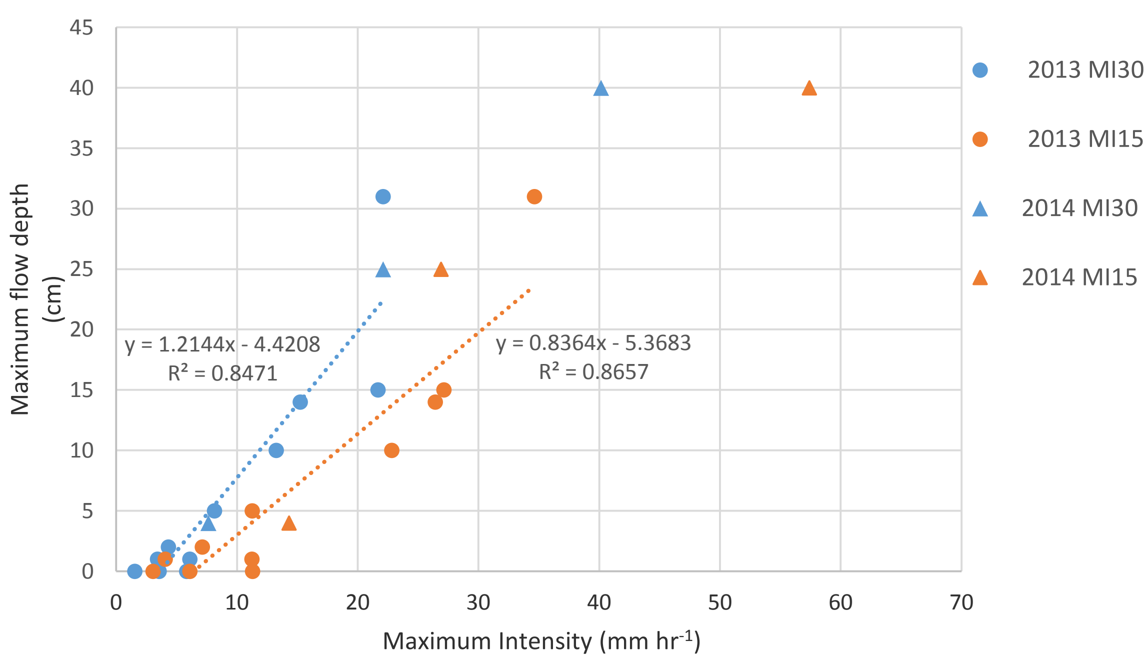

Figure 29: 2013 and 2014 maximum flow depth versus MI_{15} and MI_{30} at WPW 3e that shows a strong positive correlation between rainfall intensity and maximum depth of flow. Regression values apply only to 2013 data.

Moody and Martin (2001b) found that MI_{30} was the best predictor of peak discharge in basins with contributing areas 17-27 km^2. Results from this study suggest that in small basins MI_{15} may have greater explanatory power in determining peak discharge, and therefore geomorphic response. Another issue that must be addressed is the differences between peak-discharge, which may exert the greatest influence on channel response (channel geometry), and the duration of elevated discharge, which may control the total quantity of sediment produced at the basin scale. Threshold response at the hillslope scale as well as in the channel network make integration of erosion response across spatial scales challenging.

It is important to recognize the linear relationship shown between rainfall intensity and stage likely indicates a non-linear relationship between rainfall and discharge, since the relationship between stage and discharge is non-linear. Furthermore, maximum stage values reported in this study are underestimates, as demonstrated by the scour and fill dynamic revealed by the scour chains at WPW XS 3e.

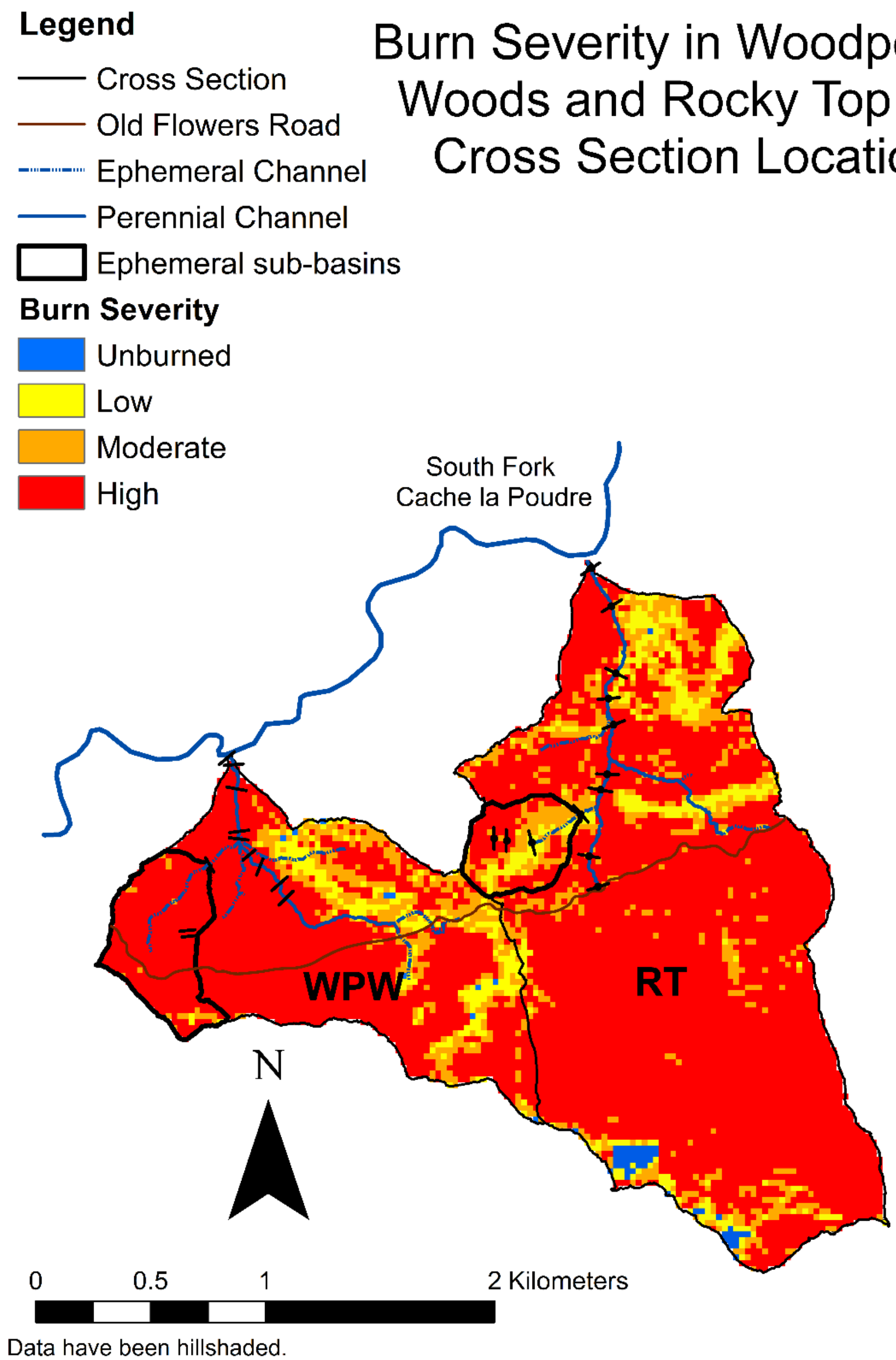

Figure 30: Burn Severity in WPW and RT and locations of cross sections.

Ground cover surveys in 2013 and 2014 indicated that there was significantly more ground cover in the RT ephemeral sub-basin than the WPW ephemeral sub-basin (Table 11), a finding that is supported by the burn severity map (Figure 29). This finding however, demonstrates an additional challenge when attempting to assess the influence of mulch on channel response. Because the control basin, despite being unmulched, had higher levels of ground cover than the treated basin, evaluating the role of mulch is unrealistic. It is also worth noting that ground cover surveys were not completed until after the 7/1/2013 storm that transported significant quantities of mulch (Figure 18).

Table 13: Bare soil and ground cover in WPW and RT in 2013 and 2014. Survey was completed during the second week of July during both field seasons. Ground cover was classified as rock, bare soil, ash, live vegetation, organic, mulch, charcoal, or wood. Bare soil includes only the bare soil, rock, and ash categories.

	2013		2014	
	Bare soil	Ground cover	Bare soil	Ground cover
WPW	0.72	0.28	0.70	0.30
RT	0.53	0.47	0.43	0.57

The table shows that ground cover recovery was greater in RT than in WPW during the course of the study. This difference, which is opposite of what is suggested by the mulch treatment is likely due to, (1) the removal of mulch by the 7/1/2013 storm rendering it ineffective at promoting regrowth of vegetation, and (2) differences in burn severity that encouraged quicker vegetative regrowth in RT.

APPENDIX C: 2013 AND 2014 RAINFALL CHARACTERISTICS

Table 14: 2013 Rainfall event characteristics in WPW and RT.

WPW				**RT**			
Date	Depth (mm)	MI_{30} (mm/hr)	EI_{30} (MJ mm ha^{-1} hr^{-1})	Date	Depth (mm)	MI_{30} (mm/hr)	EI_{30} (MJ mm ha^{-1} hr^{-1})
7/1/2013	16.3*	NA*	NA*	7/1/2013	NA*	NA*	NA*
7/12/2013	3.1	3.6	2.1	7/12/2013	3.3	4.1	2.4
7/13/2013	9.7	15.2	33.1	7/13/2013	8.4	12.7	22.7
7/14/2013	11.7	21.7	55.4	7/14/2013	9.7	18.3	41.8
7/18/2013	17.8	13.2	48.9	7/18/2013	9.4	6.6	10.7
7/20/2013	11.1	22.1	61.1	7/20/2013	11.8	23.2	63.9
7/27/2013	1.5	3.0	0.7	7/27/2013	2.0	4.1	1.4
7/28/2013	4.1	3.4	2.2	7/28/2013	3.7	3.6	2.0
8/8/2013	0.8	1.5	0.2	8/8/2013	2.4	4.8	2.2
8/9/2013	3.1	6.1	3.4	8/9/2013	1.5	3.1	0.7
8/18/2013	3.2	5.8	3.5	8/18/2013	0.8	1.5	0.2
8/23/2013	2.3	4.3	2.0	8/23/2013	1.3	1.3	0.3
8/26/2013	1.8	2.0	0.5	8/26/2013	2.3	3.5	1.0
8/27/2013	4.1	7.6	5.2	8/27/2013	2.5	4.6	1.7
8/30/2013a	8.4	15.7	27.1	8/30/2013a	9.9	18.2	40.1
8/30/2013b	2.0	4.1	1.2	8/30/2013b	2.0	3.5	1.0
9/5/2013	4.1	8.1	6.9	9/5/2013	6.2	12.5	18.6
9/8/2013	12.2	6.6	11.6	9/8/2013	16.0	12.6	35.0
9/9/2013	2.5	3.5	1.5	9/9/2013	6.4	10.4	14.3
9/10 - 9/13/2013	166.1	13.2	320.7	9-10 to 9-13-2013	152.7	13.7	298.9
9/14/2013	2.0	4.1	1.0	9/14/2013	2.3	4.0	1.2
9/15/2013	13.7	4.5	7.2	9/15/2013	14.2	5.6	9.6

Table 15: 2014 Rainfall event characteristics in WPW and RT.

WPW Date	Depth (mm)	MI_{30} (mm/hr)	EI_{30} (MJ mm ha^{-1} hr^{-1})	RT Date	Depth (mm)	MI_{30} (mm/hr)	EI_{30} (MJ mm ha^{-1} hr^{-1})
6/23/2014	2.5	5.1	2.0	6/23/2014	5.8	10.7	11.2
6/24/2014	2.8	5.6	3.2	6/24/2014	2.8	5.6	2.9
7/3/2014	2.4	4.1	1.2	7/3/2014	1.4	2.8	0.5
7/4/2014	2.8	5.6	2.9	7/4/2014	2.8	5.6	3.2
7/7/2014	6.0	8.6	8.3	7/7/2014	7.1	11.9	18.0
7/9/2014	1.3	1.5	0.2	7/9/2014	1.5	1.8	0.5
7/10/2014	2.9	5.8	3.8	7/10/2014	1.4	2.0	0.3
7-11-2014a	2.8	4.8	2.2	7-11-2014a	5.6	8.2	11.5
7-11-2014b	2.8	3.6	1.4	7-11-2014b	1.8	2.1	0.5
7/12/2014	21.8	40.1	215.2	7/12/2014	15.4	27.1	101.6
7/13/2014	3.8	7.1	4.4	7/13/2014	3.8	7.3	4.5
7-15-2014a	2.3	4.1	1.4	7-15-2014a	1.8	3.0	0.8
7-15-2014b	1.3	2.0	0.2	7-15-2014b	2.3	3.4	1.1
7-16-2014a	1.5	3.1	0.8	7-16-2014a	1.7	3.3	1.0
7-16-2014b	5.3	8.8	8.4	7-16-2014b	3.3	3.8	1.7
7/29/2014	63.5	22.1	189.3	7/29/2014	66.8	13.2	116.0
8/5/2014	1.3	2.5	0.4	8/5/2014	2.3	4.6	1.9
8/15/2014	4.1	7.6	6.1	8/15/2014	4.3	7.9	7.6
8/19/2014	6.1	11.5	12.1	8/19/2014	4.6	7.9	6.5
8/25/2014	4.6	4.1	2.1	8/25/2014	3.9	3.1	1.5
8/29/2014	0.8	1.5	0.1	8/29/2014	1.7	3.3	0.9

APPENDIX D: P-VALUES FOR PREDICTING ΔMBE AND ΔD

Table 16: **P-values for all predictor and response variables in 2014. The relationship between slope and ΔMBE for the 7/12/2014 storm (p-value 0.07) was positive, suggesting that increasing slope leads to increasing aggradation.**

Storm	data set	predictor	response	p-value	Storm	data set	predictor	response	p-value
7/12/2014	Wpper	slope	ΔMBE	0.071	7/29/2014	Wpper	slope	ΔMBE	0.62
		slope*area		0.51			slope*area		0.76
		area		0.25			area		0.51
		slope+area		0.18			slope+area		0.79
		w:d		0.57			w:d		0.44
7/12/2014	Wpper	slope	ΔD	0.127	7/29/2014	Wpper	slope	ΔD	0.43
		slope*area		0.99			slope*area		0.51
		area		0.09			area		0.96
		slope+area		0.14			slope+area		0.72
		w:d		0.49			w:d		0.73
7/12/2014	Rtper	slope	ΔMBE	0.54	7/29/2014	Rtper	slope	ΔMBE	0.72
		slope*area		0.86			slope*area		0.42
		area		0.52			area		0.49
		slope+area		0.66			slope+area		0.77
		w:d		0.97			w:d		0.29
7/12/2014	Rtper	slope	ΔD	0.22	7/29/2014	Rtper	slope	ΔD	0.64
		slope*area		0.46			slope*area		0.87
		area		0.94			area		0.53
		slope+area		0.5			slope+area		0.72
		w:d		0.66			w:d		0.66
7/12/2014	WP + RT per	slope	ΔMBE	0.61	7/29/2014	WP + RT per	slope	ΔMBE	0.61
		slope*area		0.37			slope*area		0.37
		area		0.33			area		0.33
		slope+area		0.5			slope+area		0.5
		w:d		0.75			w:d		0.75
7/12/2014	WP + RT per	slope	ΔD	0.93	7/29/2014	WP + RT per	slope	ΔD	0.93
		slope*area		0.73			slope*area		0.73
		area		0.91			area		0.91
		slope+area		0.99			slope+area		0.99
		w:d		0.82			w:d		0.82

APPENDIX E: SUSPENDED SEDIMENT CONCENTRATION

Table 17: 2013 SSC, MI_{30}, peak timing, and stage differences in WPW and RT. "Stage difference at peak" refers the difference in stage at the max SSC comparted to base flow, "Max. stage difference" is the difference between base flow and the maximum stage of the event. Bold values indicate a dam release is responsible for the rise in stage.

WPW Date	SSC (mg L^{-1})	MI_{30} (mm hr^{-1})	Time at peak	Stage difference at SSC (m)	Max. stage difference (m)
7/13/2013	3043	15.2	19:20	0.02	0.11
7/14/2013	3144	21.7	23:50	0.04	0.04
7/18/2013	2935	13.2	13:40	0.03	0.03
7/20/2013	2976	22.1	15:40	0.05	0.09
7/27/2013	**186**	**0**	**21:50**	**0.06**	**0.10**
8/9/2013	645	6.1	17:00	0.00	0.01
8/14/2013	**85**	**0**	**15:50**	**0.07**	**0.07**
8/27/2013	781	7.6	23:00	0.01	0.01
8/30/2013	3180	15.7	13:30	0.02	0.03
9/5/2013	3283	8.1	17:30	0.01	0.09
9/8/2013	3069	6.6	15:50	0.02	0.10
9/9/2013	1375	3.5	14:10	0.01	0.01
RT Date	SSC (mg L^{-1})	MI_{30} (mm hr^{-1})	Time at peak	Stage difference at SSC (m)	Max. stage difference (m)
7/13/2013	NA	12.7	NA	NA	NA
7/14/2013	3528	18.3	0:00	0.07	0.07
7/18/2013	1248	6.6	14:40	0.03	0.03
7/20/2013	3884	23.2	16:20	0.04	0.12
7/27/2013	**233**	**0**	**22:30**	**0.08**	**0.09**
8/9/2013	419	3.1	18:30	0.00	0.01
8/14/2013	**101**	**0**	**16:10**	**0.06**	**0.07**
8/27/2013	166	4.6	0:30	0.01	0.01
8/30/2013	3348	18.2	13:40	0.03	0.07
9/5/2013	3771	12.5	16:00	0.01	0.09
9/8/2013	NA	12.6	NA	NA	NA
9/9/2013	3869	10.4	14:20	NA	NA

Table 18: 2014 SSC, MI_{30}, peak timing, and stage differences in WPW and RT. Bold values indicate upstream dam release.

WPW Date	SSC (mg L^{-1})	MI_{30} (mm hr^{-1})	Time at peak	Stage difference at peak SSC (m)	Max. stage difference (m)
7/12/2014	1326	40.1	16:30	0.12	0.13
7/16/2014	408	8.8	15:10	0.02	0.05
7/29/2014	1153	22.1	13:30	0.04	0.19
8/9/2014	**82**	**0**	**17:30**	**0.13**	**0.13**
8/14/2014	65	0	23:00	0	0
8/15/2014	214	7.6	13:40	0.01	0.01
8/16/2014	**69**	**0**	**18:20**	**0.15**	**0.16**
8/19/2014	27	11.5	16:20	0	0
RT Date	SSC (mg L^{-1})	MI_{30} (mm hr^{-1})	Time at peak	Stage difference at peak SSC (m)	Max. stage difference (m)
7/12/2014	3104	27.1	17:00	0.08	0.22
7/16/2014	167	3.8	15:50	0.02	0.04
7/29/2014	994	13.2	17:40	0.05	0.19
8/9/2014	**75**	**0**	**18:00**	**0.13**	**0.13**
8/14/2014	55	0	21:30	0	0
8/15/2014	230	7.9	14:40	0.01	0.02
8/16/2014	**58**	**0**	**19:00**	**0.16**	**0.17**
8/19/2014	17	7.9	17:00	0	0

APPENDIX F: LONGITUDINAL PROFILE SURVEYS

Table 19: Reach length and slope in WPW and RT.

	Slope	Length (m)
Wr1p	0.04	42
Wr2p	0.1	70
Wr3p	0.08	83
Wr4p	0.15	90
Rr1p	0.09	100
Rr2p	0.1	100
Rr3p	0.07	120
Rr4p	0.1	100
Wr1s	0.22	104
Wr2e	0.06	270
Rr1s	0.28	150
Rr2e	0.15	160
Rr3e	0.11	130

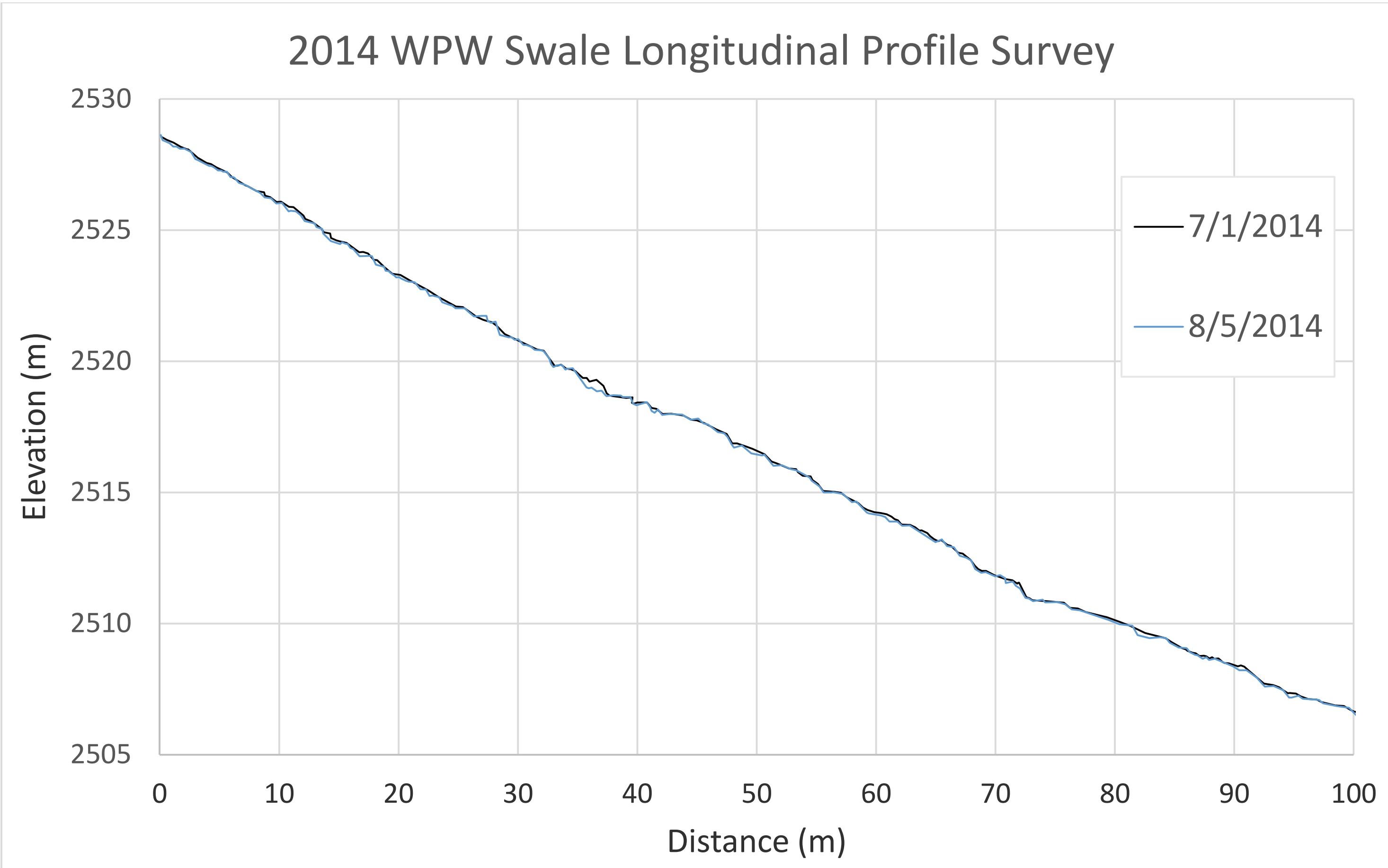

Figure 31: 2014 WPW swale longitudinal profile survey. Profile indicates the dominant response along this reach was degradation. ΔMTE was -5.2cm.

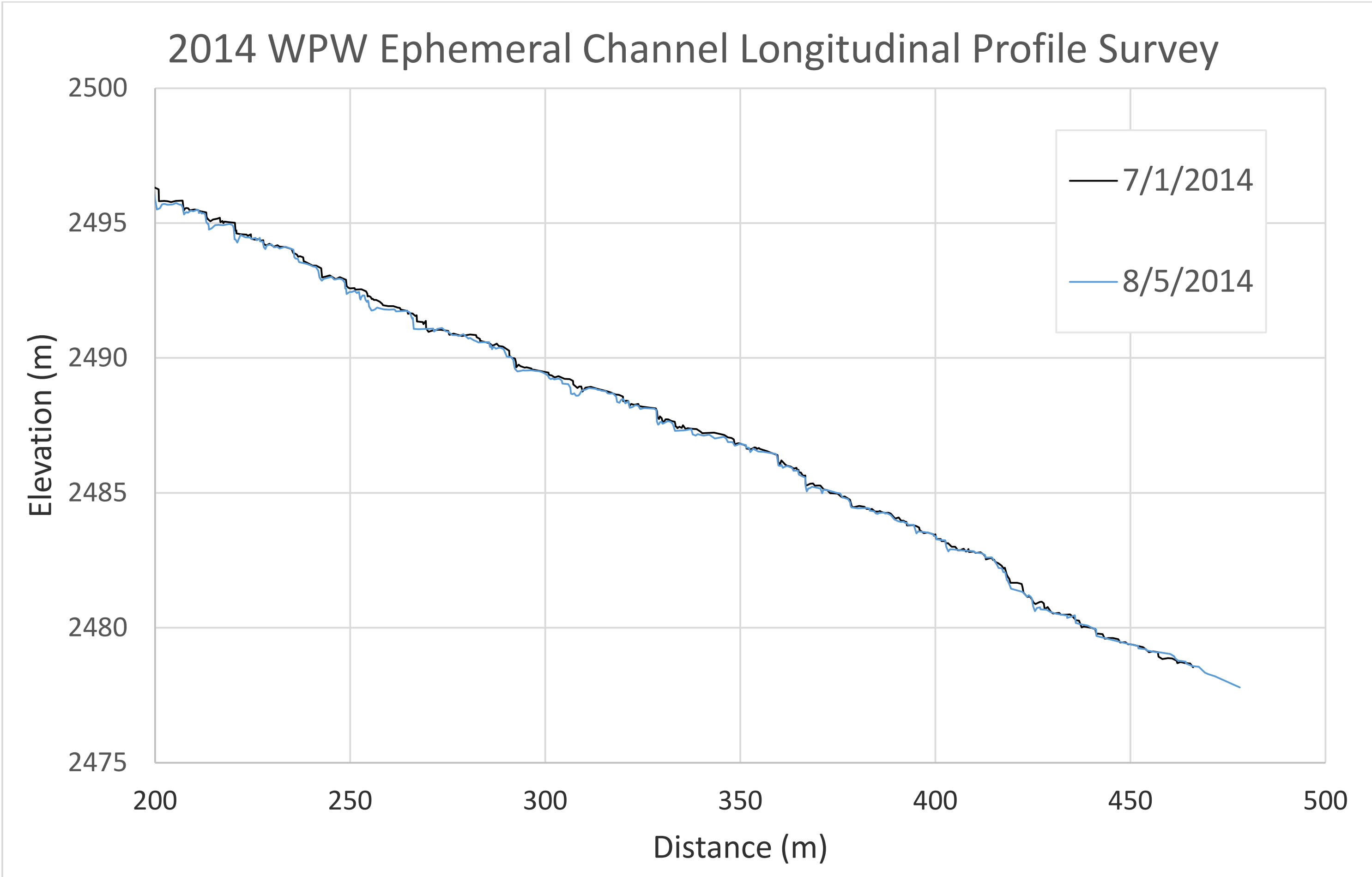

Figure 32: 2014 WPW ephemeral channel longitudinal profile. Profiles indicate that the dominant response was degradation. Degradation appears to be the result of the creation of knickpoints and headward erosion, and the creation and deepening of scour pools.

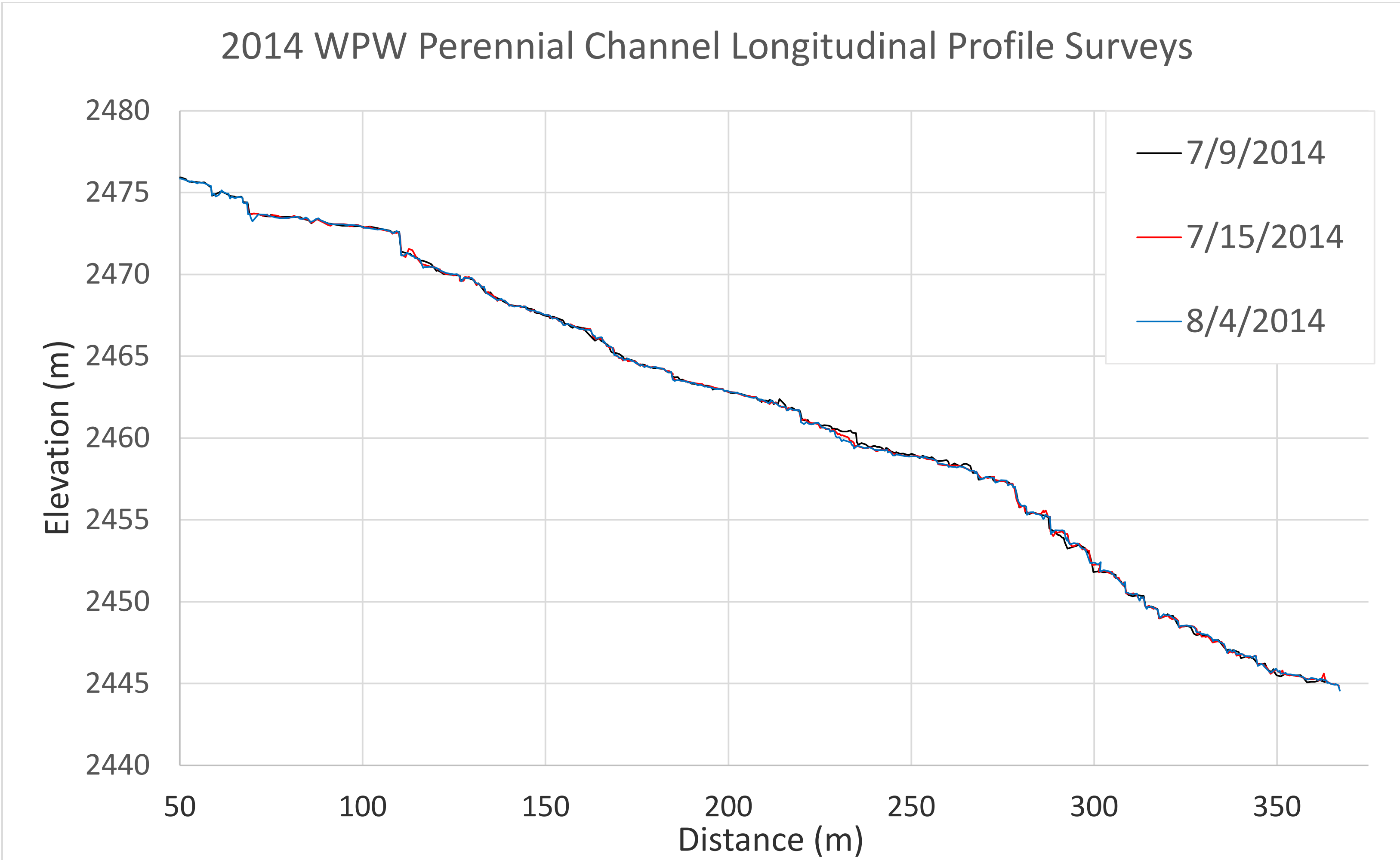

Figure 33: 2014 WPW perennial channel longitudinal profile. The three profiles account for changes caused by the 7/12/2014 and 7/29/2014 storms and reveals a channel largely resistant to change despite numerous knickpoints. The profiles do not show any areas of extensive aggradation or degradation during the survey period.

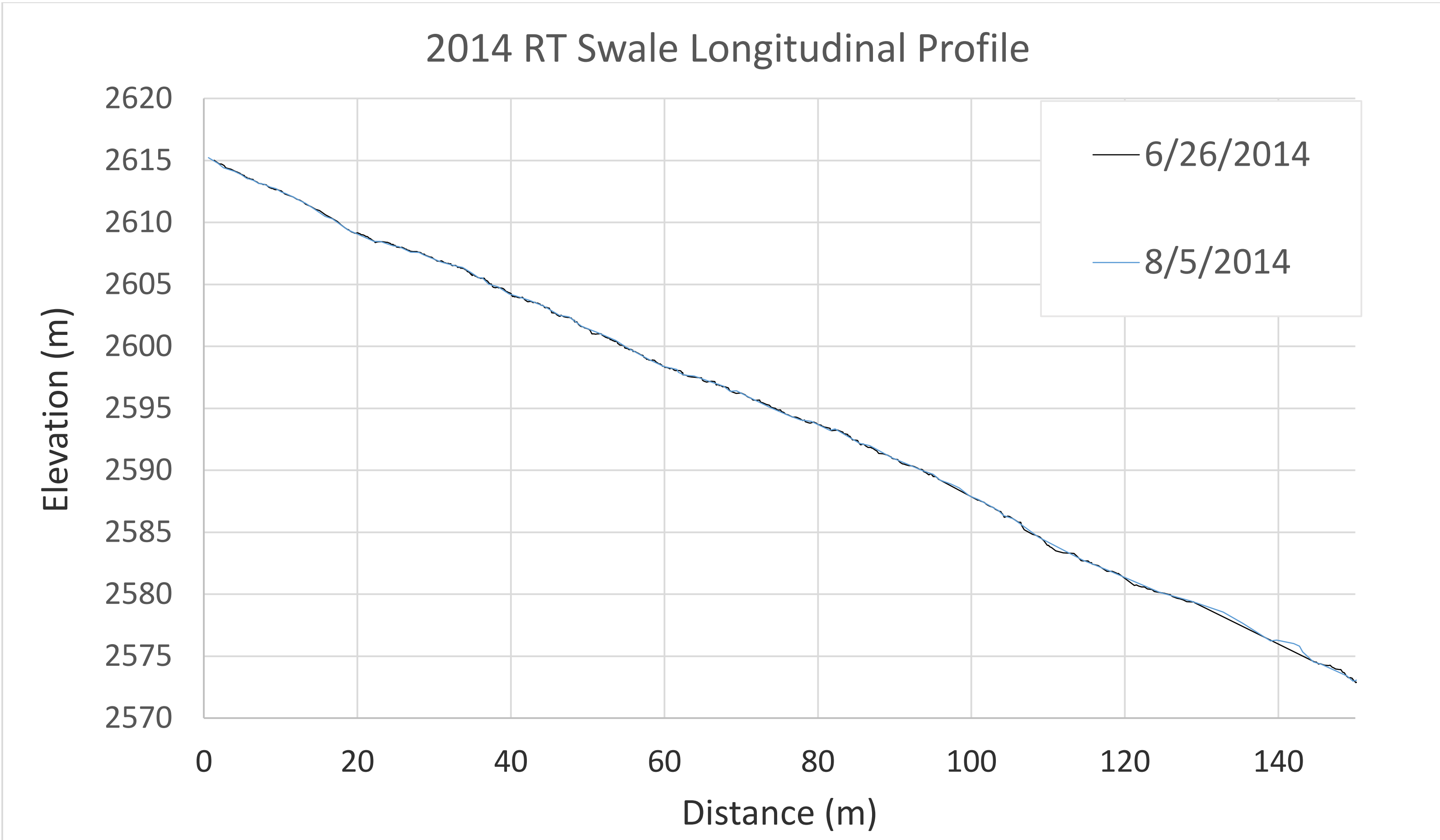

Figure 34: 2014 RT swale longitudinal profile. The dominant response of the swale during summer 2014 was degradation, ΔMTE = -3.7 cm.

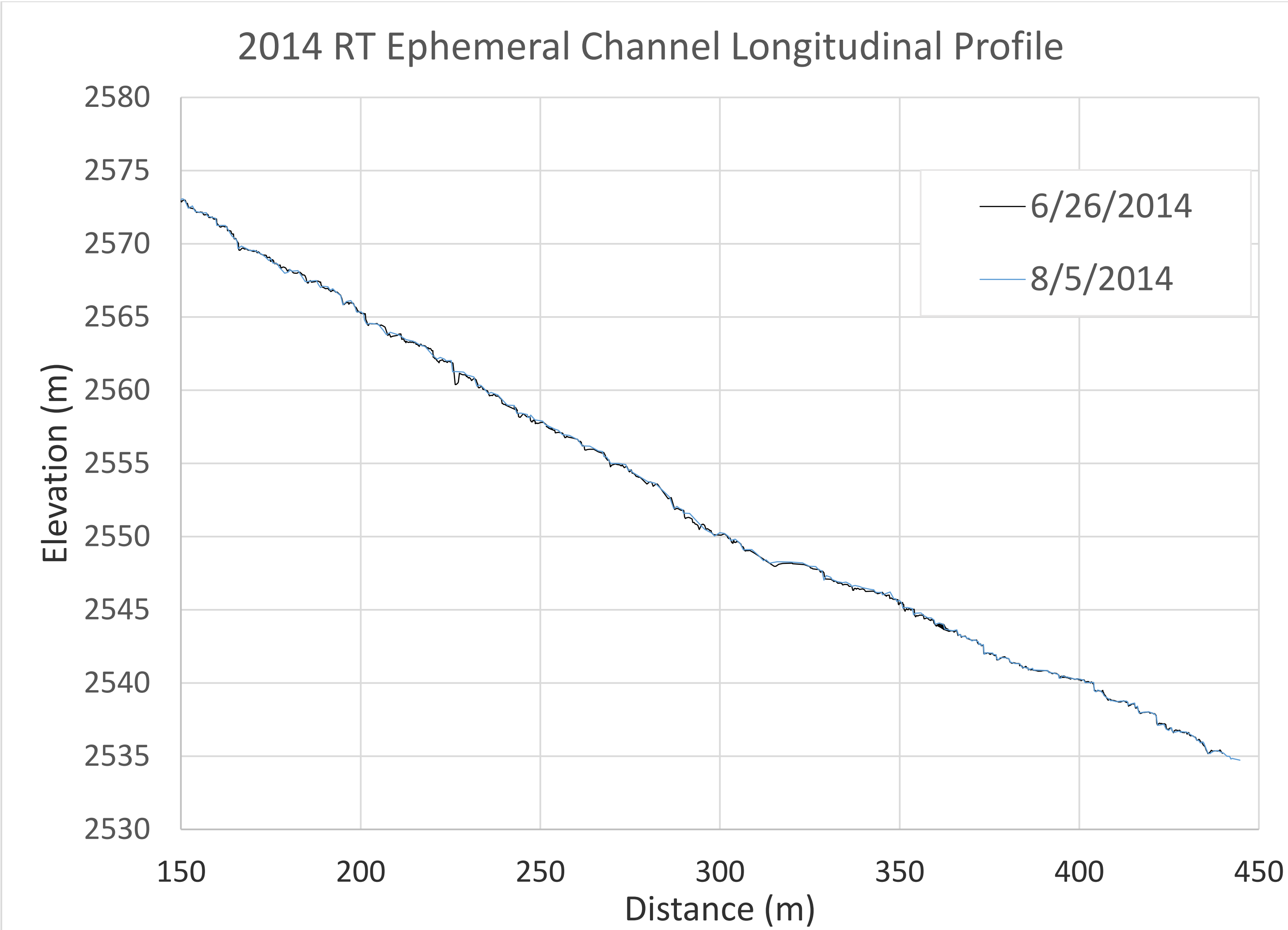

Figure 35: 2014 RT ephemeral channel longitudinal profile that reveals a channel largely resistant to change during summer 2014, despite numerous knickpoints.

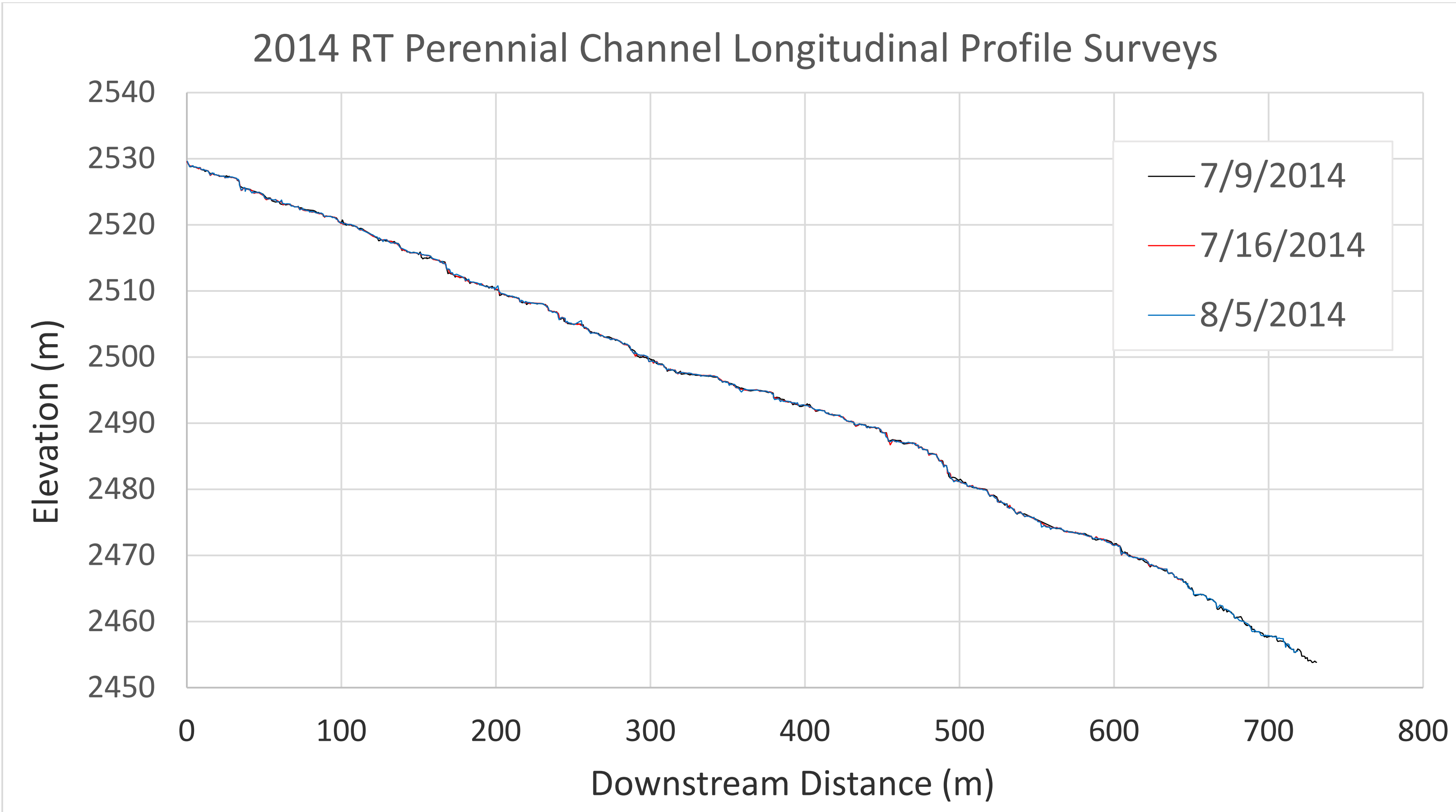

Figure 36: 2014 RT perennial channel longitudinal profile surveys. The three profiles account for changes caused by the 7/12/2014 and 7/29/2014 storms. The profiles show a channel largely resistant to change despite numerous knickpoints. The profiles do not show any areas of extensive aggradation or degradation during the survey period.